Theses, Dissertations, and Other Capstone Projects

2010

Bioinformatic and Sequence Analysis of Four Resuscitation Promoting Factor (Rpf) Gene Homologues in Mycobacterium avium subsp. paratuberculosis (Mpt), and Expression of the Putative Mpt rpf B in Escherichia coli.

David Dale Hedlund
Minnesota State University - Mankato

Follow this and additional works at: http://cornerstone.lib.mnsu.edu/etds

Part of the Microbiology Commons

Bioinformatic and Sequence Analysis of Four Resuscitation

Promoting Factor (Rpf) Gene Homologues in *Mycobacterium*

avium subsp. *paratuberculosis* (Mpt)*,* and Expression of the

Putative Mpt *rpfB* in *Escherichia coli.*

By

David D. Hedlund

A Thesis

Submitted in Partial Fulfillment

Of the Requirements for

Master of Science

In

Biology

Minnesota State University, Mankato

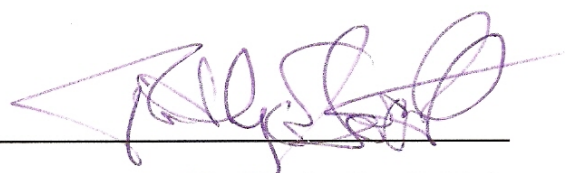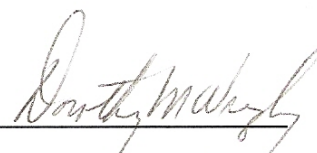Mankato, Minnesota

December 2010

Date: _11/11/2010_

This thesis has been examined and approved.

Examining Committee:

_____

Dr. Timothy Secott, Chair

_____

Dr. Dorothy Wrigley

_____

Dr. Robert Sorensen

For my loving family.

Acknowledgements

Abstract

Mycobacterium avium subsp. *paratuberculosis* (Mpt)*,* the causative agent of

Johne's disease (JD), is a global problem in the agricultural industry. It is estimated that

25% of all U.S. dairy herds are JD positive. One obstacle in the management of JD is the

lack a sensitive diagnostic test for use during the early stages of infection. Resuscitation

promoting factors (Rpf) are proteins that promote the growth of many species of

Actinobacteria. If Rpf proteins could enhance the growth of Mpt, the sensitivity of

diagnostic fecal culture could be improved, and the impact of JD on the dairy industry

would be significantly reduced. The putative *rpf* translation products from four open

reading frames (ORFs) in the genome of Mpt have been designated as Rpf homologues,

but their function as true Rpf proteins has not been demonstrated. Bioinformatic and

sequence alignment analysis supported the previous identification of four ORFs as *rpf*

homologues in Mpt, and further indicated that each of these homologues contains motifs

demonstrated to be critical for Rpf function. I cloned the Mpt homologue of *rpfB* in *E.*

coli and optimized the conditions necessary for expression. The recovered expression

products were tested against dormant Mpt. Although the recombinant protein exhibited

effects in *E. coli* consistent with Rpf expression, dormant Mpt did not respond to

recombinant RpfB. This may have been due to the loss of functional conformation

during the purification process. Further, RpfB alone may not be sufficient to resuscitate

dormant Mpt.

Table of Contents

List of Tables and Figures

Introduction

Animal disease accounts for a significant annual economic loss to the agricultural industry. Farmers must invest in controlling animal disease to ensure a healthy herd, and a product of consumable quality. The farmer's investment must be returned in order to justify the costs accrued. Those who consume the products will make up the cost of investing in the herd. If the cost of managing animal diseases can be reduced, the market price for products from animals will also be reduced.

Johne's disease (JD), caused by *Mycobacterium avium* subsp. *paratuberculosis* (Mpt), is a chronic wasting disease that is particularly significant in dairy and beef cattle, sheep, and goats; however it can also be found among wild ruminants (18). In 2008, the prevalence of JD in dairy herds was estimated to be 25% (101). The average economic cost of JD can be $229/cow/year (81). Estimates have placed the annual cost of JD to be as much as $1.5 billion (90). Efforts to eradicate Mpt from the agricultural process have been unsuccessful. Current JD management practices have helped decrease the incidence of JD. However, the current diagnostic techniques are insufficient in distinguishing uninfected animals from animals in the early stages of infection.

The course of JD can be broken down into 3 stages. Stage 1 is classified as early infection, most commonly seen in animals less than 2 years of age. During this period the infected animal does not show signs of disease, and Mpt is shed from the infected animal at levels below the limits of detection. The second stage is classified as subclinical infection. Subclinical infection is seen in animals that have been infected for

approximately 2-4 years. The infected host appears to be healthy, but may be a threat to surrounding stock due to an increase in the amount of Mpt being shed. The final stage of infection is classified as clinical infection. During clinical disease, animals progressively show signs including emaciation, watery diarrhea, and a decrease in milk production. Evidence of Mpt infection is easily accomplished during this stage of disease.

The organism is spread from animal to animal through the fecal-oral route by way of contaminated food and water, nursing from infected dams, or transplacentally (18). The infectious dose of Mpt has not been clearly established. The onset and progression of JD can vary depending on the number of organisms ingested, as well as the age of the animal (3). Mpt inocula at concentrations between 10^8 and 10^{10} are commonly used to experimentally infect animals through ingestion (18). However, orally administered doses of Mpt at concentrations as low as 10^3 have also successfully produced an infection (18). It is estimated that animals in the clinical stage of infection shed 5×10^{12} mycobacteria per day (14). Currently, the most effective way to control the spread of the organism is through hygienic herd management, early detection, and culling of infected animals.

Early detection of infection is one of the objectives in the successful management of JD. Fecal culture (FC) is the "gold standard" for detecting Mpt. FC is laborious, expensive, has a slow turn around time, and frequently leads to false-negative diagnoses due to poor sensitivity during the early stages of JD. Considering that FC is the gold standard used in the diagnosis of JD, the efficiencies of all other diagnostic tests are evaluated against FC. Diagnostic tests that are manipulated to have higher sensitivities than FC are considered to give false-positive results, due to the accepted consideration

that animals not shedding Mpt do not have JD. Improving the sensitivity of FC during the early and subclinical stages of disease would legitimize the elevated sensitivities of other diagnostic methods that are inexpensive and have rapid turn around times, and would lead to fewer false-negative diagnoses.

In order to increase the efficacy of JD diagnostics, work must first be done to improve the diagnostic gold standard. The first thing we must learn about Mpt infections is whether or not an infected host in the early stages of disease is always shedding Mpt. It is currently held that Mpt-infected hosts intermittently shed Mpt during the early stages of disease. However, infected hosts may always be shedding Mpt, but the accepted methods of FC may only support the intermittent detection of Mpt during the early stages of disease. If it is found that Mpt is always being shed from infected animals, it will be likely that a fraction of the Mpt is in a non-culturable state. Although the available diagnostic growth media have been optimized for the recovery of culturable Mpt, it is poorly understood how viable but not culturable bacteria respond to these media.

The sensitivity of FC may be affected by the physiological state of Mpt. It is possible that organisms in a physiologically dormant state cannot be successfully cultured by standard FC methods. Dormancy results when conditions for growth are less than optimal, possibly similar to those encountered within a granuloma. Reactivation of dormant cells can result in the reactivation of a latent infection, diffusion of an existing infection, or cause new infections upon entry into a new host. Recovery from dormancy is dependent on signaling factors produced by actively growing cells. Isolation of the signals that cause the resuscitation of dormant Mpt could be used in concert with FC to recover dormant Mpt *in vitro*. This would permit the means to determine whether or not

dormant Mpt are being shed from infected hosts during the stages of JD where standard FC is unreliable.

Growth factors known as Resuscitation Promoting Factors (Rpf) have been shown to promote the growth of related organisms that were previously dormant. Rpf proteins are highly conserved among Actinobacteria. The Rpf proteins of *M. tuberculosis* have been shown to greatly increase the culturability of previously uncultivable mycobacteria. To the writer's knowledge, only one experiment has been published on the ability of a Rpf to stimulate the growth of Mpt *in vitro* (117).

In the annotated genome of Mpt, there are four hypothetical proteins that share homology with Rpfs of related bacteria. If it is determined that Mpt expresses these genetic elements, recombinant Rpfs could be produced and incorporated into diagnostic culture media to facilitate a more rapid and accurate diagnosis of subclinical animals, and possibly improve the detection of Mpt-shedding animals within the early disease stage.

Our purpose in this study was to determine if Mpt contained the necessary genetic elements for functional Rpf proteins, and if dormant Mpt would respond to those Rpf proteins. We analyzed the Mpt Rpf homologues, and determined that the critical amino acids for Rpf function are present. We cloned the four *rpf* sequences into a mycobacterial expression vector; however we were unable to obtain any expression products from those vectors. We successfully expressed the putative *rpfB* in *E. coli*, and saw activity in *E. coli* consistent with that of Rpf proteins. When the purified RpfB was tested against dormant Mpt we did not detect any resuscitative response.

Literature Review

Mycobacterium avium subsp. *paratuberculosis* (Mpt) is the causative agent of paratuberculosis, or Johne's disease (JD); a chronic intestinal disease characterized by inflammation of the ileum and granulomatous enteritis of domestic and wild ruminants (12, 26, 38, 48, 68, 81, 94, 103). The economic consequences of this disease are particularly significant in dairy herds. In 1997, estimates by The National Animal Health Monitoring System (NAHMS) stated that 21.6% of dairy herds were infected (102). This number increased to 25% of dairy herds in 2008 (101). The economic consequence of JD can be as much as $1.5 billion in the dairy industry (38, 90).

Mycobacterium tuberculosis and *M. leprae* are the most well-known mycobacterial pathogens of humans, collectively infecting nearly 9.5 million new individuals each year (37, 82). Notable mycobacterial animal pathogens include *M. bovis, M. avium* subsp. *avium,* and Mpt. The common features of mycobacterial infections have led to the consideration of Mpt in the pathogenesis of Crohn's disease (8, 9, 12, 13, 36, 59, 68, 80, 105); however, this remains controversial.

Mpt has the slowest generation time of all cultivable mycobacteria, at approximately 20 hours (50). The genomic comparison of Mpt to *M. tuberculosis* indicates that this slow growth may have resulted from an insertion near *ori*C, as well as numerous nucleotide substitutions in genes encoding enzymes for purine synthesis (78). The most notable phenotypic difference between Mpt and other mycobacteria is the *in vitro* dependence of the former on mycobactin J, a siderophore. It is thought that this

dependency may be due to the truncation of the *mbtA* gene (53). The reliance on an intermediate iron supplier secures the obligate parasitism of Mpt.

Infection and Immunity

Infection begins with the consumption of milk or feed contaminated with Mpt. While moving through the small intestine, Mpt comes into contact with mucosa-associated lymphoid tissue where it crosses through M cells of the ileal Peyer's patches (38, 60). M cells are a common portal of entry for pathogens due to reduced levels of brush-border microvilli, digestive enzymes, and surface mucus at this site (32). Mpt then passes from ileal M cells to subepithelial and intraepithelial macrophages (60). Following endocytosis by macrophages of the Peyer's patches, the fate of Mpt depends on the maturation of the phagosome. If maturation occurs, the chances of Mpt surviving are greatly diminished. Maturation occurs in approximately 30% of phagocytic cases (115), and can lead to successful antigen presentation to reactive T-cell populations (26). If maturation of the phagosome does not occur, the environment Mpt encounters is less acidic and less toxic than in the case of normal phagosome trafficking.

The importance of phagosome trafficking extends to the reliance of Mpt on an intermediate iron supplier. The means by which Mpt obtains iron *in vivo* has eluded scientists to date. Brooks *et al.* characterized a 40 kDa protein called antigen D, the sequence of which resembles *E. coli* bacterioferritin (7). The role antigen D plays in iron acquisition for Mpt has yet to be confirmed. Lambrecht and Collins determined that mycobacteria are unable to access iron bound to siderophores of unrelated organisms; however, at a pH between 5-6.2, iron dissociation from host siderophores – transferrin

and lactoferrin – will promote the growth of Mpt without mycobactin (51). The pH

inside of a Mpt phagosome is 6.2-6.3 (43). In addition to this, Mpt-containing

phagosomes have increased levels of transferrin receptors (TFR), which are responsible

for transporting transferrin into early-stage endosomes (44). Mpt also produces an

extracellular ferric reductase that could play a role in Fe^{2+} acquisition from chelated Fe^{3+}

(42). Due to Mpt's lack of SOD activity, this reductase would also offer protection by

making Fe^{3+} unavailable to H_2O_2-producing enzymes (42). In addition, the increased

levels of TFR on Mpt-containing phagosomes suggest that Mpt may gain access to iron

from transferrin (43, 44).

The complexity of immune responses during this multistage disease cannot be

summed up in the simple paradigm of a Th1-Th2 shift (27). A synthesis of literature

from reports describing immune responses to Mpt infection can be confusing because of

variables such as methods and location of experimental inoculation, murine vs. ruminant

hosts, location of sampling for cytokine detection, identification and quantitation of

cytokines via mRNA transcripts vs. direct cytokine screening, and determining which

disease stage (if any) is being examined. A number of workers have reviewed the

available literature with regard to disease progression and host responses to Mpt infection

(26, 88, 91). Conclusions from these reports weighed the determinants of infection on a

controlled Th-type 1 response. If stabilized by the host, there is little likelihood that the

infection will progress to the subclinical stage, and protective immunity can result from

circulating Mpt-reactive CD8+ T lymphocytes (95).

The first response to the presence of Mpt is the production of the proinflammatory

cytokines interleukin (IL) 1α, IL-6, and gamma interferon (IFN-γ) as well as upregulation

of tumor necrosis factor associated receptor factor 1 (TRAF1) (26). Through IL-2/CD25 signaling, Th-1 and suppressor T-cell populations begin proliferation and production of IL-10, respectively (26).

Signs of IL-1α toxicity characterize the progression of infection into the sub-clinical phase. Lack of a TNF-α response sufficient to result in the formation of granulomas leads to the dissemination of infection (26). Granulomas of tuberculosis have been characterized as avascular structures consisting of 3 basic layers. The first is the outermost layer, composed of resting macrophages and lymphocytes. The second layer is composed of activated macrophages. The third layer is the caseous center, composed of viable bacteria, bacterial fragments, and killed macrophages (43).

The enhanced survival of infected macrophages may also be the result of high levels of TRAF1 surface expression, which prevent these cells from undergoing apoptosis. Mpt causes further recruitment of macrophages, and selection for and containment of suppressive T-cell populations by maintaining steady host production of IL-1α, IL-8, IL-10, and augmentation of the population shift from Th-1 to cytotoxic suppressor cells (26). Interestingly, a tie is yet to be made between the abundance of IL-8 and the lack of neutrophil infiltration.

Once the host has progressed to the clinical stage of disease, the active cell population has shifted almost exclusively to the response of macrophages, cytotoxic suppressor cells, and B cells. This combination marks total loss of control and regulation over the infection, and Mpt moves about the host unchecked. The resulting pathogenesis leads to extensive inflammation and damage to the ileum, granuloma formation, and thickening of the lumen intestinal wall (38). The distortion of villous absorptive tissue

lining the intestine leads to the subsequent development of malabsorptive diarrhea, wasting of the infected animal, and death. The explosive diarrhea that occurs during the clinical stage results in the shedding of large numbers of infectious Mpt which can be readily ingested by the surrounding stock; including those at highest risk of infection – neonatal and juvenile calves (38, 81).

Although calves become infected with Mpt, Mpt cannot be reliably recovered in culture during the early stage of disease. After this stage, calves may or may not progress to the subclinical stage (71). This puts a high demand on the development of new technologies that aid the early diagnosis by the identification of Mpt-infected animals.

Diagnosis

Fecal culture is considered to be the gold standard in detecting Mpt infection due to its near absolute specificity and high analytical sensitivity in detecting animals with clinical infection. However, fecal culture is very time consuming, taking up to 16 weeks to complete (81). Modifications to classical fecal culture techniques have significantly reduced the detection time for cattle with clinical infections (81). In contrast to clinical infection, detection of infection in asymptomatic animals is still problematic, both in terms of time and sensitivity: the sensitivity of fecal culture relative to infection is estimated to be between 30% and 50% (17, 57).

Enzyme linked immunosorbent assay (ELISA) is another method frequently used in diagnosis. Although the specificities of ELISA kits are routinely high, the specificities can vary. This can result from the quality of the Mpt antigen used in the ELISA, and whether the antibody shares cross-reactivity with other environmental mycobacteria (23,

24). The sensitivity of ELISAs vary with the age of the animal being tested (66), as well as the disease state of the host. The sensitivity of serological diagnostic methods increases with the progression of disease. ELISA testing has great utility for rapid diagnosis and guiding proper management practices, but does not provide us with a sensitivity equal to that of diagnostic culture tests (24). When the infection is controlled by the cell-mediated response, indirect ELISA has a very low sensitivity. As the animal ages and the infection progresses, the humoral response becomes active and the sensitivity increases with the production of antibodies; however, by the time antibody levels become detectable, the infection has likely progressed to a terminal stage (26). This makes ELISA suitable to examine the infectiousness of an animal, but not as a determinant of infection in early diagnosis (66).

Success has been made in modifying these tests to improve their sensitivity and specificity; however when their diagnostic efficiency is examined, it is always compared against fecal culture. Other methods for detecting Mpt infections include brightfield-microscopic examination of acid-fast smears, fluorescence *in situ* hybridization, complement fixation, agarose gel immunodiffusion, the gamma interferon assay, and IS*900* DNA detection. These methods have not been widely accepted due to their inability to distinguish among previous exposure, disease latency, and active infection, as well as the test probes lacking necessary sensitivity and/or specificity (81).

Persistence and Dormancy

Despite their apparent simplicity, prokaryotes are highly adaptive organisms that have the ability to sustain themselves under a variety of environmental conditions (93).

Survival of parasitic organisms within ecological habitats can pose a selective advantage

for them by means of transfer within biological vectors. Both Mpt and the closely related

Mycobacterium avium subsp. *avium* have been shown to survive and replicate within a

number of protozoa following both phagocytosis and encystment (78, 92, 111). This

capability affords them a greater resistance to antimicrobial drugs and chemical

disinfection (58, 111), the ability to disperse through aerosolization of Mpt-infected cysts

(78), and concurrent infection through entrance of the intestinal epithelium within

pathogenic amoeba (16).   Insects and nematodes have also been implicated as possible

biological vectors for the transfer of Mpt. Insects and insect larvae feed on the feces of

Mpt infected cattle and intestinal matter in slaughterhouses (34), and can be consumed by

potential hosts along with grasses and feed. Parasitic nematodes could possibly enhance

the virulence of Mpt by reducing the infectious dose required for infection (6, 112).

Whittington *et al.* has shown the Mpt can survive outside the host for as many as 55

weeks in the soil, and 65 weeks in distilled water (113).

It has long been held that animals in the early and sub-clinical stages of disease

shed Mpt in feces intermittently, which would explain the poor sensitivity of fecal culture

in these stages. However, it is possible that infected animals may always be shedding

Mpt, but those being shed by animals in the early stages of disease – when the host is

able to suppress replication – are not able to withstand growth on the rich, selective

media used for primary culture due to oxidative damage from increased metabolism.

In some non-spore forming bacteria, growth-limiting conditions (such as

restriction of growth in granulomas or environmental restrictions) cause organisms to

enter a non-culturable state called dormancy, which can last for decades (12, 63, 110).

Dormancy has been defined as a reversible phase in which the organism has drastically reduced its metabolism and persists without replication (104). The adoption of this inactive state can be the result of suboptimal growth conditions which lead to the reduction of metabolic activity, formation of more rigid cellular components, and a shift in catabolic pathways (110). Extended periods of time in a state of non-replicating persistence can lead to an organism remaining viable, but not culturable (VBNC) (77). This can also be referred to as non-replicating persistence (NRP).

A number of models have been tested on the transition of organisms into a state of NRP (110). To better understand the mechanisms of transition, it is important to consider the conditions under which an organism is forced to enter NRP. Pathogenic mycobacteria must overcome the obstacle of maintaining viability within granulomas. Concerning *M. tuberculosis* granulomas, the substrate availability in the caseous slurry (83, 116) and the necrotic tissue at a pH of approximately 6.5 (110) are conducive for ongoing metabolism. However, over time within a granuloma the decreased oxygen availability limits the ability of mycobacterial cells to grow and divide (10, 45, 79, 110). Granulomas that result from an Mpt infection can differ from granulomas caused by *M. tuberculosis*. They typically do not differentiate as well, and caseation only occurs in ovine hosts.

According to the Wayne dormancy model (107), when oxygen supplies diminish to approximately 1% of ambient oxygen concentrations, *M. tuberculosis* begins its decent into anaerobic respiration in what they refer to as NRP-1 (107). The organism halts division, thickens its cell wall, replicates its chromosome one final time, and with a

continued deprivation of oxygen enters a survival transition into what they refer to as

NRP-2 (107).

The use of nitrate reduction and the glyoxylate shunt are both important during

the transition to NRP. Nitrate reductase genes are induced in *M. tuberculosis* during

hypoxia and exposure to nitric oxide (89). Reducing nitrate allows this organism to

generate ATP during periods of anaerobiosis (89, 108, 110). Although putative genes for

assimilatory nitrate and nitrite reduction, and nitrate/nitrite transporters have been

identified in Mpt (2), the effects of such gene products have yet to be tested in Mpt. The

reductive amination of glyoxylate by way of the glyoxylate shunt promotes the

conservation of carbon, the preservation of biosynthetic intermediates, and the means to

regenerate NAD through the activity of glycine dehydrogenase (109). It has been

proposed by Wayne and Lin that NAD production from reductive amination of

glyoxylate would provide the means to generate the ATP required to complete a final

cycle of DNA replication before the termination of cell division (109). The sensitivity of

mycobacteria in the state of NRP, or transition to NRP, to metronidazole may indicate

that these organisms have the ability to respire anaerobically (107). However, the

reductive potential required for the activity of metronidazole may exist in a

microaerophilic environment (reductive potential below -430 mV) (31, 107).

Within a granuloma, successful entrance into NRP would require a very gradual

and organized alteration of metabolic processes. Through gradual oxygen depletion, *in

vitro* experiments have produced non-replicating bacteria that survived for 12 years (25).

Upon re-introduction into an aerated medium, these non-replicating cells grew and

divided immediately (107).

Successful recovery from a state of NRP depends heavily on the rate of entrance into NRP-1 and NRP-2 (107). Cells that are rapidly depleted of oxygen will not spend enough time in NRP-1, and their chances of survival during NRP-2 become greatly diminished (106, 109). Addressing these issues in an *in vivo* system, Canetti noted that conditions would differ greatly per granuloma, with the specific variables affecting successful NRP, including cellular composition, the extent of caseation and liquefaction, and oxygen availability (110).

In some cases of extended dormancy, mycobacteria shed their cell walls and enter a spheroplastic state (15). This allows the organism to more efficiently evade phagocytosis, and therefore remain undetected in a host for longer periods of time. Mycobacterial spheroplasts have been found to exist within a host (15). These spheroplasts are metabolically active, capable of reverting back to their normal cell-walled form, and infectious upon reversion (15, 73, 100). Recovery and reversion of experimentally induced mycobacterial spheroplasts can vary from as low as 0.1% to as high as 20% (15, 100). Rates of reversion *in vivo* are currently unknown.

Bacterial Communication

For many actinomycetes, successful resumption of growth from dormancy is dependent on signaling factors produced by the population of cells (61, 63, 64). When gene expression is determined by population density, it is referred to as quorum sensing (QS) (96). QS plays a role in the activation of genes that are beneficial at high bacterial load, commonly exemplified by the bioluminescence of *Vibrio fischeri* following the activation of the *lux* operon of that organism (96, 114). It has been demonstrated that

Gram-positive organisms also use a pheromone-based QS motif (61). The effects of this include competence, virulence, antimicrobial peptide production, and possibly resuscitation.

The classical mechanism of QS in Gram-positive bacteria starts with a post-translationally modified peptide that gets secreted via an ATP-binding-cassette (ABC) exporter. The signal is received by a transmembrane sensor, which becomes phosphorylated. The phosphorylated component combines with the response regulator to act as an inducer molecule for the operon. The process is autoregulated by having the genes that code for the signaling peptide, the ABC exporter, and the two-component regulatory system transcriptionally linked (49). This particular model is specific to biological molecules that are produced as a means of direct communication and population sampling.

There is also a means of biochemical signaling by molecules that are not produced with the sole intent of communication, but their presence can result in phenotypic changes in the organism detecting them. One example includes muropeptides incorporated into the peptidoglycan of bacterial cell walls. When serving their primary purpose, they contribute to the structural integrity of an organism. When recognized as a free-floating entity, they can act as a regulatory stimulus (30, 35, 47, 76). Peptidoglycan can act as a signaling molecule by way of serine/threonine protein kinases (STPK) (85). While studying the PASTA (penicillin-binding protein and serine/threonine kinase associated) domain kinase PrkC, Shah *et al.* showed that *m*-DAP- containing muropeptides acted as a strong stimulus for the germination of *Bacillus* endospores (47, 84). Mycobacteria express an essential STPK homologue to PrkC called PknB, that is

downregulated in response to carbon starvation, and therefore activated during periods of growth (4, 33). The possible significance of PknB in relation to peptidoglycan structure will be discussed below.

Resuscitation Promoting Factors

Micrococcus luteus, a member of Order Actinomycetales (high G+C content bacteria), produces an autoinducing proteinaceous growth factor known as resuscitation-promoting factor (Rpf protein) (12, 38, 61). It has been shown by Mukamolova and colleagues that Rpf proteins are highly conserved and promote growth of many Actinobacteria, including several species of mycobacteria (64). Their importance has even extended to infectious mycobacteriophages that conserve them within protein tails for the purpose of cell wall penetration, and possible cell-cycle initiation (70). Analysis of N-terminal processing has suggested that Rpf proteins could be uniquely involved in autocrine and paracrine signaling (61, 64).

Mukamolova and colleagues have shown that there is cross-species interaction among mycobacteria that produce Rpf proteins. In one such instance, picomolar concentrations of the Rpf proteins of *M. tuberculosis* were able to stimulate a >10-fold increase in the population of previously dormant *M. bovis* within a 60-day incubation period, while reducing the time for induction of logarithmic growth to approximately 20 days (depending on which Rpf was assayed) (64). Zhu *et al.* confirmed that Mpt also responded to Rpf proteins at picomolar concentrations (117). Their work showed that Mpt could be recovered from a dormant state when recombinant putative Mpt RpfA was added to culture media at concentrations between 8 and 128 picomolar.

There are five *rpf* genes in the genome of *M. tuberculosis* designated *rpfA* (Rv0867c), *rpfB* (Rv1009), *rpfC* (Rv1884c), *rpfD* (Rv2389c), and *rpfE* (Rv2450c) (28, 29, 64, 98, 99). Basic Local Alignment Sequencing Tool (BLAST) (1) searches have revealed that each of the genes *rpfA, rpfB, rpfC,* and *rpfE* has a homologue within the genome of Mpt (47). If the function of these homologues in Mpt is similar to Rpf function in *M. tuberculosis*, it may be possible to incorporate products of these *rpf* homologues into culture media to improve the sensitivity of diagnostic culture.

It was initially presumed by Mukamolova *et al.* that rather than functional redundancy, each Rpf might be expected to serve a unique purpose in specific situations (61). Work with mutants harboring null mutations in the *rpf* sequences has shown that *rpf* mutations do not affect the growth of *M. tuberculosis* in liquid media (46, 98). All Rpfs are dispensable for *in vivo* and *in vitro* growth; however progressive Rpf deletions impair virulence, colony-forming ability on solid agar, and the ability to spontaneously recover from a dormant state (46).

Downing and colleagues suggested a regulatory interdependence and communication among Rpf gene products when considering single, double, and triple mutants (28). Using the Erdman type *M. tuberculosis* strain, Downing *et al.* showed that triple mutants of Δ*rpfA* Δ*rpfC* Δ*rpfB* and Δ*rpfA* Δ*rpfC* Δ*rpfD* showed a significant deficiency in resuscitation (P <0.001); with the effects of losing *rpfB* in combination with -*A* and -*C* being more catastrophic to the organism than the loss of *rpfD* in combination with –*A* and -*C* (29). Tufariello *et al.* confirmed the importance of RpfB (relative to the other single *rpf* deletions) with respect to resuscitation of dormant cells with their Erdman type *M. tuberculosis* single mutant ΔRv1009 (*rpfB*) (99). This indicates that

there is not complete redundancy within the Rpf family of proteins, and with respect solely to resuscitation, there is a greater importance to the conservation of certain *rpf* sequences.

Kana *et al.* created quadruple *rpf* mutants of *M. tuberculosis* that displayed no upregulatory compensation by expression of the remaining *rpf*, which refute any suggestion of significant crosstalk among or between *rpf* genes (46). Some of the transcriptional regulators of *rpf* genes have now been recognized (72, 74). Kana *et al.* also saw a hierarchy within the family of proteins that placed the importance of RpfB and -E retention greater than RpfA, -C, and -D (46).

Initially, the Rpf protein was classified as a bacterial cytokine due to its potency at low concentrations (61). More recent work has led to the classification of Rpf proteins as peptidoglycan hydrolases (62, 97). Rpf proteins exhibit hydrolytic activity on the cell walls of both Gram-positive and Gram-negative organisms, as well as artificial lysozyme substrates. However, a decrease in the ability to break down artificial peptidoglycan substrates indicates that the activity of Rpfs is highly specific. When assayed with fluorescamine-labeled cell walls, the *M. luteus* Rpf exhibited a five- to six-fold decrease in peptidoglycan hydrolysis when compared to that of lysozyme (62). When assayed with 4-methylumbelliferyl-ß-D-N-N′-N″-triacetylchitotriose (MUF tri-NAG), the activity of the *M. luteus* Rpf diminished an additional 45 fold comparatively (62). Recent structural modeling has shown that conserved regions of Rpf proteins share structural homology with that of lysozyme and a family of lytic transglycosylases (20, 21, 62). Rpf proteins could play unique roles in the reorganization of peptidoglycan, cleavage of the

septum, transport of molecules across the cell wall, or production of signaling muropeptides in the resuscitation of dormant Mpt (62).

Among all members of the Rpf family there is an invariant glutamate residue at position 54, that when altered, greatly diminishes the muralytic activity of the protein (62, 97). Two cysteine residues at the beginning and end of the 70-residue conserved Rpf domain may play a role in the binding of a cofactor (62), or serve as the sole disulfide bridge in the cleft area (20). Other important structural components include a glycine-X-X-glutamine turn motif, and glycan binding threonine and tryptophan residues (20).

A recent discovery has shown that RpfB and -E also interact with Rpf-interacting protein A (RipA) (39, 40). RipA is a peptidoglycan endopeptidase that co-localizes with RpfB at the septum of dividing cells. RpfB is thought to cleave the ß-1,4-glycosidic bonds in peptidoglycan, while RipA hydrolyzes peptide cross-linkages (39, 40). Hett *et al.* (39) showed that RipA is vital for actively growing cells, and provided further evidence that RpfB alone is insufficient. They also showed that the combined effort of both enzymes cleaves peptidoglycan much more efficiently than does either enzyme individually (39); however, no trials were completed on cultures grown to a dormant state. Due to the potential lethality of unregulated peptidoglycan hydrolases, it would not be striking to find more protein-protein interactions existing within the Rpf family (41).

Interestingly, *Mycobacterium leprae,* which through reductive evolution has lost ~30% of its genome and ~40% of its protein-coding genes when compared to other mycobacteria, has retained its genes for RpfA, -B, and -C (22, 29). This may indicate that homologues in this, and other pathogenic species, are essential.

Expression profiling from Tufariello *et al.* showed that all five *M. tuberculosis rpf* mRNA transcripts were produced, and peaked at their earliest measured interval (day 4 of growth at OD_{600} = 0.125; $3.1x10^7$ CFU/ml) (98). From this point, expression levels varied throughout the time intervals of the experiment; but unlike the *M. luteus* Rpf, *M. tuberculosis* Rpf mRNA transcripts, as well as 23s ribosomal rRNA, were still detectable 4 months into extended-stationary phase (98). Their presence was also detected in an *in vivo* murine model (98).

This brings up two interesting questions. First, how deep into stationary phase must the organism be before the effects of Rpfs are exerted? Second, why are cells in a 4-month extended stationary phase producing Rpfs (assuming translation is occurring) that are not having an auto-inducing effect? The following are suggestions to address these questions.

1)   The concentrations of Rpf proteins are not optimal to induce resuscitation.

2)   There are additional factors required to exit dormancy, i.e. oxygen, nutrients, metabolic products, declining immunity.

3)   If additional factors are required, lasting Rpf proteins could provide the means to a more rapid and ensured recovery when conditions improve.

4)   The Rpf mRNA transcripts are stabilized and inactivated during the onset of dormancy.

5)   The peptidoglycan rearranging ability of lytic transglycosylases could provide the means to ensuring a more rigid and durable cell wall during transitions into dormancy.

6)   The combined hydrolytic and transglycolytic ability of Rpfs serve to aid the

recycling of cell wall material during adaptation into a spheroplastic state when

dormancy becomes extended.

It is more likely that in considering the properties of Rpfs, including the short half

life (*in vitro*) (64), recovery from dormancy comes from their expression within lag phase

when the organism must begin alteration of the cell wall to accommodate cell division; or

during lag and exponential phase, when it would be beneficial to signal related cells to

exit dormancy and begin a cooperative assault against the host. In the Tufariello *et al.*

2003 study, their earliest attempts at detect Rpf transcripts were limited to early-

exponential phase (98).

Cell Walls of Dormant Organisms

It has been shown that when entering dormancy, both Gram-positive and Gram-

negative organisms will increase the total number of peptidoglycan cross linkages by

converting dimers to trimers, tetramers, pentamers, and higher oligomers (69, 86). In

addition to these changes, *Enterococcus faecalis* (a Gram-positive organism) will

produce thicker and more durable cell walls, increase the amount of lipoteichoic acid,

increase the number of penicillin-binding proteins (PBPs), and increase the amount of the

active cell-wall bound autolysin – muramidase (69, 86, 87). PBP1 is a high-molecular-

weight enzyme with both transglycosylase and transpeptidase activity. PBP5 is a low-

molecular-weight enzyme that promotes the maturation of peptidoglycan. Low-

molecular-weight PBPs have either carboxypeptidase or DD-endopeptidase activity.

Muramidases are also required for the cleaving of peptidoglycan during cell division.

Eighty-five percent of Mur1 (a muramidase) is located in the cytoplasm of exponentially

growing cells (87). It is inactive until it becomes transported to the cell wall. There is a

3-fold increase in the amount of Mur1 located in the cell walls of VBNC Gram-positive

cells (87). Mur1 has an increased affinity for hyper-linked peptidoglycan; however, there

is also an increase in the amount of lipoteichoic acid in the cell walls of dormant

organisms, which inhibits the activity of autolysins (19). Addressing mycobacterial

peptidoglycan specifically, during entrance into stationary phase there is a significant

reduction of 4→3 peptide bonds between *m*-DAP and D-Ala, and increased

transpeptidation of 3→3 linkages between *m*-DAP-*m*-DAP (Figure 1) (4, 47, 52).

This rearrangement may alter the conformation of peptidoglycan, such that a

specialized enzyme may be required to break the linkages once cell division is to resume.

It may also change the shape of released peptidoglycan fragments, which may act as

signaling factors in two-component regulatory systems. If acting through two-component

regulatory systems, the resuscitation of mycobacteria may be an act of quorum sensing

similar the quorum sensing means of Gram-positive organisms.

It has been hypothesized by Signoretto and colleagues that the combination of

these events will both promote greater endurance during dormancy, as well as a means to

recovery when growth conditions improve (87). With a redesigned cell wall, and all

enzymes in place and waiting, the proposed transglycosylase and lysozyme properties of

Rpf could be the missing link in the onset of recovery from a dormant state. Upon

reactivation, Rpf mediated carboxypeptidase cleavage and release of muropeptides,

particularly *m*-DAP-terminating disaccharide tripeptides generated during the entrance

into dormancy, could possibly act through PknB signaling to release the organism from its dormant state (47).

Materials and Methods

Bacterial Cultures

Mycobacterium avium subsp. *paratuberculosis* (Mpt) was propagated in Middlebrook 7H9 broth (Becton Dickinson, Franklin Lakes, NJ) supplemented with 10% oleic acid-albumin-dextrose-catalase (Becton Dickinson), 0.05% Tween 80 (Becton Dickinson), and 2 µg Mycobactin J (Allied Monitor, Fayette, MO) (M7H9C), in sealed tissue culture flasks. *Mycobacterium smegmatis* and *E. coli* cultures were propagated in LB broth (Becton Dickinson). All strains containing plasmids were grown in LB broth supplemented with 30-50 µg/ml kanamycin sulfate (Sigma, St. Louis, MO) or 50 µg/ml ampicillin (Sigma), depending on the resistance encoded within the vector.

Dormant Mpt were prepared by inoculating 1 ml of Mpt into 10 ml M7H9C in 15 ml serum vials. The vials were sealed with a rubber septum, and held at 37ºC for a minimum of 2 years. Before use, a viability assay was performed via flow cytometry to analyze the condition of the cells.

E. coli XL-1*, E. coli* (*lacZΔM15*)*, E. coli* BL21(DE3), and *M. smegmatis* mc^{2}155 cultures were propagated in LB broth and held at -80ºC after an electrocompetency preparation as described in the appendix.

Identification of Genomic *rpf* Sequences

All annotated and hypothetical Rpf protein sequences were mined from the following mycobacterial species using the NCBI website: *M. abscessus, M. ulcerans, M.*

marinum, M. tuberculosis, M. bovis, M. avium, and *M. smegmatis.* Once determined,

pairwise alignments were created using the protein sequences of each Rpf using CLC

Free Workbench. A consensus sequence produced from the alignments was used to

probe the proteome of Mpt. Sequences that showed homology were then realigned with

the mycobacterial Rpf proteins to analyze the placement of each critical amino acid.

Polymerase Chain Reaction

Primers were designed to amplify the 4 *rpf* sequences identified in the Mpt

genome (*rpfA, rpfB, rpfC,* and *rpfE*). Restriction sites were added to the 5′ tails of the

forward and reverse oligos, and additional nucleotides were added as needed for the

purpose of cloning in frame with the *hsp60* promoter, and hexahistidine tag within the

pMV261-derived vector, pMTS088 (Minnesota State University – Mankato, culture

collection). Primers were ordered from Integrated DNA Technologies (Coralville, IA)

and diluted as 50 µM stocks. A detailed explanation of how the primers were used is

discussed below.

Polymerase Chain Reactions (PCR) were set up in 50 µl aliquots to contain final

concentrations of: 1X buffer (50 mM Tris/HCl, 10 mM KCl, 5 mM $(NH_4)_2SO_4$, 2 mM

$MgCl_2$, pH 8.3/ 25°C), 1X GC-Rich solution (Roche, Indianapolis, IN), 5% DMSO, 200

µM dNTPs, forward and reverse primers at 1 µM each, 4 units DyNAzyme™ II DNA

polymerase (Finnzymes, Lafayette, CO), and DNA templates varying in concentration

from 5 ng to a whole cell lysate. Reactions were carried out in an Eppendorf,

Mastercycler® Gradient thermal cycler (Eppendorf, Hauppauge, NY) using a denaturing

temperature of 95°C for 5 minutes, a thermal gradient across 12 lanes ranging from 50°C

to 70.5°C, and an extension temperature of 72°C over 35 cycles.

Cloning

Primers designed to isolate hypothetical *rpf* sequences from the genome of Mpt

are as follows: Rpf1F and Rpf1R (*rpfA*), Rpf2F and Rpf2R (*rpfE*), RpfB Forw10 and

RpfB Rev10 (*rpfB*), RpfC/D Forw10 and RpfC/D Rev10 (*rpfC*). PCR amplicons

generated from genomic Mpt templates were TA cloned into the plasmid vector, pSC-A,

using a Stratagene (Santa Clara, CA) StrataClone™ PCR cloning kit at a 2:1 vol./vol.

insert:vector ratio. The pSC-A constructs were propagated in the *E. coli* strain provided

by the manufacturer. Blue-white screening was performed using LB agar (Becton

Dickinson) supplemented with 50 μg/ml kanamycin (Fisher, Pittsburgh, PA) and 2% 5-

bromo-4-chloro-3-indolyl-b-D-galactopyranoside (X-Gal) (Zymo Research, Orange, CA).

Selected transformants were screened using PCR.

Secondary primer sets were required to incorporate restriction tails into the *rpfA*

and *rpfE* sequences. These primers included Rpf1D and Rpf1BR for the amplification of

rpfA, and Rpf2D and Rpf2DR for the amplification of *rpfE*. The pMTS089 and

pMTS090 vectors served as templates for these PCRs. Nucleotide sequences generated

from these reactions were TA cloned into pSC-A, and selected for as previously

described.

Transformants containing the *rpf* insert were grown overnight at 37°C in LB broth

supplemented with 50 μg/ml kanamycin. Plasmids were extracted using a Zyppy™

Plasmid Miniprep Kit (Zymo Research), and digested eccentrically to confirm insert

orientation. Inserts were removed from vectors using restriction endonucleases respective to sites incorporated into the primer tails, and gel purified using a Zymoclean™ DNA Gel Recovery Kit (Zymo Research). Recovered inserts were then ligated downstream and in frame with the *hsp60* promoter, and upstream and in frame with the hexahistidine tag in the plasmid vector pMTS088. The pMTS088 vector is a modified pMV261 construct, which contains a mycobacterial cell entry (Mce) sequence between the flanking *hsp60* promoter and hexahistidine tag. Mce has no affect on cell growth, and was used as a hexahistidine-tagged mycobacterial protein control in this study. The pMTS088 derived *rpf* constructs were propagated using *E. coli* XL-1 following electroporation using a Gene Pulser Xcell™ (Bio-Rad , Hercules, CA) set to 2,500 V, 25 µF, and 200 Ω. Once insert screening and orientation were confirmed, plasmids were extracted and electroporated into electrocompetent *Mycobacterium smegmatis* mc^{2}155 at 1250 V, 25 µF, and 800 Ω in a 2mm cuvette.

Expression

    M. smegmatis mc^{2}155 transformants were grown at 37°C for 72-96 hours in 30 ml LB with 50 µg/ml kanamycin (Fisher), and harvested using centrifugation for 10 minutes at 10,000 x *g*. Pellets were resuspended in 250 µl 1X phosphate-buffered saline (PBS) with 1 mM phenylmethylsulfonyl fluoride (PMSF) (Sigma) and boiled for 15 minutes. Alternatively, cultures were harvested using centrifugation, washed twice in 1X PBS, and resuspended in 1 ml 1X PBS. Cells were then pulse sonicated for 20-second intervals with three repetitions, and PMSF added to a final concentration of 10 mM. The protein fraction of cell lysates was quantitated using the bicinchoninic acid (BCA) assay (Pierce)

standardized with bovine serum albumin (BSA) (Rockland, Gilbertsville, PA). Equal

quantities of protein from boiled lysates were sent through SDS-PAGE, and streamlined

into western blots. Blotting was performed with a biotin affinity-purified rabbit anti-6X

His antibody (Rockland).

Plasmid vector pMTS079 (a pET28b+ derivative) was used as a second parent

vector for the expression of *rpfB*. The pMTS079 vector was digested using *Nco*I

(Fermentas, Glen Burnie, MD) and *Pst*I (Promega, Madison, WI), allowing *rpfB* to be

inserted downstream and in frame with the T7 *lac* promoter and upstream and in frame

with the histidine tag provided from pET28b+ (Novagen, San Diego, CA). The new

construct – pMTS115 – and pMTS079 were electroporated into electrocompetent *E. coli*

BL21(DE3) (Novagen) using the same parameters as described for *E. coli* XL-1.

Expression conditions were optimized by growing cultures at room temperature, 30°C,

and 37°C. Each of the cultures was induced between 0.6 and 0.8 OD_{590} units with

isopropyl-1thiol-(d)-galacto-pyranoside (IPTG) (EMD Chemicals, Gibbstown, NJ) at

final concentrations of 0.05 mM, 0.1 mM, 0.5 mM, and 1 mM. Ten-milliliter samples

were drawn each hour over the four-hour period and processed for the detection of his-

tagged proteins.

Recombinant Protein Isolation and Purification

Cultures were harvested by centrifugation at 10,000 x *g* for 10 min, washed in 20

mM Tris-HCl pH 8.0, and spun again at 10,000 x *g* for 10 min. Pellets were resuspended

in 2 ml BugBuster® (Novagen) reagent supplemented with 1 mg/ml lysozyme (MP

Biomedicals, Solon, OH), 25 U Benzonase® nuclease (Novagen), 1 mM PMSF, and

rocked at room temperature for 30 minutes. Cell lysates were spun down at 16,000 x g

for 10 minutes, and pellets were resuspended in 1 ml BugBuster® reagent with final

concentrations of lysozyme and PMSF at 1 mg/ml and 1 mM respectively. Resuspended

pellets were sonicated on ice at 45% duty with 5.5 output control in a Branson Sonifier

450 (Danbury, CT) for three 10 sec pulses between 30 sec breaks.

Soluble fractions were separated from insoluble fractions by centrifugation at

21,000 x g for 10 min.   Pellets were resuspended in 1X Ni-NTA binding buffer pH 8.0,

solubilized with either 6 M guanidine hydrochloride (Fluka, Buchs, Switzerland) or 8 M

urea (Sigma), and stored overnight at 4ºC. The following day the samples were

centrifuged at 4,000 x g for 30 minutes to separate any remaining insoluble debris.

Solubilized fractions were sent through HisPur™ Ni-NTA Resin (Pierce, Rockford, IL)

and eluted in four 500 µl fractions. Eluted fractions were desalted using D-Salt™

Dextran Desalting Columns (Pierce) with 3mls of 10 mM Tris-HCl pH 6.8 in 500 µl

increments. Samples were stored at -20ºC in 10 µl aliquots. Eluates containing peak

protein fractions were determined photometrically at OD_{280}. Once the peaks were

determined, samples were run through SDS-PAGE and western blots. The optical

density of the RpfB and Mce protein bands relative to the co-purifying contaminating

bands were measured using UVP LabWorks BioImaging Software (Upland, CA). The

total protein concentrations in each sample were determined using the BCA assay

standardized with BSA.

Experiment Assembly

A 2 ml aliquot of dormant Mpt was drawn from serum vials with a 3 cc syringe fitted with a 25-gauge needle. Cells were centrifuged at 10,000 x g for 7 minutes and resuspended in 1 ml 1X PBST. Half the volume was diluted with 1X PBST to a photometric reading of 30% transmission ($2.0x10^8$ CFU/ml) at OD_{590}. The remaining 500 µl was centrifuged at 10,000 x g for 7 minutes, and resuspended in an equal volume of M7H9C required to get the density to 30% transmission. The culture was then serially diluted to a final concentration of $2.0x10^4$ CFU/ml in 10 ml M7H9C. Alternatively, cultures were serially diluted to final concentrations of $2.0x10^6$ CFU/ml in 10 ml M7H9C. Prior to inoculation, a viability assay was done on the dormant Mpt cultures using SYTO9® and propidium iodide (Invitrogen, Eugene, OR) by way of flow cytometry (Millipore, Billerica, MA).

Recombinant RpfB and Mce were tested at two different starting concentrations. For the first preparation, purified recombinant Mce and RpfB were diluted to total protein concentrations of 1 nM in volumes of, at minimum, 100 µl M7H9C. The second preparations were setup identically with RpfB and Mce at final concentrations of 12.8 nM.

Eight doubling dilutions of Mce and RpfB were tested against dormant Mpt, each in 5 replicate sets per plate. This accounted for 10 of the 12 columns of each plate. Of the remaining 2 columns, 1 contained only dormant Mpt, and the other contained only M7H9C (Appendix Figure 1, Appendix Figure 2, Appendix Figure 3, Appendix Figure 4).

Microplate wells were covered with a transparent seal to prevent evaporation and contamination. Microplates were placed in sterile plastic containers with a benzalkonium chloride soaked paper towel between the microplate and the bottom of the container to prevent desiccation and contamination. Containers were incubated at 37ºC. Before optical densities were measured, microplates were allowed to equilibrate to room temperature in a laminar hood, and a new seal was placed over the wells. Optical densities were measured at 590 nm every 48 hours.

Results

<u>Identification of Mpt ORFs that are Homologous to *rpf* ORFs of Related</u>

<u>Actinobacteria</u>

All available annotated and hypothetical Rpf protein sequences of mycobacterial

species were aligned according to their classification as RpfA-E. Consensus sequences

were determined, and used to probe the proteome of Mpt. It was confirmed that 4

hypothetical Rpf proteins exist in Mpt. The GenBank accession numbers for those

hypothetical Rpf sequences are MAP_0805c, MAP_0974, MAP_1607c, and

MAP_2273c. Each of the hypothetical Mpt Rpf proteins was then aligned with annotated

mycobacterial Rpf proteins to verify the approximately 70-residue consensus, the

flanking cysteines, the catalytic glutamate, the glycine-X-X-glutamine turn motif, and the

NAG-binding threonine and tryptophan residues that all proteins of the Rpf family share.

The RpfA alignment is shown in figure 2. The RpfB alignment is shown in figure 3. The

RpfC alignment is shown in figure 4. The RpfE alignment is shown in figure 5.

<u>Cloning</u>

Primers were first designed to isolate the *rpf* homologues from the genome of

Mpt. Restriction tags were incorporated into the 5' tails of the primers that amplified

rpfC and *rpfB,* but not *rpfA* or *rpfE* (described in table 2). Each of the 4 *rpf* sequences

was then TA cloned into pSC-A. The names of those primers and the pSC-A derived

constructs that were produced using the amplicons generated from those primers are listed in table 3. The pSC-A vector is described in figure 6.

Once the *rpf*-pSC-A constructs were produced, a second set of primers containing restriction elements was designed to amplify *rpfA* and *rpfE* from pMTS089 and pMTS090 (described in table 2). Primer sequences are listed in table 4. The PCR amplified products were then TA cloned into pSC-A to produce the vectors pMTS099 and pMTS100. The construction of all 6 *rpf*-pSC-A plasmids was confirmed using PCR and restriction endonuclease digestion.

Following *Bam*HI and *Nsi*I digestion of the pSC-A constructs pMTS099, pMTS100, pMTS110, and *Nco*I and *Nsi*I digestion of pMTS109, all sequences were ligated into the modified pMTS088 vector (a pMV261 derivative). The pMTS088 vector is described in figure 7. DNA sequencing reactions were performed using an ABI Prism®. Primers designed for the purpose of DNA sequencing are listed in table 3. The sequence of each primer is listed in table 4. DNA sequencing allowed us to analyze the 5' and 3' linkages, and confirm that all inserted sequences were in frame with the hexahistidine tag, the heat-shock promoter of pMTS088, and the mycobacterial *hsp60* Shine-Dalgarno sequence – 5′ CGGAGGA 3′ (55, 65). The DNA sequencing results were aligned with the predicted *rpf* constructs to verify the predicted constructs were assembled correctly. All sequences were confirmed, with the exception of pMTS105 (thought to contain *rpfE*), which contained a mismatched section upstream of the 3′ *Nsi*I/*Pst*I link (figure 9). The pMTS104 sequencing results are shown in figure 8. The pMTS105 sequencing results are shown in figure 9. The pMTS112 sequencing results are shown in figure 10. The pMTS113 sequencing results are shown in figure 11. The

rpfB sequence was also ligated into the modified pMTS079 vector (a pET28b+ derivative), producing the vector pMTS115. The presence of *rpfB* in pMTS115 was confirmed using PCR and restriction endonuclease digestion. The pMTS079 vector is described in figure 12. The pMTS115 vector is described in figure 13. Detailed descriptions of each pSC-A, pMV261, and pET28b+ derived construct are given in table 1.

Expression

No his-tagged proteins were detected from any attempts at expression within *M. smegmatis* mc^{2}155, including pMTS088 – the positive control (figure 14). Previous attempts at expression of recombinant his-tagged *mce* from pMTS088 in *M. smegmatis* mc^{2}155 have been successful (Secott, unpublished) however those results could not be replicated. For this reason, the plan to express recombinant-mycobacterial proteins in a mycobacterial host was abandoned, and efforts were put towards the expression of *rpfB* and *mce* in *E. coli* BL21(DE3) from pET28-derived vectors.

Initial attempts at detecting recombinant RpfB from *E. coli* BL21(DE3) proved difficult due to the lysis of the expressing cells (figure 15). The initial attempts were carried out according to the manufacturer's instructions, inducing with 1 mM IPTG and harvesting after a 3 hour expression time. Upon further investigation it was found that there was a considerable loss of detectable recombinant RpfB using extended expression times (figure 16). Considering that RpfB has the potential to be a lethal protein due to its ability to break glycosidic bonds of the cells wall, the graph in figure 15 gives reason to believe that the Mpt *rpfB* ORF codes for a functional protein, and *E. coli* BL21(DE3) is

able to express it in its functional conformation. For this reason, growth and expression conditions were optimized with the primary interest of recovering soluble RpfB, and secondarily, to produce the greatest detectable quantity (see materials and methods).

Although it is assumed that there is an active, soluble quantity of RpfB being translated due to the lysis of expressing cells, detection of soluble RpfB was not successful (exemplified in figure 16). The conditions that promoted the best expression (in terms of cellular-retained quantity) were when the cells were grown at 37ºC, induced with 1mM IPTG between 0.6 and 0.8 OD_{590} units, and harvested at 1 hour post induction (figure 16). This procedure, as well as all others tried, produced recombinant his-tagged proteins in the form of inclusion bodies.

The Thermo Scientific Pierce Blue Prestained Protein MW Marker was used to distinguish the size of recombinant proteins in SDS-PAGE gels. The Mce and RpfB proteins were expected to be 48 kDa and 42 kDa, respectively. Recombinant Mce migrated at a slightly slower rate than ovalbumin (47 kDa), and RpfB migrated at a slightly faster rate (figure 16).

Protein OD_{280} peaks following the desalting of Ni-NTA consistently occurred within the first 3 ml eluted. Quantitative differences in the Mce and RpfB protein purifications differed between expression trials from as much as 146 µg/ml, to as little as 6.5 µg/ml. Although the majority of protein that eluted from the Ni-NTA column was consistent with the expected molecular weight of Mce and RpfB, the actual quantity of recombinant protein recovered was skewed by the presence of co-purifying contaminant proteins (seen in figure 17 and figure 18).   Optical densitometry was used to measure the proportion of RpfB and Mce relative to the amount of co-purifying contaminant bands.

The differences in optical density ranged from as little as 35% purity to as much as 100% purity.

Increasing the concentration of imidazole in the column wash buffer from 20 mM to 50 mM appeared to increase the purity of recombinant proteins that were recovered (Figure 17), without affecting the affinity of hexahistidine-fused proteins to the column resin. However, this varied between experiments. Increasing the concentration of imidazole in the column elution buffer from 250 mM to 500 mM resulted in a product of comparable quantity, and lesser purity (Figure 18). Decreasing the pH of the binding, wash, and elution buffers from pH 8.0 to pH 6.3 did not have an effect on the purity of eluted histidine-fused proteins (data not shown). To avoid potential problems resulting from protein carbamylation, all proteins that were tested for bioactivity came from chromatography preparations in which urea was used in concert with Ni-NTA buffers at a slightly alkaline pH. There did not appear to be a difference in the quantity or purity of recombinant proteins when inclusion bodies were solubilized with urea compared to their solubilization with guanidine hydrochloride (data not shown).

Effects of Recombinant RpfB on Dormant Mpt

The viability assay on dormant Mpt calculated an approximate 3.5% culture viability. Results showing the growth stasis of dormant Mpt with and without the addition of recombinant Mce and RpfB are shown in Figure 19. The results displayed in figure 19 are consistent with the optical densities of all 24 plates monitored. Dormant Mpt cultures did not exceed baseline turbidity levels in any of the 24 plates monitored.

Table 1: Vector nomenclature and hosts.

Plasmid	Parent Vector	Modified Parent used for Cloning	Sequence Inserted	Sequence Template	Host
pSC-A	N/A	N/A	N/A	N/A	*E. coli* (StrataClone™)
pMTS089	pSC-A	N/A	*rpfA*[*]	Mpt Genome	*E. coli* (StrataClone™)
pMTS090	pSC-A	N/A	*rpfE*[*]	Mpt Genome	*E. coli* (StrataClone™)
pMTS099	pSC-A	N/A	*rpfA*	pMTS089	*E. coli* (StrataClone™)
pMTS100	pSC-A	N/A	*rpfE*	pMTS090	*E. coli* (StrataClone™)
pMTS109	pSC-A	N/A	*rpfB*	Mpt Genome	*E. coli* (StrataClone™)
pMTS110	pSC-A	N/A	*rpfC*	Mpt Genome	*E. coli* (StrataClone™)
pMV261	N/A	N/A	N/A	N/A	*M. smegmatis* mc^{2}155
pMTS088	pMV261	pBluescriptII SK+, pSC-A, pET28b+	*mce*	pMTS079	*M. smegmatis* mc^{2}155
pMTS104	pMV261	pMTS088	*rpfA*	pMTS099	*M. smegmatis* mc^{2}155
pMTS105	pMV261	pMTS088	*rpfE*	pMTS100	*M. smegmatis* mc^{2}155
pMTS112	pMV261	pMTS088	*rpfB*	pMTS109	*M. smegmatis* mc^{2}155
pMTS113	pMV261	pMTS088	*rpfC*	pMTS110	*M. smegmatis* mc^{2}155
pET28b+	N/A	N/A	N/A	N/A	*E. coli* BL21(DE3)
pMTS079	pET28b+	pBluescriptII SK+, pSC-A	*mce*	Mpt Genome	*E. coli* BL21(DE3)
pMTS115	pET28b+	pMTS079	*rpfB*	pMTS109	*E. coli* BL21(DE3)

---

[*] Primers used to generate the *rpf* amplicon were designed to anneal approximately 400 base pairs outside of the ORF in the genome of Mpt. The construct was then used as a template for directional *rpf* cloning.

Table 2: Cloning and expression detail.

Plasmid	Forward Restriction	Reverse Restriction	Promoter / Expression Tag	Sequence Verification Method	Sequence Confirmed	Expression Detected
pSC-A	N/A	N/A	N/A	N/A	N/A	N/A
pMTS089	N/A	N/A	N/A	RE, PCR	Yes, Yes	N/A
pMTS090	N/A	N/A	N/A	RE, PCR	Yes, Yes	N/A
pMTS099	*Bam*HI	*Nsi*I	N/A	RE, PCR	Yes, Yes	N/A
pMTS100	*Bam*HI	*Nsi*I	N/A	RE, PCR	Yes, Yes	N/A
pMTS109	*Nco*I	*Nsi*I	N/A	RE, PCR	Yes, Yes	N/A
pMTS110	*Bam*HI	*Nsi*I	N/A	RE, PCR	Yes, Yes	N/A
pMV261	N/A	N/A	*hsp60* / N/A	N/A	N/A	N/A
pMTS088	*Bam*HI, *Nco*I	*Pst*I	*hsp60* / 6XHis	RE, PCR	Yes, Yes	No
pMTS104	N/A	N/A	*hsp60* / 6XHis	RE, PCR, Sequenced	Yes, Yes, Yes	No
pMTS105	N/A	N/A	*hsp60* / 6XHis	RE, PCR, Sequenced	Yes, Yes, No*	No
pMTS112	N/A	N/A	*hsp60* / 6XHis	RE, PCR, Sequenced	Yes, Yes, Yes	No
pMTS113	N/A	N/A	*hsp60* / 6XHis	RE, PCR, Sequenced	Yes, Yes, Yes	No
pET28b+	N/A	N/A	T7 *lac* / 6XHis	N/A	N/A	N/A
pMTS079	*Nco*I	*Pst*I	T7 *lac* / 6XHis	RE, PCR	Yes, Yes	Yes
pMTS115	N/A	N/A	T7 *lac* / 6XHis	RE, PCR	Yes, Yes	Yes

---

* Sequencing showed the 3′ ligation occurred between NsiI-PstI restriction sites, however the sequence upstream of the linkage did not match that of the hypothetical *rpfE*. See Figure 25 for further explanation.
RE = Restriction Endonuclease Digestion.

Table 3: Primer nomenclature and antibiotic resistance markers.

Plasmid	Cloning Primers[*]	5′ Sequencing Primers[*]	3′ Sequencing Primers[*]	Antibiotic (50 µg/ml)
pSC-A	N/A	N/A	N/A	Kan
pMTS089	Rpf1F, Rpf1R	N/A	N/A	Amp
pMTS090	Rpf2F, Rpf2R	N/A	N/A	Amp
pMTS099	Rpf1D, Rpf1BR	N/A	N/A	Kan
pMTS100	Rpf2D, Rrf2BR	N/A	N/A	Kan
pMTS109	RpfB Forw10, RpfB Rev10	N/A	N/A	Kan
pMTS110	RpfC/D Forw10, RpfC/D Rev10	N/A	N/A	Kan
pMV261	N/A	N/A	N/A	Kan
pMTS088	N/A	N/A	N/A	Kan
pMTS104	N/A	088 HspF Link ID, 1D HspR Link ID	109F1, MsMceHisR	Kan
pMTS105	N/A	088 Hsp Link ID, E HspR Link ID	109F1, MsMceHisR	Kan
pMTS112	N/A	088 Hsp Link ID, B HspR Link ID	109F1, MsMceHisR	Kan
pMTS113	N/A	088 Hsp Link ID, C/D HspR Link ID	109F1, MsMceHisR	Kan
pET28b+	N/A	N/A	N/A	Kan
pMTS079	N/A	N/A	N/A	Kan
pMTS115	N/A	N/A	N/A	Kan

---

[*] See Table 4 for the corresponding sequences and templates of each primer.

Table 4: Primer nomenclature.

Primer ID	Amplified Sequence	Template	Primer Sequence 5′ → 3′	RE Tag
Rpf1F	*rpfA*	Mpt Genome	gtgacgagagaggaatacatcg	N/A
Rpf1R	*rpfA*	Mpt Genome	tgtggaagcaccagttcttc	N/A
Rpf1D	*rpfA*	pMTS089	taatGGATCCagagaggaatacatcggcgcgtatgagtgg	*Bam*HI
Rpf1BR	*rpfA*	pMTS089	taatATGCATggcgctgggtgcgggctgcaccagggcg	*Nsi*I
Rpf2F	*rpfE*	Mpt Genome	caacgggttacggaagagta	N/A
Rpf2R	*rpfE*	Mpt Genome	ggtagccccatacaagacaa	N/A
Rpf2D	*rpfE*	pMTS090	taatGGATCCtcgtgcccgacccagacggcacgtcccg	*Bam*HI
Rpf2BR	*rpfE*	pMTS090	gctgATGCATgccgcggcggccgcacaccgggccacgcgc	*Nsi*I
RpfB Forw10	*rpfB*	Mpt Genome	CCATGGcccgcgcgttgagtgtattgacaaa	*Nco*I
RpfB Rev10	*rpfB*	Mpt Genome	ATGCATaccagctcttccgctgcaca	*Nsi*I
RpfC/D Forw10	*rpfC*	Mpt Genome	GGATCCtaacgccttgttttcgcctgccgaaatg	*Bam*HI
RpfC/D Rev10	*rpfC*	Mpt Genome	ATGCATcgggaccgccgcctggatca	*Nsi*I
088 HspF Link ID	Sequencing amplicon	All pMV261 derived vectors	agtggcagcgaggacaacttgag	N/A
1D HspR Link ID	*rpfA* sequencing amplicon	pMTS104	gcaatcttggcgacgctgacac	N/A
B HspR Link ID	*rpfB* sequencing amplicon	pMTS112	gcacaccgaaaccgcgtatc	N/A
C/D HspR Link ID	*rpfC* sequencing amplicon	pMTS113	tgtggccaaagcgttacctattcg	N/A
E HspR Link ID	*rpfE* sequencing amplicon	pMTS105	gctgaggctgttggttgaatgc	N/A
109F1	Sequencing amplicon	All pMV261 derived vectors	gaatcacttcgcaatggccaagac	N/A
MsMceHisR	Sequencing amplicon	All pMTS088 derived vectors	ataTTCGAAgccaactcagcttcctttcggg	*Bst*BI
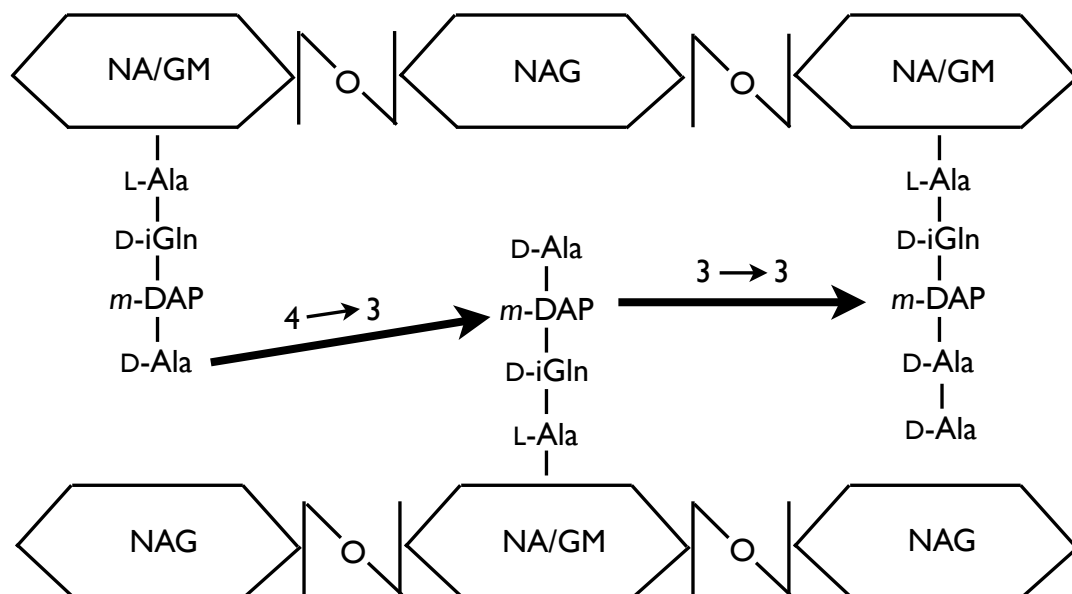
Figure 1: Proposed model of peptidoglycan alterations during the transition from exponential growth into stationary phase. The diagram is a simplified reproduction of a model produced by Kana *et al.* (47). The NA/GM polymer represents the *N*-acetyl or *N*-glycolyl muropeptide that mycobacteria contain (56). The left side shows the typical arrangement of peptidoglycan during exponential growth. The right side shows the proposed arrangement of peptidoglycan in dormant mycobacteria.
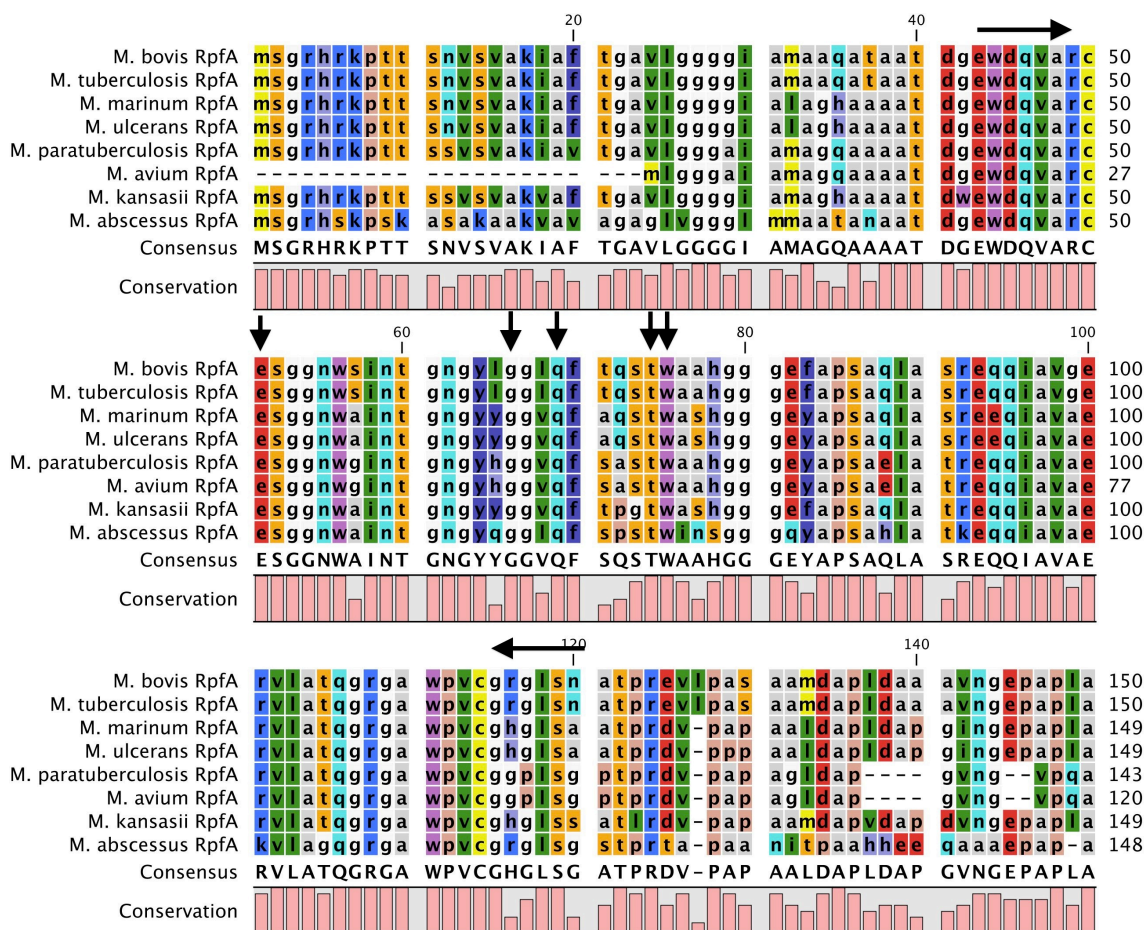
Figure 2: Partial pairwise alignment of the annotated and hypothetical mycobacterial RpfA sequences. All sequences were identified using the NCBI website. Alignment was created using CLC Free Workbench. Horizontal arrows indicate the flanking cysteine residues near to the beginning and end of the approximately 70-residue core Rpf sequence. Vertical arrows indicate the invariant glutamate, the glycine-X-X-glutamine turn motif, and the NAG-binding threonine and tryptophan residues that all members of the Rpf family share. This alignment shows the similarities that all annotated and hypothetical RpfA proteins share.
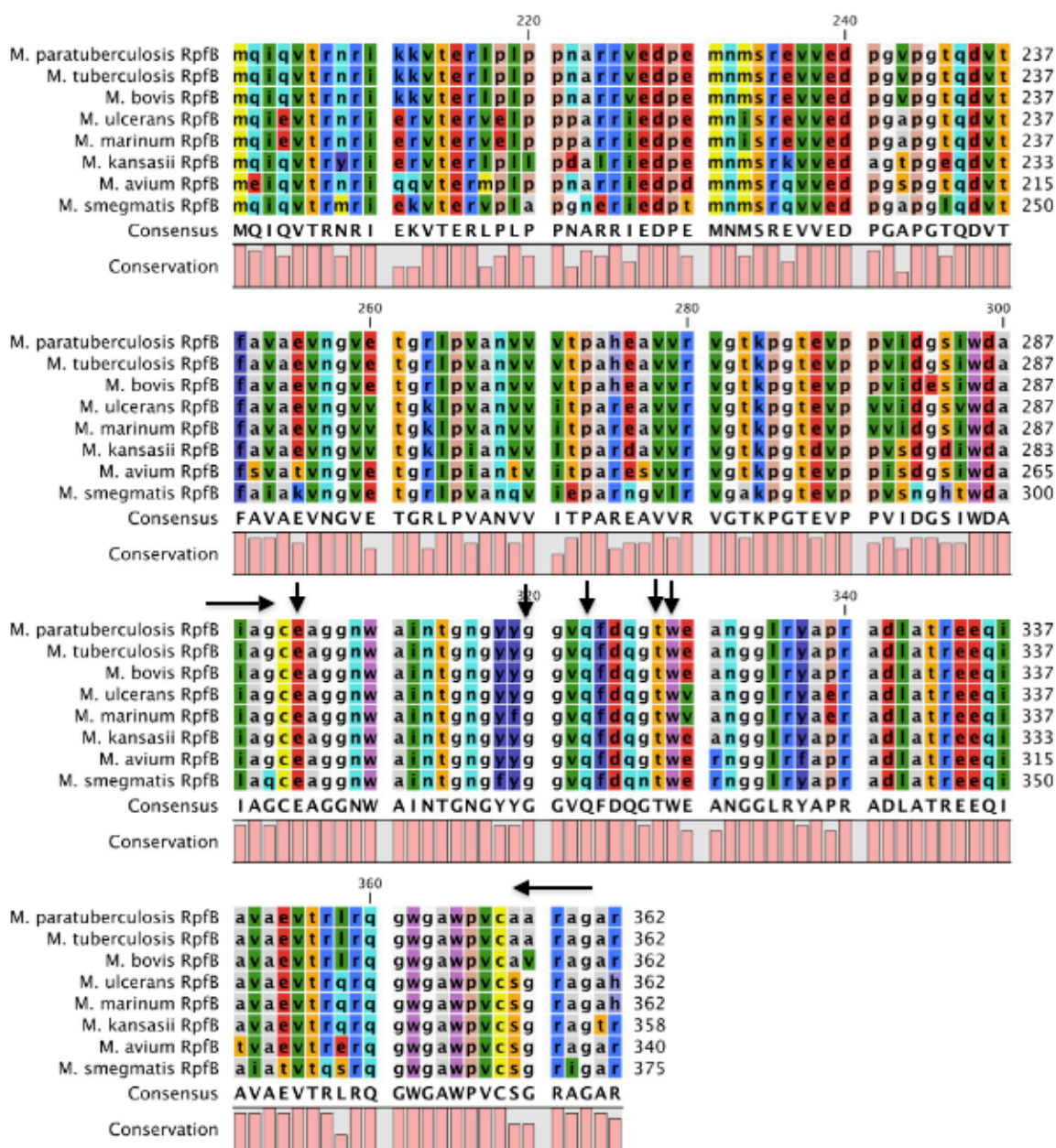
Figure 3: Partial pairwise alignment of the annotated and hypothetical mycobacterial RpfB sequences. All sequences were identified using the NCBI website. Alignment was created using CLC Free Workbench. Horizontal arrows indicate the flanking cysteine residues near to the beginning and end of the approximately 70-residue core Rpf sequence. Vertical arrows indicate the invariant glutamate, the glycine-X-X-glutamine turn motif, and the NAG-binding threonine and tryptophan residues that all members of the Rpf family share. This alignment shows the similarities that all annotated and hypothetical RpfB proteins share.
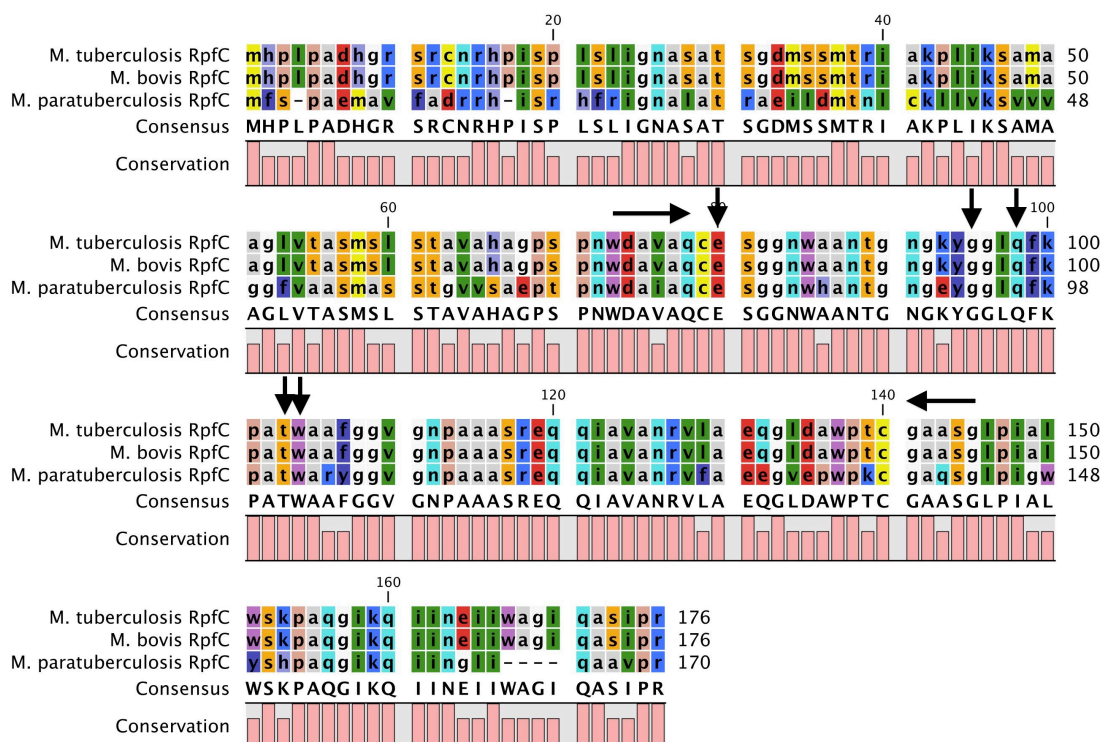
Figure 4: Pairwise alignment of the annotated and hypothetical mycobacterial RpfC sequences. All sequences were identified using the NCBI website. Alignment was created using CLC Free Workbench. Horizontal arrows indicate the flanking cysteine residues near to the beginning and end of the approximately 70-residue core Rpf sequence. Vertical arrows indicate the invariant glutamate, the glycine-X-X-glutamine turn motif, and the NAG-binding threonine and tryptophan residues that all members of the Rpf family share. This alignment shows the similarities that all annotated and hypothetical RpfC proteins share.

Figure 5: Pairwise alignment of the annotated and hypothetical mycobacterial RpfE sequences. All sequences were identified using the NCBI website. Alignment was created using CLC Free Workbench. Horizontal arrows indicate the flanking cysteine residues near to the beginning and end of the approximately 70-residue core Rpf sequence. Vertical arrows indicate the invariant glutamate, the glycine-X-X-glutamine turn motif, and the NAG-binding threonine and tryptophan residues that all members of the Rpf family share. This alignment shows the similarities that all annotated and hypothetical RpfE proteins share.

Figure 6: pSC-A. Plasmid vector pSC-A was used as a parent vector for the propagation of *rpf* sequences that were amplified directly from the genome of Mpt using PCR. Amplified *rpf* sequences were TA cloned into the *lacZ* gene coding for α-fragment of β-galactosidase.

Figure 7: pMTS088, a pMV261 derived construct. The pMTS088 vector was constructed by Secott and Johnson during a previous study. The vector was designed to express histidine-fused mycobacterial proteins in a mycobacterial host. The *hsp60* promoter and the hexahistidine tag in pMTS088 flank the *mce* sequence, which encodes a mycobacterial cell entry protein. Before the *mce* sequence was cloned into pMV261 it was shuttled through pBluescriptII SK+, pET28b+, and pSC-A. The 3′ tail of the *mce* sequence carried with it a portion of the MCS from pBluescriptII SK+, and a portion of the MCS from pET28b+ containing the C-terminal hexahistidine tag. Digesting the pMTS088 vector with the restriction nucleases that are shown opened the vector for *rpf* cloning.

A: *rpfA* 5′ Link in pMTS104
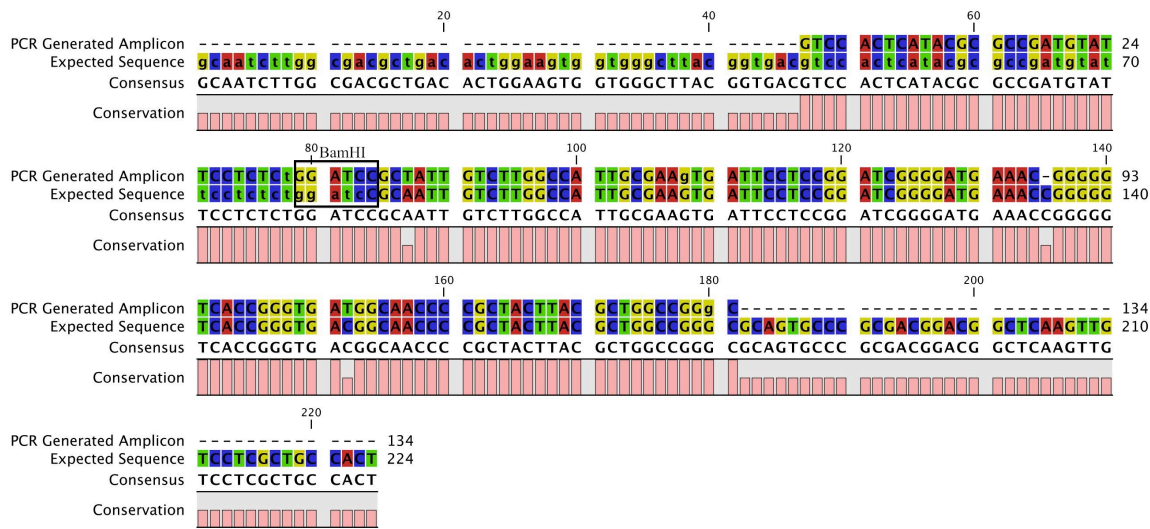
B: *rpfA* 3′ Link in pMTS104
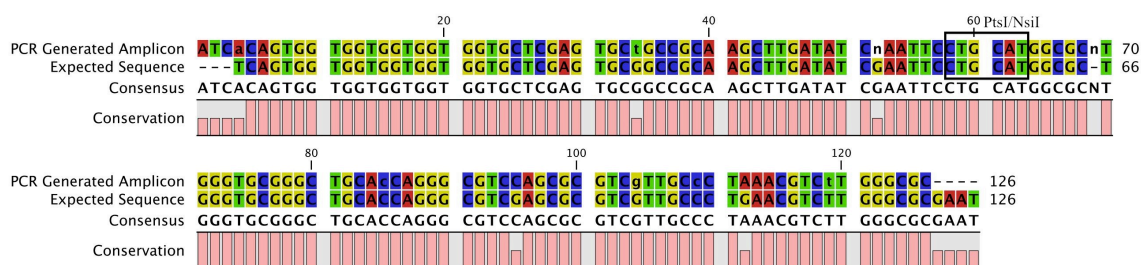
Figure 8: DNA sequencing results confirming the insertion of *rpfA* into the former pMTS088 construct. The 5′ PCR amplicon (A) was amplified from pMTS104 using primers 088 HspF Link ID and 1D HspR Link ID. The 3′ PCR amplicon (B) was amplified from pMTS104 using primers 109F1 and MsMceHisR. DNA sequencing was performed in Dr. Robert Sorensen's lab at Minnesota State University – Mankato, MN. The pairwise alignments was produced using CLC Free Workbench to show that the 5′ *Bam*HI and 3′ *Nsi*I/*Pst*I ligations occurred, and the sequences up and downstream of the linkages matched those of the expected pMTS104 sequence. The boxes note the location of the restriction sites. Nucleotides to the left of the boxes are part of the pMTS088 sequence. Nucleotides to the right of the boxes are part of the *rpfA* sequence.

A: *rpfE* 5′ Link in pMTS105
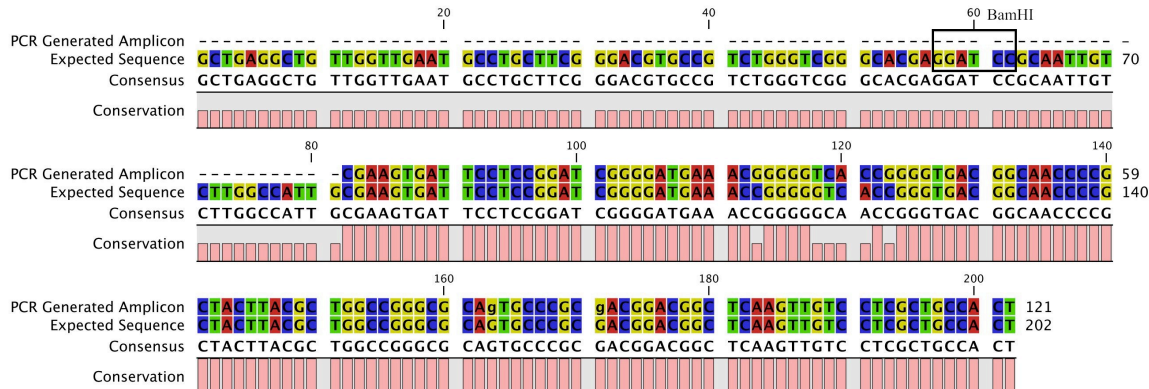
B: *rpfE* 3′ Link in pMTS105
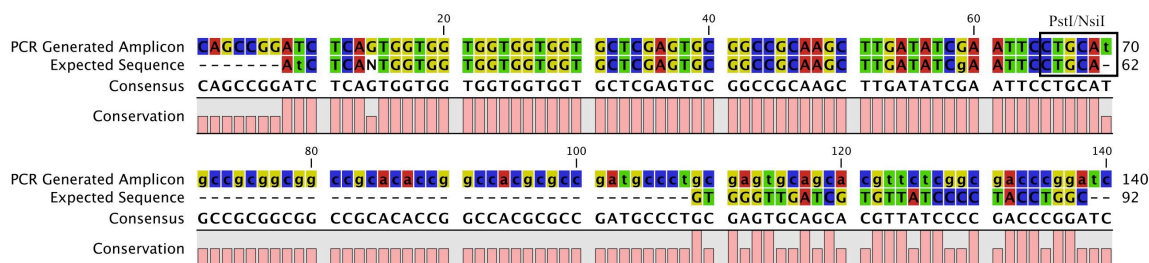
Figure 9: DNA sequencing results confirming the insertion of *rpfE* into the former pMTS088 construct did not occur. The 5′ PCR amplicon (A) was amplified from pMTS104 using primers 088 HspF Link ID and E HspR Link ID. The 3′ PCR amplicon (B) was amplified from pMTS105 using primers 109F1 and MsMceHisR. DNA sequencing was performed in Dr. Robert Sorensen's lab at Minnesota State University – Mankato, MN. The pairwise alignment was produced using CLC Free Workbench to show that the 5′ *Bam*HI and 3′ *Nsi*I/*Pst*I ligations occurred, and the sequences up and downstream of the linkages matched those of the expected pMTS105 sequence. The boxes note the location of the restriction sites. Nucleotides to the left of the boxes are part of the pMTS088 sequence. Nucleotides to the right of the boxes are part of the *rpfA* sequence. Although the sequencing reaction missed the targeted *Bam*HI site in the 5′ link, the sequence of the *rpfE* PCR amplicon shares homology with the expected sequence. The *rpfE* 3′ link does not share homology with the expected sequence. Further investigation showed that the 3′ link shared homology with the *mce* sequence that was expectedly removed from pMTS088.

A: *rpfB* 5′ Link in pMTS112

B: *rpfB* 3′ Link in pMTS112

Figure 10: DNA sequencing results confirming the insertion of *rpfB* into the former pMTS088 construct. The 5′ PCR amplicon (A) was amplified from pMTS112 using primers 088 HspF Link ID and 1D HspR Link ID. The 3′ PCR amplicon (B) was amplified from pMTS112 using primers 109F1 and MsMceHisR. DNA sequencing was performed in Dr. Robert Sorensen's lab at Minnesota State University – Mankato, MN. The pairwise alignment was produced using CLC Free Workbench to show that the 5′ *Nco*I and 3′ *Nsi*I/*Pst*I ligations occurred, and the sequences up and downstream of the linkages matched those of the expected pMTS112 sequence. The boxes note the location of the restriction sites. Nucleotides to the left of the boxes are part of the pMTS088 sequence. Nucleotides to the right of the boxes are part of the *rpfB* sequence.

A: *rpfC* 5′ Link in pMTS113

B: *rpfC* 3′ Link in pMTS113
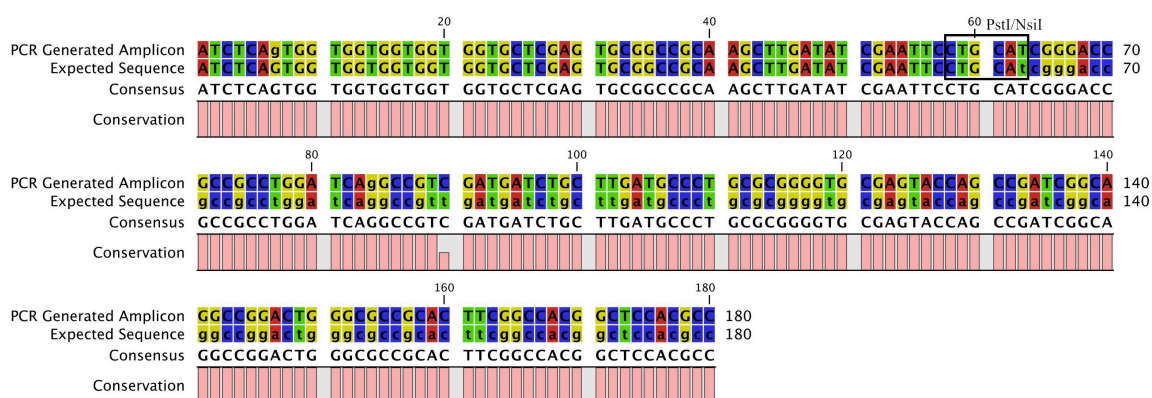
Figure 11: DNA sequencing results confirming the insertion of *rpfC* into the former pMTS088 construct. The 5′ PCR amplicon (A) was amplified from pMTS113 using primers 088 HspF Link ID and 1D HspR Link ID. The 3′ PCR amplicon (B) was amplified from pMTS113 using primers 109F1 and MsMceHisR. DNA sequencing was performed in Dr. Robert Sorensen's lab at Minnesota State University – Mankato, MN. The pairwise alignment was produced using CLC Free Workbench to show that the 5′ *Bam*HI and 3′ *Nsi*I/*Pst*I ligations occurred, and the sequences up and downstream of the linkages matched those of the expected pMTS113 sequence. The boxes note the location of the restriction sites. Nucleotides to the left of the boxes are part of the pMTS088 sequence. Nucleotides to the right of the boxes are part of the *rpfC* sequence.
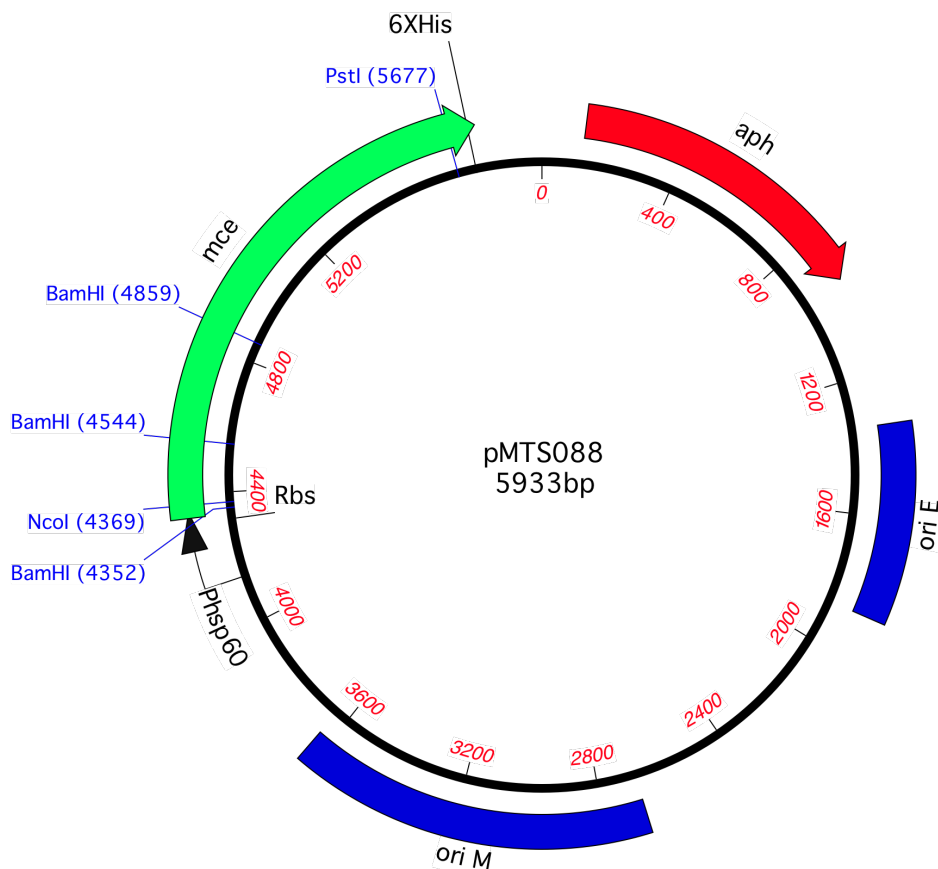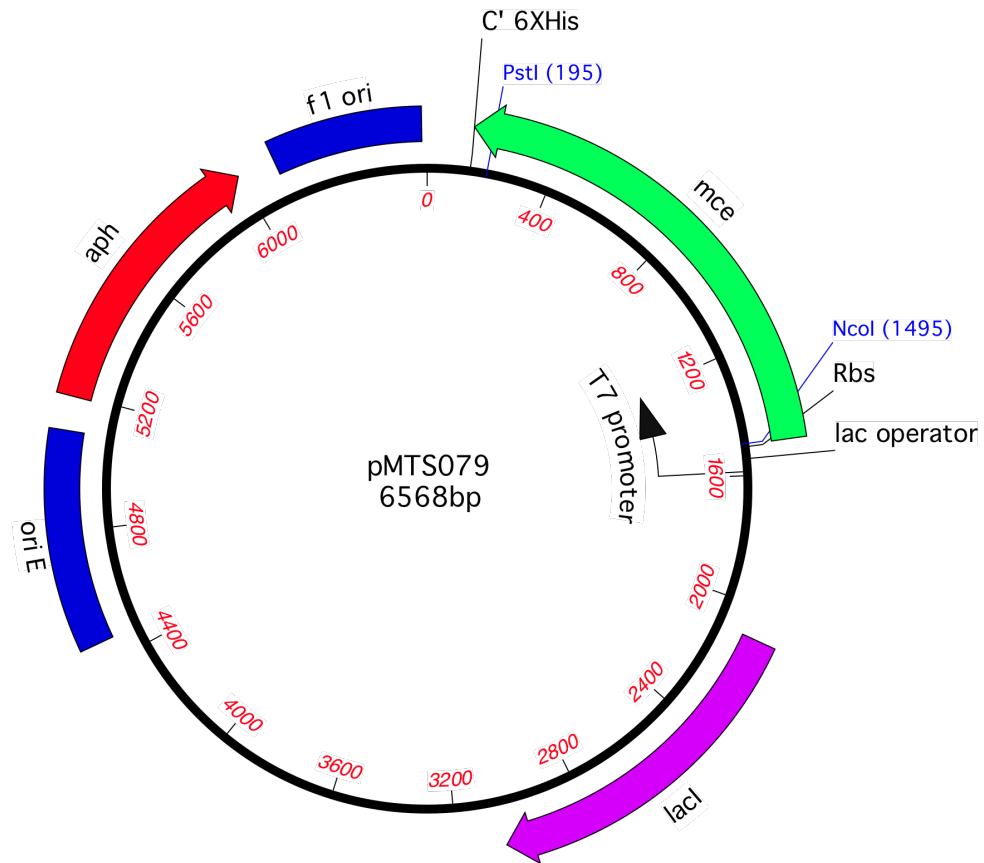
Figure 12: pMTS079, a pET28b+ derived construct. The pMTS079 vector was constructed by Secott and Johnson during a previous study. The *mce* sequence encodes a mycobacterial cell entry protein. The *Nco*I restriction site in pET28b+ and the *Pst*I restriction site in the *mce* sequence provided the means to cloning *rpfB* inframe with the T7 *lac* promoter and C-terminal 6XHis of pET28b+.
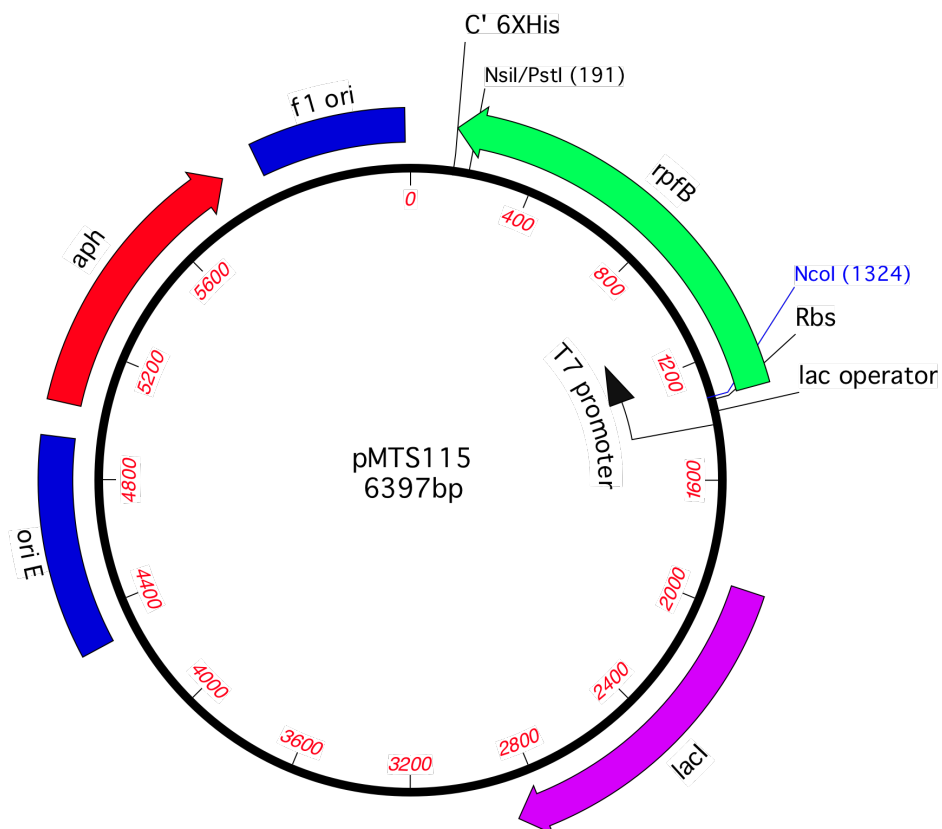
Figure 13: pMTS115, a pET28b+ derived construct. The pMTS115 vector was constructed for the expression of *rpfB* in an *E. coli* system. The *rpfB* sequence was first removed from the pMTS109 vector using the restriction endonucleases *Nco*I and *Nsi*I. The *mce* sequence was removed from pMTS079 using the restriction endonucleases *Nco*I, and the *Nsi*I isoschizomer, *Pst*I. The pMTS115 vector was then constructed by ligating *rpfB* into pMTS079 at the *Nco*I and *Nsi*I/*Pst*I cohesive ends. This placed *rpfB* inframe with the T7 *lac* promoter and 6XHis tag of pET28b+.
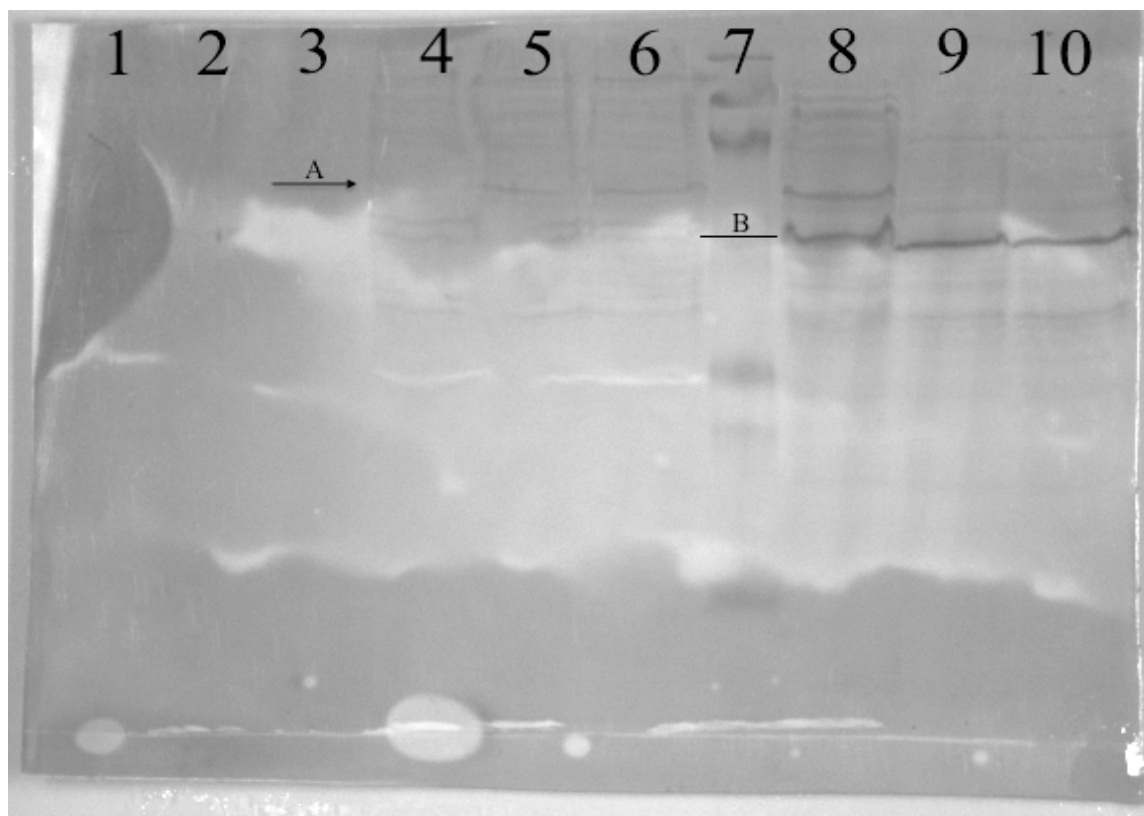
Figure 14: Western blot of *mce* and *rpfB* expression trials in *M. smegmatis* mc^{2}155. *M. smegmatis* mc^{2}155 cultures containing either pMV261, pMTS088, or pMTS112 were grown for 96 hours at 37ºC. Cultures were processed according to the methods protocol for the purification of hexahistidine-fused proteins. Lanes 1-10 are described from left to right: lanes 1-3, concentrated culture supernates of pMV261, pMTS088, and pMTS112, respectively; lanes 4-6, Soluble fractions of pMV261, pMTS088, and pMTS112 cell lysates, respectively; lane 7, MW marker; lanes 8-10, Insoluble fractions of pMV261, pMTS088, and pMTS112 cell lysates, respectively. Bands of interest are those that are present in RpfB and Mce preparations, and absent in pMV261 preparations. This is seen at one location, indicated by the horizontal arrow (A). However, previous research has shown that recombinant Mce expressed from *M. smegmatis* mc^{2}155 migrates at a rate equal to proteins that have a molecular weight of 50 kDa (B). The location of the indicated band is >50 kDa. Along with this, RpfB is expected to migrate faster than Mce due its molecular weight of 42 kDa when expressed from pMTS112. This shows that there is no expression of *mce* or *rpfB* from *M. smegmatis* mc^{2}155.
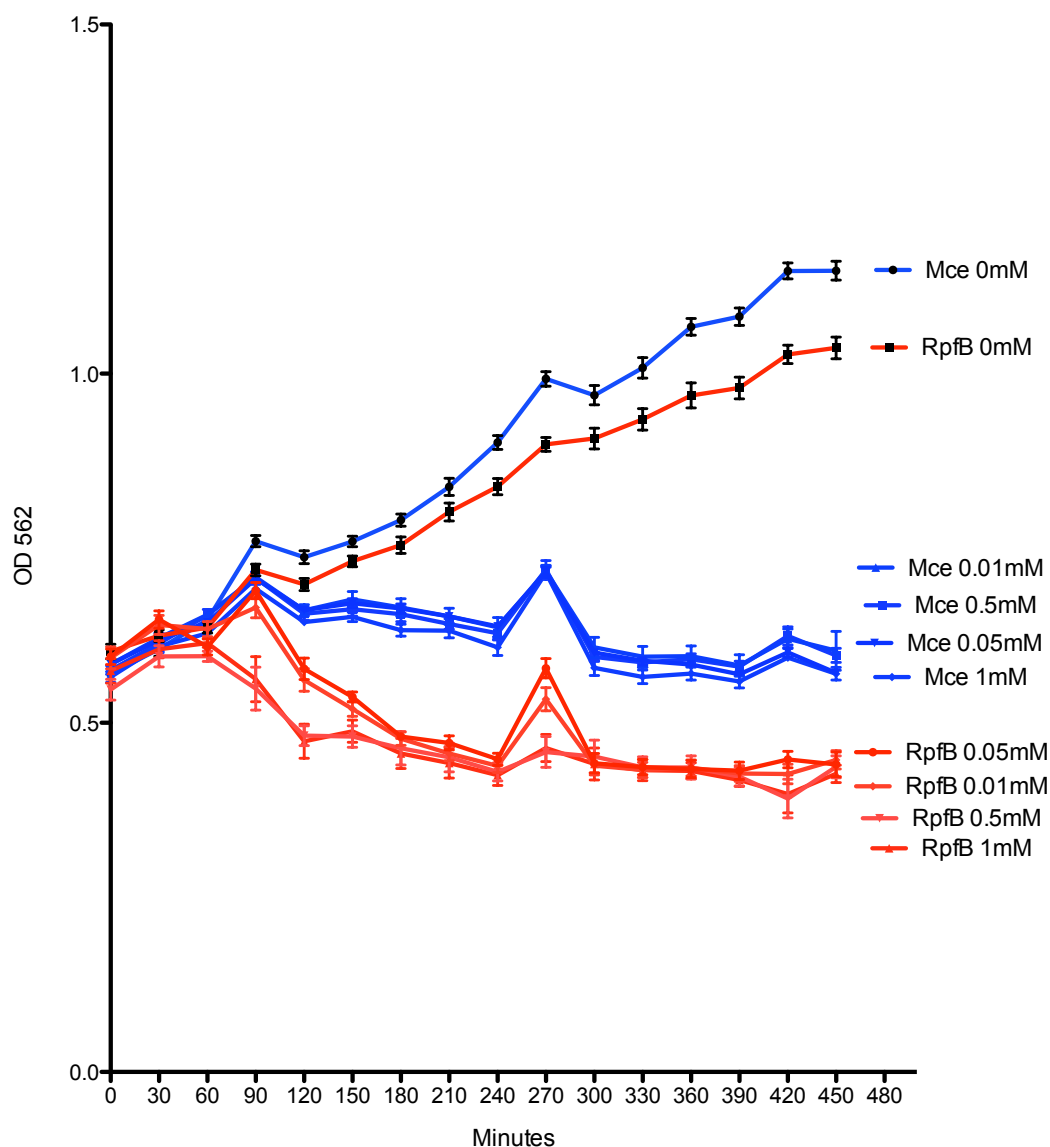
Figure 15: Growth curves of *E. coli* BL21(DE3) after induction with 5 different IPTG concentrations. Blue lines represent cultures expressing *mce* from pMTS079, and red lines represent cultures expressing *rpfB* from pMTS115. The legends are listed in order from highest absorbance to lowest absorbance at 7.5 hours. Cultures were induced with IPTG at OD_{590} 0.6. Cell division stopped after 90 minutes in all concentrations of IPTG for cultures expressing *mce*. After this time the absorbance decreased slowly until an optical density of approximately 0.58. Cell division stopped at 90 minutes in cultures expressing *rpfB* at IPTG concentrations of 0.05 mM and 0.1 mM. From this point there was a rapid decline in absorbance until it reached an optical density of approximately 0.44. Cell division stopped at 60 minutes in cultures expressing *rpfB* at IPTG concentrations of 0.5 mM and 1 mM. From this point there was a dramatic decline in absorbance until it reached an optical density of approximately 0.44. This indicates there is lytic activity of RpfB on expressing cells.

Panel A
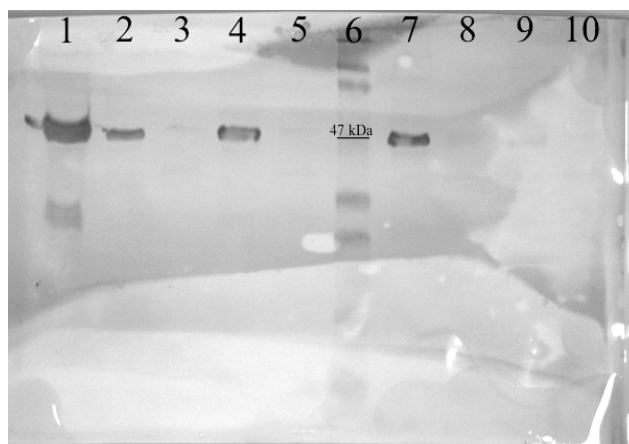
Panel B
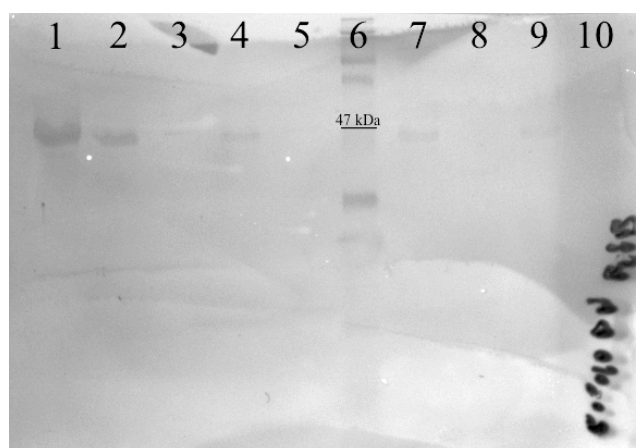
Figure 16: Comparative expression of *mce* (Panel A) and *rpfB* (Panel B) from *E. coli* BL21(DE3) using 1 mM IPTG for 1 hour at 37ºC vs. induction with 0.05 mM IPTG over 4 hours at 37ºC. Cultures were induced with IPTG between OD_{590} 0.6-0.8. Ten milliliters of the culture induced with 1 mM IPTG was and processed at 1 hour post induction. Ten milliliters of the culture induced with 0.05 mM IPTG was drawn and processed each hour over 4 hours. Fifteen microliters of the soluble lysate, and urea-solubilized lysate was then sent through a western blot using an anti-6XHis antibody at a 1:1000 dilution. Lane 1 is the urea-solubilized fraction of the culture induced with 1 mM IPTG at 1 hour post induction. Lanes 2, 4, 7, 9 are urea-solubilized cell lysates at 1, 2, 3, and 4 hour intervals, respectively. Lanes 3, 5, 8, 10 are soluble fractions of the cell lysates at 1, 2, 3, and 4 hour intervals, respectively. Lane 6 is the MW Marker. This shows that the recombinant proteins separate with the insoluble fraction, and the largest quantities of recombinant protein are produced when cells are grown at 37ºC, induced with 1 mM IPTG, and harvested after 1 hour of expression.

Panel A   **Panel B**
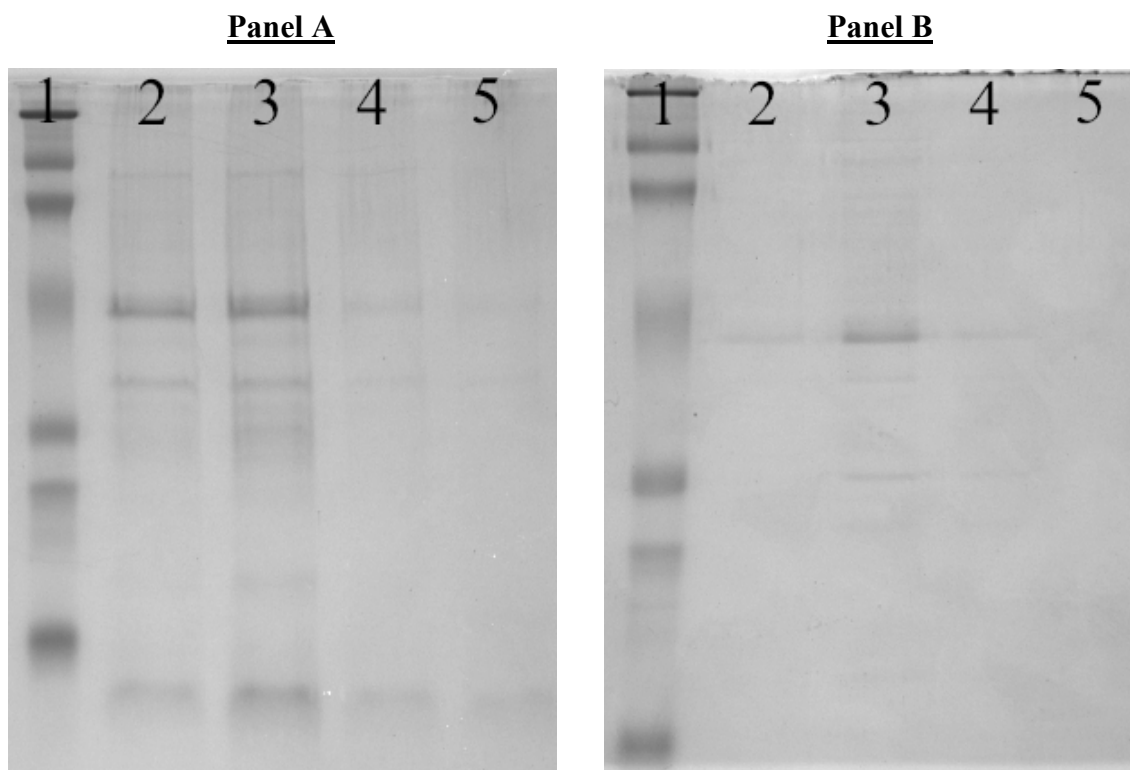
Figure 17: Increasing the concentration of imidazole in the Ni-NTA wash buffer decreases the amount contaminating proteins in the Ni-NTA eluates. Expression of *rpfB* after 1 hour induction with 1 mM IPTG. Inclusion bodies were solubilized with 8 M urea and sent through Ni-NTA resin. Ten-millimolar imidazole was used in the binding buffer, 20 mM imidazole (Panel A) or 50 mM imidazole (Panel B) was used in the wash buffer, and 250 mM imidazole was used in the elution buffer. Four 500 μl volumes of elution buffer were applied to the resin, collected, and 15 μl of each eluate was sent through a 10% acrylamide gel (lanes 2-5). Lane 1 is the MW Marker. This shows that when compared to a 50 mM imidazole wash (Panel B), RpfB elutes with more contaminating bands

Panel A   **Panel B**
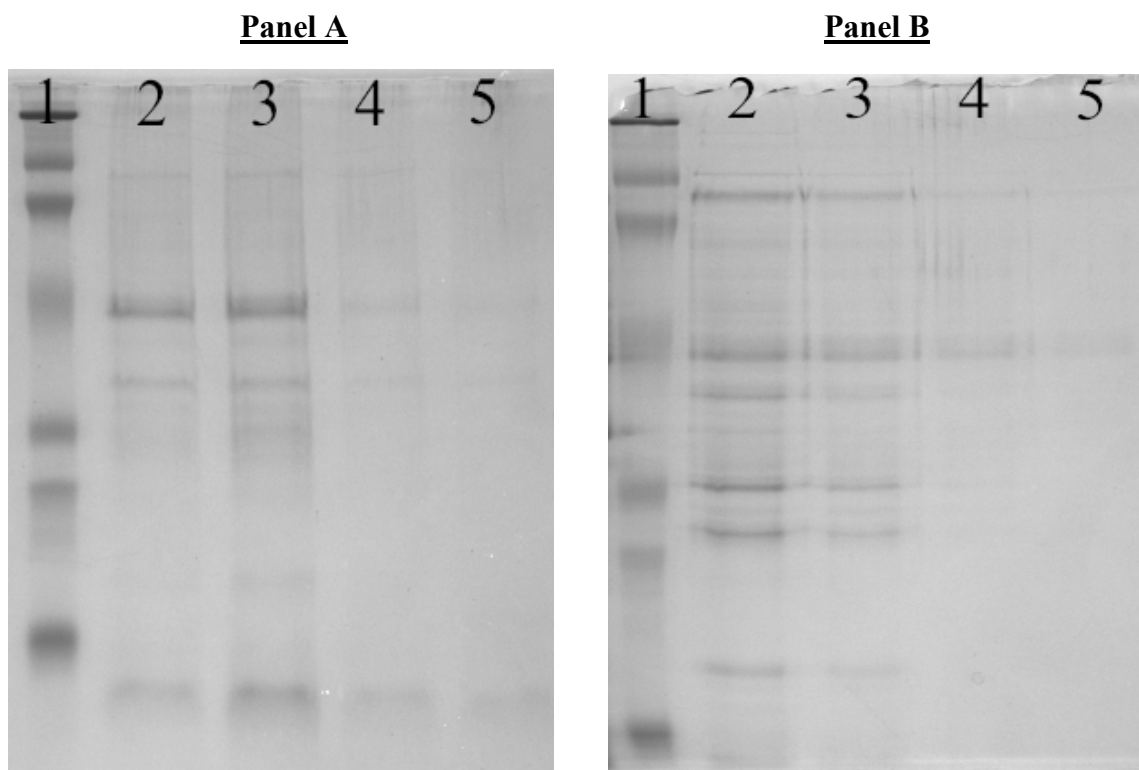
Figure 18: Increasing the concentration of imidazole in the Ni-NTA elution buffer increases the amount contaminating proteins in the Ni-NTA eluates. Expression of *rpfB* after 1 hour induction with 1 mM IPTG. Inclusion bodies were solubilized with 8 M urea and sent through Ni-NTA resin. Ten-millimolar imidazole was used in the binding buffer, 20 mM imidazole was used in the wash buffer, and 250 mM imidazole (Panel A) or 500 mM imidazole (Panel B) was used in the elution buffer. Four 500 μl volumes of elution buffer were applied to the resin, collected, and 15 μl of each eluate was sent through a 10% acrylamide gel (lanes 2-5). Lane 1 is the MW Marker. This shows that when compared to a 500 mM imidazole elution (Panel B), RpfB elutes with fewer contaminating bands.
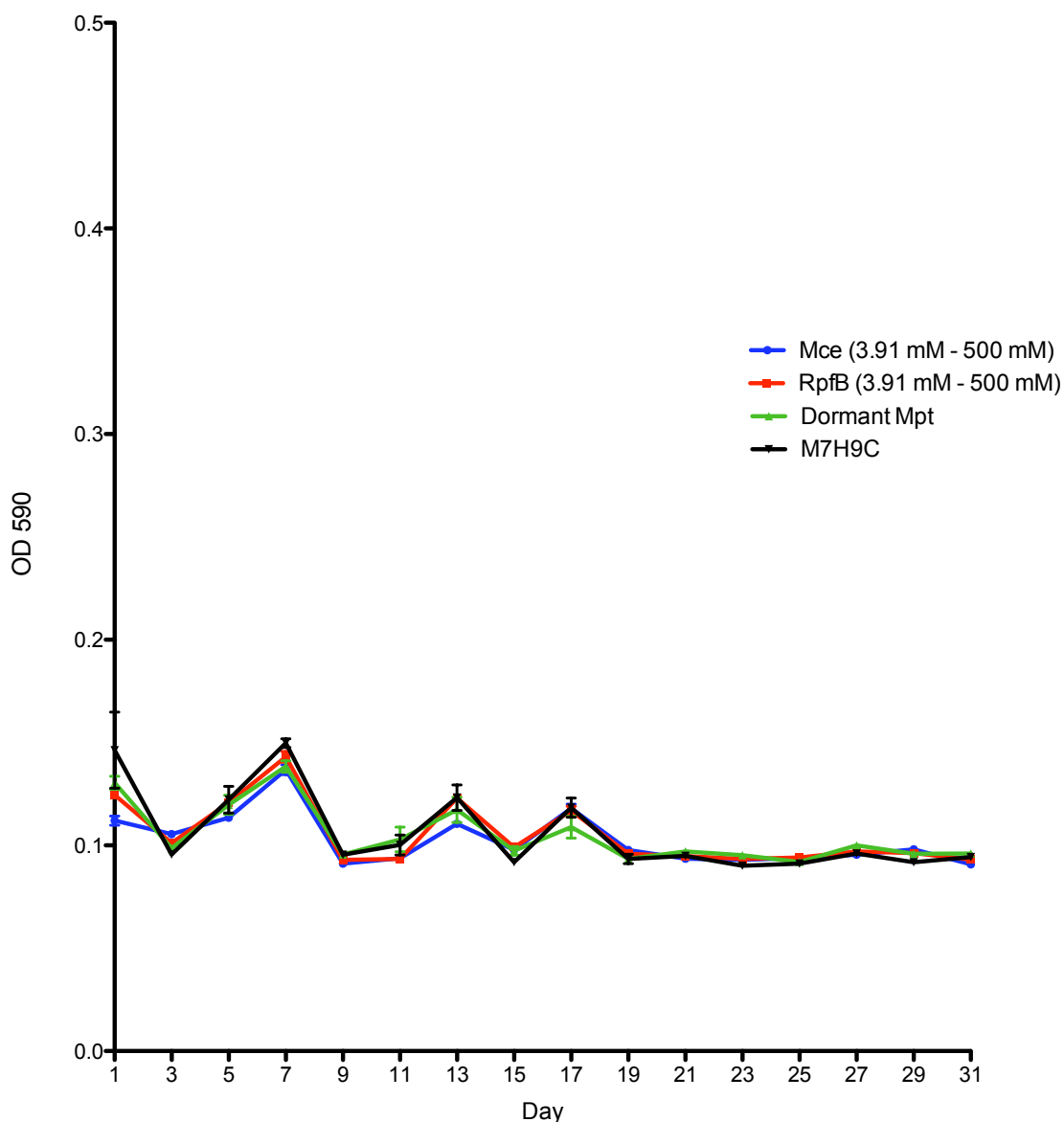
Figure 19: Growth curves of Mpt in M7H9C with and without the addition of recombinant Mce and RpfB. The 96-well plate used in this assay contained 5 replicate trials that tested doubling dilutions of recombinant Mce and RpfB from 500 mM to 3.91 mM on dormant Mpt in M7H9C, 8 replicate tests on dormant Mpt in M7H9C , and 8 replicate tests on M7H9C. Optical densities were measured over 31 days. Since there was no difference between any of the trials testing varying recombinant protein concentrations, all 40 wells containing Mce (5 replicates of 8 different protein concentrations) were treated as 40 replicates to produce 1 line. The same was done for RpfB-containing wells. This figure shows that Recombinant RpfB has no effect on the recovery of dormant Mpt.

Discussion

Our purpose in this study was to test the ability of recombinant Mpt RpfA-E to promote the growth of dormant Mpt. Our bioinformatic analysis revealed four *rpf* ORFs in the genome of Mpt, consistent with the accession numbers published by Kana *et al.* (47). DNA sequencing revealed that the Mpt *rpfA, rpfB,* and *rpfC* sequences were successfully cloned into the pMV261 derived vector. Our attempts at producing recombinant Mce, RpfA, RpfB, and RpfC from a modified pMV261 vector in *M. smegmatis* mc^{2}155 were unsuccessful. Reasons for this are unclear when considering that previous attempts at expressing *mce* from the pMV261-derived construct were successful. Investigations are currently in process to determine a consistent and repeatable means of expressing recombinant proteins from these pMV261 derived constructs. Once this is accomplished, there is a greater likelihood of recovering a functional Rpf product, which can be tested to resuscitate dormant Mpt.

We examined the ability of *E. coli* BL21(DE3) to express two mycobacterial proteins (Mce and RpfB) from pET28b+ derived vectors. We also examined the potential functionality of the recombinant Mce and RpfB proteins on cultures of dormant Mpt. Our results determined that the optimal conditions for the expression of these proteins in *E. coli*, in terms of greatest cellular-retained quantity, occur when the cultures are induced at OD$_{590}$ 0.6-0.8 with 1 mM IPTG, incubated at 37ºC, and harvested at 1 hr post induction. These conditions, however, resulted in the aggregation of fusion proteins as inclusion bodies. These inclusion bodies had to be solubilized with chemical denaturants

in order to isolate the fusion proteins from the rest of the cell lysate. In doing so, fusion proteins are linearized, and the potential functionality may have been compromised. Some proteins are known to spontaneously refold after their removal from denaturing conditions (i.e. RNase and prion proteins). In considering the possibility of that some spontaneous reformation occurred, total protein concentrations from desalted Ni-NTA eluates were tested against dormant Mpt at concentrations up to 640 times greater than optimal RpfB concentrations required for the resuscitation of related species. For the resuscitation of related species, the optimal concentration of RpfB is approximately ~13 pM (64).

When testing the bioactivity of recombinant proteins, it is preferable to optimize the expression conditions so that the protein can be isolated from a soluble fraction. When *E. coli* is being used for the expression of a foreign gene, uncertainties in the quality and/or quantity of an expression product can result from (i) questionable folding of unique protein structures, (ii) tRNA availability and rare codon demand, (iii) mRNA folding and stability, (iv) translational efficiency, (v) protease activity in *E. coli*, (vi) potential lethality of the recombinant expression product (54), (vii) a Met, His, or Glu residue being called for at the +2 location of the mRNA transcript (5), (viii) and negative repeating nucleic acid elements. These variables, as well as the rate of recombinant protein expression and recognizable signal cleavage sites can play a role in the production and solubility of recombinant proteins. A number of commercially available *E. coli* strains have been developed to overcome some of these obstacles, and a number of molecular techniques can be used to alter the rare codon demand of foreign sequences.

The following characteristics of the *mce* and *rpfB* sequences used in this experiment may make them less suitable for expression in *E. coli*: (i) use of the rare *E. coli* codons AGG, AGA, CGA, CGG (all of which code for arginine), and CCC (coding for proline) (11), (ii) codon adaption indices (CAI) of 0.72 and 0.74, respectively, (iii) rare codon frequency distributions (CFD) of 8% and 6%, respectively, (iv) and nucleic acid sequences containing 18 and 26 negative repeating elements (NRE), respectively (CAI, CFD, and NRE values were calculated using the algorithm from www.genscript.com/cgi-bin/tools/rare_codon_analysis). *E. coli* BL21(DE3) was able to overcome these obstacles; however, we were unable to obtain a soluble product. It is worth noting that, although a pause in translation due to the lack of appropriate tRNA can cause premature termination, significant reductions in total soluble protein concentrations have been observed in systems where codon bias was adjusted (75).

Previous studies that attempted the expression of Rpf proteins in *E. coli* have produced mixed results. The Zhu *et al.* study was successful in developing a functional Rpf protein in *E. coli* (117). Tufariello and colleagues were unsuccessful in inducing a resuscitative response in dormant *M. tuberculosis* cultures using recombinant Rpf proteins expressed from *E. coli* (98). Mukamolova and colleagues had difficulty expressing a soluble and functional *M. luteus rpf* from pET19b using *E. coli* (62). They were successful in using *E. coli* to produce a recombinant *M. luteus* Rpf from the pBAD/gIIIb vector (62). However they were unable to test the activity of the recombinant *M. luteus* Rpf due the high level of endogenous Rpf activity in expressing cells, which resulted in cell lysis during expression (62). In this study, expression of *rpfB* in *E. coli* from the pET28b+ vector was complicated by the incorporation of recombinant

RpfB into inclusion bodies and aggregation during cell lysis. However, this study does suggest (i) the Mpt putative *rpfB* ORF codes for a functional Rpf, (ii) the Mpt *rpfB* was successfully cloned into the pET28b+ derivative, and (iii) *E. coli* BL21(DE3) were able to fold the protein properly. The fact that inclusion bodies were our source of Rpf purification suggests additional possibilities: (i) there are two forms of RpfB being produced – one of which is functional, and one of which is aggregated; (ii) during expression of *rpfB,* the initial recombinant products produced are secreted through the periplasm, and as the endogenous level rises with continued expression, their accumulation results in aggregation. This could explain why lysis was seen in the expressing cells, yet inclusion bodies were still detected.

Although fusion proteins were obtained from *E. coli* expression of *mce* and *rpfB*, the purity and quantity of those proteins following Ni-chelate chromatography was less than desired, and replicate expression trials frequently led to differences in the purity and quantity of recombinant protein. Hexahistidine fused contaminants were not expected due to the fact that our cloning designs utilized restriction sites upstream of the N-terminal hexahistidine tag in pET28b+.

The following ideas are possible explanations for the differences seen in purity and quantity of recombinant proteins. (i) More recombinant protein is released from cells expressing *rpfB* compared to cells expressing *mce* due to a more complete lysis caused by high endogenous levels of active RpfB. (ii) The use of denaturants may expose histidine-dense regions in other *E. coli* proteins that may competitively bind to the nickel resin. (iii) Hydrophobic interactions occurring between the chromatography resin and contaminating proteins may affect the purity of the histidine tagged proteins. Results

may be improved if a different purification tag is used. Some tags, such as GST, promote

the solubility of recombinant proteins. Others, such as the affinity tags FLAG and HPC,

promote greater purity of recombinant proteins due to specific epitope interactions (54).

It is difficult to say with certainty that the differences seen from adjusting

parameters such as imidazole concentrations and pH of the chromatography buffers had a

direct affect on the purity and quantity of recovered proteins. This is due to the

comparisons being made between expression trials, and not within expression trials. The

differences may have resulted from inconsistencies in the total amount of recombinant

protein expressed from cell lines, or different amounts of cellular debris solubilized with

the inclusion bodies. The ratio of cells transcribing recombinant sequences vs. cells that

have adapted a resistance to IPTG may change over time, negatively affecting the

quantity of recombinant protein relative to the total protein expressed for normal cell

operations. It is presumed that less than 2% of the culture is unaffected by IPTG (67).

This percentage may vary from culture to culture, and may increase over time with

extended storage at -80ºC, culture passage, or freeze-thaw cycling.

Recombinant RpfB and Mce were tested against dormant Mpt, despite the issues

of absolute purity. The analysis of the SDS-PAGE gels using optical densitometry

helped in deciphering the quantity of hexahistidine-fused protein that was being applied

to dormant Mpt, relative to contaminating proteins. The concentrations of Mpt RpfB that

were tested against dormant Mpt varied in concentration from as high as 6.4 nM to as low

as 3.91 nM. Again, the exact concentration of recombinant protein added could not be

calculated due to the protein-contaminated preparations. None of these concentrations

induced a response from dormant Mpt cultures when dormant cultures were added at

concentrations of 1.0×10^4 CFU/well, or 1.0×10^6 CFU/well (calculated by 30%T at OD_{590}). Through the use of a viability assay using flow cytometry, the actual number of viable cells was likely 3.54×10^1 CFU/well and 3.54×10^3 CFU/well, respective the photometric calculations.

To my knowledge, this study is the second attempt at resuscitating dormant Mpt through the use of autologous Mpt Rpfs. The first attempt was done by Zhu and colleagues, who tested the potential functionality of the putative Mpt RpfA (117). The optimal concentration of Mpt RpfA observed to resuscitate dormant Mpt was 100 pM in the Zhu study. No other data exists on the optimal concentrations of Rpfs required to resuscitate dormant Mpt, and all other studies have used mycobacterial cultures that had been dormant for months, not years. Considering that optimal Rpf concentrations are typically consistent across genera, and even families, it is unlikely that optimal Rpf concentrations required for the resuscitation of dormant Mpt will differ. However, this will not be certain until optimal Rpf concentrations required for the resuscitation of dormant Mpt are determined.

Mycobacterial cells that have been dormant for years may differ structurally from cells that have been dormant for months. As previously stated, Mpt can enter a spheroplastic state during periods of extended dormancy. The high energy demand required to maintain the mycolates of the outer cell membrane will likely not be supported, and with time, the acid-fast cell wall will diminish. When this occurs, the optimal concentrations of Rpf proteins required to resuscitate dormant cells may be much lower than concentrations required to recover "younger" dormant cultures due to the accessibility of exposed mycobacterial peptidoglycan.

As cells age in dormancy and take on a true spheroplastic state, the peptidoglycan disappears. If Rpf proteins induce resuscitation by hydrolyzing glycosidic bonds of structurally modified cell walls, then no resuscitation would be seen from cells in a spheroplastic state. However, Rpf induced recovery from dormancy may be possible for cells in a spheroplastic state if recovery is dependant on the products of Rpf substrate cleavage rather than direct Rpf hydrolysis of the cell wall. Peptidoglycan fragments are activators of two-component regulatory systems, and the serine threonine protein kinase PknB is an essential growth mechanism in *M. tuberculosis* (33). This kinase has also been hypothesized to serve a role in resuscitation – particularly through the means of recognizing structurally modified peptidoglycan that has been cleaved by Rpf proteins (47). Since PknB is essential for growth, it is possible that PknB is maintained throughout dormancy.

Other protein-protein interactions may exist for the proper function of RpfB on dormant Mpt. RipA, for example, has been shown to co-localize with RpfB at the septum of dividing cells (39, 40). Studies have been done to examine the effects of numerous *rpf* deletions, and results from those studies have concluded that there is a hierarchy of importance in the retention of certain *rpf* sequences when considering the ability to induce resuscitation. However, no studies have shown the effects of adding combined Rpf proteins to dormant cultures. Keeping in mind that (i) peptidoglycan hydrolases are tightly regulated by the cell, (ii) *rpfs* are being found to be controlled by different transcriptional regulators, (iii) work with Rpf null mutants has shown diminished resuscitative capability with sequential deletions, (iv) expressions of all *rpfs* seem to overlap at some point during growth, and (v) redundancy among 4 conserved proteins

seems unlikely (especially considering that 3 homologues still exist in *M. leprae*), it may

be possible that the Rpf proteins associate to form a larger complex.

This study has produced many avenues for future research. Now that all of the

Mpt *rpf* ORFs are cloned into a mycobacterial expression vector, conditions to express

the sequences and effects of the recombinant products can be tested against dormant Mpt.

To make future study compare well with other Rpf studies, dormant Mpt should be tested

within months of entering dormancy. The choice of growth media should be better

investigated in future trials. Some studies show that Middlebrook 7H9 inhibits the

recovery from dormancy (117). This may be due to the increased metabolism resulting in

the production of an overwhelming amount of reactive-oxygen intermediates. If this is

the case, the addition of Rpf proteins in combination with oxygen reducing agents may

result in a greater number of cells recovering from dormancy.

Antibodies could be produced to the RpfB proteins that were produced in this

experiment. These antibodies could then be applied to cultures of Mpt to determine if,

and during what stages of growth RpfB is expressed in Mpt.

Much work is yet to be done on the study of Mpt dormancy and the effects of Rpf

proteins on dormant Mpt.   With continued investigation, it may be found that Rpf

proteins are the key to increasing the sensitivity of diagnostic culture, and lowering the

incidence of JD.

References

1.   **Altschul, S. F., W. Gish, W. Miller, E. W. Myers, and D. J. Lipman.** 1990. Basic local alignment search tool. J Mol Biol **215:**403-10.

2.   **Amon, J., F. Titgemeyer, and A. Burkovski.** 2009. A genomic view on nitrogen metabolism and nitrogen control in mycobacteria. J Mol Microbiol Biotechnol **17:**20-9.

3.   **Begg, D. J., and R. J. Whittington.** 2008. Experimental animal infection models for Johne's disease, an infectious enteropathy caused by *Mycobacterium avium* subsp. *paratuberculosis*. Vet J **176:**129-45.

4.   **Betts, J. C., P. T. Lukey, L. C. Robb, R. A. McAdam, and K. Duncan.** 2002. Evaluation of a nutrient starvation model of *Mycobacterium tuberculosis* persistence by gene and protein expression profiling. Mol Microbiol **43:**717-31.

5.   **Bivona, L., Z. Zou, N. Stutzman, and P. D. Sun.** Influence of the second amino acid on recombinant protein expression. Protein Expr Purif.

6.   **Bottjer, K. P., D. C. Hirst, and G. F. Slonka.** 1978. *Nematospiroides dubius* as a vector for *Salmonella typhimurium*. Am J Vet Res **39:**151-3.

7.   **Brooks, B. W., N. M. Young, D. C. Watson, R. H. Robertson, E. A. Sugden, K. H. Nielsen, and S. A. Becker.** 1991. *Mycobacterium paratuberculosis* antigen D: characterization and evidence that it is a bacterioferritin. J Clin Microbiol **29:**1652-8.

8.   **Bull, T. J., E. J. McMinn, K. Sidi-Boumedine, A. Skull, D. Durkin, P. Neild, G. Rhodes, R. Pickup, and J. Hermon-Taylor.** 2003. Detection and verification of *Mycobacterium avium* subsp. *paratuberculosis* in fresh ileocolonic mucosal biopsy specimens from individuals with and without Crohn's disease. J Clin Microbiol **41:**2915-23.

9.   **Chamberlin, W., T. Borody, and S. Naser.** 2007. MAP-associated Crohn's disease MAP, Koch's postulates, causality and Crohn's disease. Dig Liver Dis **39:**792-4.

10.   **Chang, Z., T. P. Primm, J. Jakana, I. H. Lee, I. Serysheva, W. Chiu, H. F. Gilbert, and F. A. Quiocho.** 1996. *Mycobacterium tuberculosis* 16-kDa antigen (Hsp16.3) functions as an oligomeric structure in vitro to suppress thermal aggregation. J Biol Chem **271:**7218-23.

11.   **Chen, D., and D. E. Texada.** 2006. Low-usage codons and rare codons of *Escherichia coli*. Gene Ther Mol Biol **10:**1-12.

12.   **Chiodini, R. J.** 1989. Crohn's disease and the mycobacterioses: a review and comparison of two disease entities. Clin Microbiol Rev **2:**90-117.

13. **Chiodini, R. J., and C. A. Rossiter.** 1996. Paratuberculosis: a potential zoonosis? Vet Clin North Am Food Anim Pract **12:**457-67.

14. **Chiodini, R. J., H. J. Van Kruiningen, and R. S. Merkal.** 1984. Ruminant paratuberculosis (Johne's disease): the current status and future prospects. Cornell Vet **74:**218-62.

15. **Chiodini, R. J., H. J. Van Kruiningen, W. R. Thayer, and J. A. Coutu.** 1986. Spheroplastic phase of mycobacteria isolated from patients with Crohn's disease. J Clin Microbiol **24:**357-63.

16. **Cirillo, J. D., S. Falkow, L. S. Tompkins, and L. E. Bermudez.** 1997. Interaction of *Mycobacterium avium* with environmental amoebae enhances virulence. Infect Immun **65:**3759-67.

17. **Clark, D. L., Jr., J. J. Koziczkowski, R. P. Radcliff, R. A. Carlson, and J. L. Ellingson.** 2008. Detection of *Mycobacterium avium* subspecies *paratuberculosis*: comparing fecal culture versus serum enzyme-linked immunosorbent assay and direct fecal polymerase chain reaction. J Dairy Sci **91:**2620-7.

18. **Clarke, C. J.** 1997. The pathology and pathogenesis of paratuberculosis in ruminants and other species. J Comp Pathol **116:**217-61.

19. **Cleveland, R. F., A. J. Wicken, L. Daneo-Moore, and G. D. Shockman.** 1976. Inhibition of wall autolysis in *Streptococcus faecalis* by lipoteichoic acid and lipids. J Bacteriol **126:**192-7.

20. **Cohen-Gonsaud, M., P. Barthe, C. Bagneris, B. Henderson, J. Ward, C. Roumestand, and N. H. Keep.** 2005. The structure of a resuscitation-promoting factor domain from *Mycobacterium tuberculosis* shows homology to lysozymes. Nat Struct Mol Biol **12:**270-3.

21. **Cohen-Gonsaud, M., N. H. Keep, A. P. Davies, J. Ward, B. Henderson, and G. Labesse.** 2004. Resuscitation-promoting factors possess a lysozyme-like domain. Trends Biochem Sci **29:**7-10.

22. **Cole, S. T., K. Eiglmeier, J. Parkhill, K. D. James, N. R. Thomson, P. R. Wheeler, N. Honore, T. Garnier, C. Churcher, D. Harris, K. Mungall, D. Basham, D. Brown, T. Chillingworth, R. Connor, R. M. Davies, K. Devlin, S. Duthoy, T. Feltwell, A. Fraser, N. Hamlin, S. Holroyd, T. Hornsby, K. Jagels, C. Lacroix, J. Maclean, S. Moule, L. Murphy, K. Oliver, M. A. Quail, M. A. Rajandream, K. M. Rutherford, S. Rutter, K. Seeger, S. Simon, M. Simmonds, J. Skelton, R. Squares, S. Squares, K. Stevens, K. Taylor, S. Whitehead, J. R. Woodward, and B. G. Barrell.** 2001. Massive gene decay in the leprosy bacillus. Nature **409:**1007-11.

23. **Collins, M. T.** 1996. Diagnosis of paratuberculosis. Vet Clin North Am Food Anim Pract **12:**357-71.

24. **Collins, M. T., S. J. Wells, K. R. Petrini, J. E. Collins, R. D. Schultz, and R. H. Whitlock.** 2005. Evaluation of five antibody detection tests for diagnosis of bovine paratuberculosis. Clin Diagn Lab Immunol **12:**685-92.

25. **Corper, H., and M. Cohn.** 1933. The viability and virulence of old cultures of tubercle bacilli: studies on twelve-year broth cultures maintained at incubator temperature. Am Rev Tuberc **28:**856–874.

26. **Coussens, P. M.** 2004. Model for immune responses to *Mycobacterium avium* subspecies *paratuberculosis* in cattle. Infect Immun **72:**3089-96.

27. **Coussens, P. M., N. Verman, M. A. Coussens, M. D. Elftman, and A. M. McNulty.** 2004. Cytokine gene expression in peripheral blood mononuclear cells and tissues of cattle infected with *Mycobacterium avium* subsp. *paratuberculosis*: evidence for an inherent proinflammatory gene expression pattern. Infect Immun **72:**1409-22.

28. **Downing, K. J., J. C. Betts, D. I. Young, R. A. McAdam, F. Kelly, M. Young, and V. Mizrahi.** 2004. Global expression profiling of strains harbouring null mutations reveals that the five rpf-like genes of *Mycobacterium tuberculosis* show functional redundancy. Tuberculosis (Edinb) **84:**167-79.

29. **Downing, K. J., V. V. Mischenko, M. O. Shleeva, D. I. Young, M. Young, A. S. Kaprelyants, A. S. Apt, and V. Mizrahi.** 2005. Mutants of *Mycobacterium tuberculosis* lacking three of the five rpf-like genes are defective for growth in vivo and for resuscitation in vitro. Infect Immun **73:**3038-43.

30. **Dziarski, R.** 2003. Recognition of bacterial peptidoglycan by the innate immune system. Cell Mol Life Sci **60:**1793-804.

31. **Edwards, D. I.** 1979. Mechanism of antimicrobial action of metronidazole. J Antimicrob Chemother **5:**499-502.

32. **Featherstone, C.** 1997. M cells: portals to the mucosal immune system. Lancet **350:**1230.

33. **Fernandez, P., B. Saint-Joanis, N. Barilone, M. Jackson, B. Gicquel, S. T. Cole, and P. M. Alzari.** 2006. The Ser/Thr protein kinase PknB is essential for sustaining mycobacterial growth. J Bacteriol **188:**7778-84.

34. **Fischer, O. A., L. Matlova, L. Dvorska, P. Svastova, J. Bartl, R. T. Weston, and I. Pavlik.** 2004. Blowflies Calliphora vicina and Lucilia sericata as passive vectors of *Mycobacterium avium* subsp. *avium*, *M. a. paratuberculosis* and *M. a. hominissuis.* Med Vet Entomol **18:**116-22.

35. **Girardin, S. E., I. G. Boneca, L. A. Carneiro, A. Antignac, M. Jehanno, J. Viala, K. Tedin, M. K. Taha, A. Labigne, U. Zahringer, A. J. Coyle, P. S. DiStefano, J. Bertin, P. J. Sansonetti, and D. J. Philpott.** 2003. Nod1 detects a unique muropeptide from gram-negative bacterial peptidoglycan. Science **300:**1584-7.

36. **Greenstein, R. J.** 2003. Is Crohn's disease caused by a mycobacterium? Comparisons with leprosy, tuberculosis, and Johne's disease. Lancet Infect Dis **3:**507-14.

37. **Hanekom, W. A., S. D. Lawn, K. Dheda, and A. Whitelaw.** Tuberculosis research update. Trop Med Int Health **15:**981-9.

38. **Harris, N. B., and R. G. Barletta.** 2001. *Mycobacterium avium* subsp. *paratuberculosis* in Veterinary Medicine. Clin Microbiol Rev **14:**489-512.

39. **Hett, E. C., M. C. Chao, L. L. Deng, and E. J. Rubin.** 2008. A mycobacterial enzyme essential for cell division synergizes with resuscitation-promoting factor. PLoS Pathog **4:**e1000001.

40. **Hett, E. C., M. C. Chao, A. J. Steyn, S. M. Fortune, L. L. Deng, and E. J. Rubin.** 2007. A partner for the resuscitation-promoting factors of *Mycobacterium tuberculosis*. Mol Microbiol **66:**658-68.

41. **Hett, E. C., and E. J. Rubin.** 2008. Bacterial growth and cell division: a mycobacterial perspective. Microbiol Mol Biol Rev **72:**126-56, table of contents.

42. **Homuth, M., P. Valentin-Weigand, M. Rohde, and G. F. Gerlach.** 1998. Identification and characterization of a novel extracellular ferric reductase from *Mycobacterium paratuberculosis*. Infect Immun **66:**710-6.

43. **Honer zu Bentrup, K., and D. G. Russell.** 2001. Mycobacterial persistence: adaptation to a changing environment. Trends Microbiol **9:**597-605.

44. **Hostetter, J., E. Steadham, J. Haynes, T. Bailey, and N. Cheville.** 2003. Phagosomal maturation and intracellular survival of *Mycobacterium avium* subspecies *paratuberculosis* in J774 cells. Comp Immunol Microbiol Infect Dis **26:**269-83.

45. **Imboden, P., and G. K. Schoolnik.** 1998. Construction and characterization of a partial *Mycobacterium tuberculosis* cDNA library of genes expressed at reduced oxygen tension. Gene **213:**107-17.

46. **Kana, B. D., B. G. Gordhan, K. J. Downing, N. Sung, G. Vostroktunova, E. E. Machowski, L. Tsenova, M. Young, A. Kaprelyants, G. Kaplan, and V. Mizrahi.** 2008. The resuscitation-promoting factors of *Mycobacterium tuberculosis* are required for virulence and resuscitation from dormancy but are collectively dispensable for growth in vitro. Mol Microbiol **67:**672-84.

47. **Kana, B. D., and V. Mizrahi.** Resuscitation-promoting factors as lytic enzymes for bacterial growth and signaling. FEMS Immunol Med Microbiol **58:**39-50.

48. **Kao, R. R., M. G. Roberts, and T. J. Ryan.** 1997. A model of bovine tuberculosis control in domesticated cattle herds. Proc Biol Sci **264:**1069-76.

49. **Kleerebezem, M., L. E. Quadri, O. P. Kuipers, and W. M. de Vos.** 1997. Quorum sensing by peptide pheromones and two-component signal-transduction systems in Gram-positive bacteria. Mol Microbiol **24:**895-904.

50. **Lambrecht, R. S., J. F. Carriere, and M. T. Collins.** 1988. A model for analyzing growth kinetics of a slowly growing *Mycobacterium* sp. Appl Environ Microbiol **54:**910-6.

51. **Lambrecht, R. S., and M. T. Collins.** 1993. Inability to detect mycobactin in mycobacteria-infected tissues suggests an alternative iron acquisition mechanism by mycobacteria in vivo. Microb Pathog **14:**229-38.

52. **Lavollay, M., M. Arthur, M. Fourgeaud, L. Dubost, A. Marie, N. Veziris, D. Blanot, L. Gutmann, and J. L. Mainardi.** 2008. The peptidoglycan of stationary-phase *Mycobacterium tuberculosis* predominantly contains cross-links generated by L,D-transpeptidation. J Bacteriol **190:**4360-6.

53. **Li, L., J. P. Bannantine, Q. Zhang, A. Amonsin, B. J. May, D. Alt, N. Banerji, S. Kanjilal, and V. Kapur.** 2005. The complete genome sequence of *Mycobacterium avium* subspecies *paratuberculosis*. Proc Natl Acad Sci U S A **102:**12344-9.

54. **Lichty, J. J., J. L. Malecki, H. D. Agnew, D. J. Michelson-Horowitz, and S. Tan.** 2005. Comparison of affinity tags for protein purification. Protein Expr Purif **41:**98-105.

55. **Ma, J., A. Campbell, and S. Karlin.** 2002. Correlations between Shine-Dalgarno sequences and gene features such as predicted expression levels and operon structures. J Bacteriol **184:**5733-45.

56. **Mahapatra, S., H. Scherman, P. J. Brennan, and D. C. Crick.** 2005. N Glycolylation of the nucleotide precursors of peptidoglycan biosynthesis of *Mycobacterium* spp. is altered by drug treatment. J Bacteriol **187:**2341-7.

57. **McNab, W. B., A. H. Meek, J. R. Duncan, B. W. Brooks, A. A. Van Dreumel, S. W. Martin, K. H. Nielsen, E. A. Sugden, and C. Turcotte.** 1991. An evaluation of selected screening tests for bovine paratuberculosis. Can J Vet Res **55:**252-9.

58. **Miltner, E. C., and L. E. Bermudez.** 2000. *Mycobacterium avium* grown in *Acanthamoeba castellanii* is protected from the effects of antimicrobials. Antimicrob Agents Chemother **44:**1990-4.

59. **Mishina, D., P. Katsel, S. T. Brown, E. C. Gilberts, and R. J. Greenstein.** 1996. On the etiology of Crohn disease. Proc Natl Acad Sci U S A **93:**9816-20.

60. **Momotani, E., D. L. Whipple, A. B. Thiermann, and N. F. Cheville.** 1988. Role of M cells and macrophages in the entrance of *Mycobacterium paratuberculosis* into domes of ileal Peyer's patches in calves. Vet Pathol **25:**131-7.

61. **Mukamolova, G. V., A. S. Kaprelyants, D. I. Young, M. Young, and D. B. Kell.** 1998. A bacterial cytokine. Proc Natl Acad Sci U S A **95:**8916-21.

62. **Mukamolova, G. V., A. G. Murzin, E. G. Salina, G. R. Demina, D. B. Kell, A. S. Kaprelyants, and M. Young.** 2006. Muralytic activity of *Micrococcus luteus* Rpf and its relationship to physiological activity in promoting bacterial growth and resuscitation. Mol Microbiol **59:**84-98.

63. **Mukamolova, G. V., O. A. Turapov, K. Kazarian, M. Telkov, A. S. Kaprelyants, D. B. Kell, and M. Young.** 2002. The *rpf* gene of *Micrococcus luteus* encodes an essential secreted growth factor. Mol Microbiol **46:**611-21.

64. **Mukamolova, G. V., O. A. Turapov, D. I. Young, A. S. Kaprelyants, D. B. Kell, and M. Young.** 2002. A family of autocrine growth factors in *Mycobacterium tuberculosis*. Mol Microbiol **46:**623-35.

65. **Mulder, M. A., H. Zappe, and L. M. Steyn.** 1997. Mycobacterial promoters. Tuber Lung Dis **78:**211-23.

66. **Nielsen, S. S., and N. Toft.** 2006. Age-specific characteristics of ELISA and fecal culture for purpose-specific testing for paratuberculosis. J Dairy Sci **89:**569-79.

67. **Novgen.** 2002. pET Sytems Manual. 10 ed.

68. **Pickup, R. W., G. Rhodes, S. Arnott, K. Sidi-Boumedine, T. J. Bull, A. Weightman, M. Hurley, and J. Hermon-Taylor.** 2005. *Mycobacterium avium* subsp. *paratuberculosis* in the catchment area and water of the River Taff in South Wales, United Kingdom, and its potential relationship to clustering of Crohn's disease cases in the city of Cardiff. Appl Environ Microbiol **71:**2130-9.

69. **Pisabarro, A. G., M. A. de Pedro, and D. Vazquez.** 1985. Structural modifications in the peptidoglycan of *Escherichia coli* associated with changes in the state of growth of the culture. J Bacteriol **161:**238-42.

70. **Piuri, M., and G. F. Hatfull.** 2006. A peptidoglycan hydrolase motif within the mycobacteriophage TM4 tape measure protein promotes efficient infection of stationary phase cells. Mol Microbiol **62:**1569-85.

71. **Raizman, E. A., J. Fetrow, S. J. Wells, S. M. Godden, M. J. Oakes, and G. Vazquez.** 2007. The association between *Mycobacterium avium* subsp. *paratuberculosis* fecal shedding or clinical Johne's disease and lactation performance on two Minnesota, USA dairy farms. Prev Vet Med **78:**179-95.

72. **Raman, S., R. Hazra, C. C. Dascher, and R. N. Husson.** 2004. Transcription regulation by the *Mycobacterium tuberculosis* alternative sigma factor SigD and its role in virulence. J Bacteriol **186:**6605-16.

73. **Ratnam, S., and S. Chandrasekhar.** 1976. The pathogenicity of spheroplasts of *Mycobacterium tuberculosis*. Am Rev Respir Dis **114:**549-54.

74. **Rickman, L., C. Scott, D. M. Hunt, T. Hutchinson, M. C. Menendez, R. Whalan, J. Hinds, M. J. Colston, J. Green, and R. S. Buxton.** 2005. A member of the cAMP receptor protein family of transcription regulators in *Mycobacterium tuberculosis* is required for virulence in mice and controls transcription of the *rpfA* gene coding for a resuscitation promoting factor. Mol Microbiol **56:**1274-86.

75. **Rosano, G. L., and E. A. Ceccarelli.** 2009. Rare codon content affects the solubility of recombinant proteins in a codon bias-adjusted *Escherichia coli* strain. Microb Cell Fact **8:**41.

76. **Rosenthal, R. S., W. Nogami, B. T. Cookson, W. E. Goldman, and W. J. Folkening.** 1987. Major fragment of soluble peptidoglycan released from growing *Bordetella pertussis* is tracheal cytotoxin. Infect Immun **55:**2117-20.

77. **Roszak, D. B., and R. R. Colwell.** 1987. Survival strategies of bacteria in the natural environment. Microbiol Rev **51:**365-79.

78. **Rowe, M. T., and I. R. Grant.** 2006. *Mycobacterium avium* ssp. *paratuberculosis* and its potential survival tactics. Lett Appl Microbiol **42:**305-11.

79. **Russel, W. F., S. H. Dressler, G. Middlebrook, and J. Denst.** 1955. Implications of the phenomenon of open cavity healing for the chemotherapy of pulmonary tuberculosis. Am Rev Tuberc **71:**441-6.

80. **Scanu, A. M., T. J. Bull, S. Cannas, J. D. Sanderson, L. A. Sechi, G. Dettori, S. Zanetti, and J. Hermon-Taylor.** 2007. *Mycobacterium avium* subspecies *paratuberculosis* infection in cases of irritable bowel syndrome and comparison with Crohn's disease and Johne's disease: common neural and immune pathogenicities. J Clin Microbiol **45:**3883-90.

81. **Secott, T. E., A. M. Ohme, K. S. Barton, C. C. Wu, and F. A. Rommel.** 1999. *Mycobacterium paratuberculosis* detection in bovine feces is improved by coupling agar culture enrichment to an IS900-specific polymerase chain reaction assay. J Vet Diagn Invest **11:**441-7.

82. **Sehgal, V. N., K. Sardana, and S. Dogra.** 2008. The imperatives of leprosy treatment in the pre- and post-global leprosy elimination era: appraisal of changing the scenario to current status. J Dermatolog Treat **19:**82-91.

83. **Sever, J. L., and G. P. Youmans.** 1957. Enumeration of viable tubercle bacilli from the organs of nonimmunized and immunized mice. Am Rev Tuberc **76:**616-35.

84. **Shah, I. M., M. H. Laaberki, D. L. Popham, and J. Dworkin.** 2008. A eukaryotic-like Ser/Thr kinase signals bacteria to exit dormancy in response to peptidoglycan fragments. Cell **135:**486-96.

85. **Shi, L., M. Potts, and P. J. Kennelly.** 1998. The serine, threonine, and/or tyrosine-specific protein kinases and protein phosphatases of prokaryotic organisms: a family portrait. FEMS Microbiol Rev **22:**229-53.

86. **Signoretto, C., M. M. Lleo, and P. Canepari.** 2002. Modification of the peptidoglycan of *Escherichia coli* in the viable but nonculturable state. Curr Microbiol **44:**125-31.

87. **Signoretto, C., M. M. Lleo, M. C. Tafi, and P. Canepari.** 2000. Cell wall chemical composition of *Enterococcus faecalis* in the viable but nonculturable state. Appl Environ Microbiol **66:**1953-9.

88. **Sohal, J. S., S. V. Singh, P. Tyagi, S. Subhodh, P. K. Singh, A. V. Singh, K. Narayanasamy, N. Sheoran, and K. Singh Sandhu.** 2008. Immunology of mycobacterial infections: with special reference to *Mycobacterium avium* subspecies *paratuberculosis*. Immunobiology **213:**585-98.

89. **Sohaskey, C. D.** 2008. Nitrate enhances the survival of *Mycobacterium tuberculosis* during inhibition of respiration. J Bacteriol **190:**2981-6.

90. **Stabel, J. R.** 1998. Johne's disease: a hidden threat. J Dairy Sci **81:**283-8.

91.   **Stabel, J. R.** 2000. Transitions in immune responses to *Mycobacterium paratuberculosis*. Vet Microbiol **77:**465-73.

92.   **Steinert, M., K. Birkness, E. White, B. Fields, and F. Quinn.** 1998. *Mycobacterium avium* bacilli grow saprozoically in coculture with *Acanthamoeba polyphaga* and survive within cyst walls. Appl Environ Microbiol **64:**2256-61.

93.   **Stephenson, K., Y. Yamaguchi, and J. A. Hoch.** 2000. The mechanism of action of inhibitors of bacterial two-component signal transduction systems. J Biol Chem **275:**38900-4.

94.   **Stewart, D. J., J. A. Vaughan, P. L. Stiles, P. J. Noske, M. L. Tizard, S. J. Prowse, W. P. Michalski, K. L. Butler, and S. L. Jones.** 2007. A long-term bacteriological and immunological study in Holstein-Friesian cattle experimentally infected with *Mycobacterium avium* subsp. *paratuberculosis* and necropsy culture results for Holstein-Friesian cattle, Merino sheep and Angora goats. Vet Microbiol.

95.   **Storset, A. K., H. J. Hasvold, M. Valheim, H. Brun-Hansen, G. Berntsen, S. K. Whist, B. Djonne, C. M. Press, G. Holstad, and H. J. Larsen.** 2001. Subclinical paratuberculosis in goats following experimental infection. An immunological and microbiological study. Vet Immunol Immunopathol **80:**271-87.

96.   **Taga, M. E., and B. L. Bassler.** 2003. Chemical communication among bacteria. Proc Natl Acad Sci U S A **100 Suppl 2:**14549-54.

97.   **Telkov, M. V., G. R. Demina, S. A. Voloshin, E. G. Salina, T. V. Dudik, T. N. Stekhanova, G. V. Mukamolova, K. A. Kazaryan, A. V. Goncharenko, M. Young, and A. S. Kaprelyants.** 2006. Proteins of the Rpf (resuscitation promoting factor) family are peptidoglycan hydrolases. Biochemistry (Mosc) **71:**414-22.

98.   **Tufariello, J. M., W. R. Jacobs, Jr., and J. Chan.** 2004. Individual *Mycobacterium tuberculosis* resuscitation-promoting factor homologues are dispensable for growth in vitro and in vivo. Infect Immun **72:**515-26.

99.   **Tufariello, J. M., K. Mi, J. Xu, Y. C. Manabe, A. K. Kesavan, J. Drumm, K. Tanaka, W. R. Jacobs, Jr., and J. Chan.** 2006. Deletion of the *Mycobacterium tuberculosis* resuscitation-promoting factor Rv1009 gene results in delayed reactivation from chronic tuberculosis. Infect Immun **74:**2985-95.

100.   **Udou, T., M. Ogawa, and Y. Mizuguchi.** 1982. Spheroplast formation of *Mycobacterium smegmatis* and morphological aspects of their reversion to the bacillary form. J Bacteriol **151:**1035-9.

101.   **USDA.** 2008. Johne's Disease on U.S. Dairy Operations. *In* NAHMS (ed.). USDA:APHIS:VS, CEAH, Fort Collins, CO, USA.

102.   **USDA.** 1997. Johne's Disease on U.S. Dairy Operations. *In* NAHMS (ed.). USDA:APHIS:VS:CEAH, Fort Collins, CO, USA.

103. **van Roermund H.J.W., D. B., P.T.J. Willemsen, M.C.M. de Jong.** 2007. Horizontal transmission of *Mycobacterium avium* subsp. *paratuberculosis* in cattle in an experimental setting: Calves can transmit the infection to other calves. Vet Microbiol.

104. **Votyakova, T. V., A. S. Kaprelyants, and D. B. Kell.** 1994. Influence of Viable Cells on the Resuscitation of Dormant Cells in *Micrococcus luteus* Cultures Held in an Extended Stationary Phase: the Population Effect. Appl Environ Microbiol **60:**3284-3291.

105. **Wall, S., Z. M. Kunze, S. Saboor, I. Soufleri, P. Seechurn, R. Chiodini, and J. J. McFadden.** 1993. Identification of spheroplast-like agents isolated from tissues of patients with Crohn's disease and control tissues by polymerase chain reaction. J. Clin. Microbiol. **31:**1241-1245.

106. **Wayne, L. G.** 1976. Dynamics of submerged growth of *Mycobacterium tuberculosis* under aerobic and microaerophilic conditions. Am Rev Respir Dis **114:**807-11.

107. **Wayne, L. G., and L. G. Hayes.** 1996. An in vitro model for sequential study of shiftdown of *Mycobacterium tuberculosis* through two stages of nonreplicating persistence. Infect Immun **64:**2062-9.

108. **Wayne, L. G., and L. G. Hayes.** 1998. Nitrate reduction as a marker for hypoxic shiftdown of *Mycobacterium tuberculosis*. Tuber Lung Dis **79:**127-32.

109. **Wayne, L. G., and K. Y. Lin.** 1982. Glyoxylate metabolism and adaptation of *Mycobacterium tuberculosis* to survival under anaerobic conditions. Infect Immun **37:**1042-9.

110. **Wayne, L. G., and C. D. Sohaskey.** 2001. Nonreplicating persistence of *Mycobacterium tuberculosis*. Annu Rev Microbiol **55:**139-63.

111. **Whan, L., I. R. Grant, and M. T. Rowe.** 2006. Interaction between *Mycobacterium avium* subsp. *paratuberculosis* and environmental protozoa. BMC Microbiol **6:**63.

112. **Whittington, R. J., J. B. Lloyd, and L. A. Reddacliff.** 2001. Recovery of *Mycobacterium avium* subsp. *paratuberculosis* from nematode larvae cultured from the faeces of sheep with Johne's disease. Vet Microbiol **81:**273-9.

113. **Whittington, R. J., D. J. Marshall, P. J. Nicholls, I. B. Marsh, and L. A. Reddacliff.** 2004. Survival and dormancy of *Mycobacterium avium* subsp. *paratuberculosis* in the environment. Appl Environ Microbiol **70:**2989-3004.

114. **Winzer, K., and P. Williams.** 2001. Quorum sensing and the regulation of virulence gene expression in pathogenic bacteria. Int J Med Microbiol **291:**131-43.

115. **Woo, S. R., J. A. Heintz, R. Albrecht, R. G. Barletta, and C. J. Czuprynski.** 2007. Life and death in bovine monocytes: the fate of *Mycobacterium avium* subsp. *paratuberculosis*. Microb Pathog **43:**106-13.

116. **Yamamura, Y., A. Walter, and H. Bloch.** 1960. Bacterial populations in experimental murine tuberculosis. I. Studies in normal mice. J Infect Dis **106:**211-22.

117. **Zhu, W., B. B. Plikaytis, and T. M. Shinnick.** 2003. Resuscitation factors from mycobacteria: homologs of *Micrococcus luteus* proteins. Tuberculosis (Edinb) **83:**261-9.

Appendix and Protocols

<u>**Agarose Gel Electrophoresis**</u>

Required: Agarose Electrophoresis Matrix, 1X TBE Buffer, Gel Cast, Loading Dye, Parafilm, Buffer Tank, Power Source, 2 mg/ml Ethidium Bromide, UV Imaging System

1. Make 1% agarose gel by adding 0.3 grams of agarose electrophoresis matrix to 29.7 ml of 1X TBE buffer. **Caution!** Ethidium bromide is a known carcinogen, always wear gloves!

2. Boil the mixture in a glass bottle for 2 minutes.

3. While the Solution is boiling, setup your gel cast by taping the open ends with masking tape so the top of the tape is level with the sides of the cast. Insert comb in the top end.

4. Once the solution has air-cooled to approximately 50ºC, poor it level with the sides of the cast, add 10 µl of 2 mg/ml ethidium bromide, and mix with the pipette tip. An agarose solution that's too hot can warp the cast. Improper cooling methods can cause inconsistencies in the gel. Ethidium bromide is photo reactive; do your best to shelter it from light.

5. Once the gel has solidified, remove the comb carefully. Squirt water over the area where comb meets gel to lubricate as it pulls out. Removing to fast can pull the agarose base of the gel through the comb slot creating an open-ended well. Remove the masking tape from the ends.

6. Place the gel, still in the cast, into the buffer tank so the wells are nearest to the cathode. Fill the buffer tank with 1X TBE buffer so that the buffer rises just over the top of the gel.

7. Mix your sample on a square of parafilm with the loading dye to a final concentration of 1X. Your final volume should not exceed 30 µl. Carefully load your samples into

the wells. If your number of samples is less the number of available wells, avoid using the outermost wells. Be sure to save one lane for your ladder.

8. Place the lid over the tank and connect the cables with concern to the cathode and anode. Switch on the power supply, and run the gel at 145 V for approximately 45 minutes, or until the bromphenol blue in the loading dye travels ¾ the distance of the gel. It should migrate with bands of approximately 500 base pairs.

9. Place the gel under UV light to reveal your samples.

NOTE: Proper clean up is a must! Your gel, running buffer, gel cast, box, and anything else you have touched will contain residual ethidium bromide.

10X TBE Buffer	
Tris Base	108 g
Boric Acid	55 g
EDTA	9.3 g
dH$_2$O	q.s. to 1 L

2 mg/ml Ethidium Bromide	
Ethidium Bromide	0.02 g
dH$_2$O	10 ml
Prepare in a 50 ml conical tube, wrap in foil, and store at 4ºC. **Caution!** Ethidium bromide is a known carcinogen! Take proper precautions.	

SDS-PAGE (Laemmli Protocol)

Required: Acrylamide:Bis 37.5:1, 4X Tris-SDS pH 8.8, 4X Tris-SDS pH 6.8, TEMED, Fresh 10% Ammonium Persulfate, 10X Tris-Glycine, 2X loading dye, Beta Mercaptoethanol, Coomassie Blue Solution, Destaining Solution, Glass Casting Plates, Casting Clamps, Buffer Tank, Power source

1. Thoroughly clean glass plates with water and 70% ethanol.

2. Place the glass-plate clamps on the bench surface, and insert the glass plates. Once you are sure they are flush, clamp them into place. If they are not your gel will leak out the bottom before it solidifies. Clamp glass-plate assemblies into the casting box, being sure the bottoms of the glass plates are seated into the foam seats.

3. Combine the following for a 10% separating gel: 5 ml Acrylamide:Bis 37.5:1, 3.75 ml 4X Tris-SDS pH 8.8, 6.25 ml dH$_2$O, 50 µl fresh ammonium persulfate, and 10 µl TEMED. Mix well, and with a P1000 micropipette dispense 5 ml between the glass plates. **Caution!** Acrylamide is a known neurotoxin!! Wear gloves!

4. Once you have 5 mls between the plates, gently dispense dH$_2$O on top of the acrylamide solution until the volume reaches the top of the front glass plate. When solidified you will see a line develop at the gel/dH$_2$O interface. Wait until you see this before proceeding.

5. Combine the following to make the stacking gel: 0.65 ml Acrylamide:Bis 37.5:1, 1.25 ml 4X SDS-Tris pH 6.8, 3.05 ml dH$_2$O, 25 µl fresh ammonium persulfate, and 10 µl TEMED. Mix well.

6. Discard the excess water from the separating gel. With a P1000 micropipette, dispense the stacking-gel solution on top of the separating gel until it reaches approximately 5 mm from the top of the front glass plate. Being sure to avoid trapping bubbles, insert the gel comb into the liquid stacking-gel solution. Some may spill over the front – clean appropriately wearing gloves. Be sure the comb is seated against the right side of the plates. As the level drops, add stacking-gel acrylamide solution in 5 µl increments to the minute gap between the left side of the comb and the glass plate until it solidifies. If you do not do this you will lose the outermost wells of your gel.

7. When the stacking gel has solidified, release the clamps and wash any residual liquid acryladmide solution from the plates. Place the gels in the clamping frame such that both of the shorter glass plates face the center, and lock into place. Place the clamping frame into the buffer tank.

8. Make 1X Tris-Glycine buffer by adding 40 mls of 10X Tris-Glycine buffer to 360 mls of dH_2O. Dispense all 400 mls into the center, between the two gels. Allow the excess buffer to flow in into the surrounding reserve of the buffer tank.

9. Dispense 300 µl of 2X loading dye into a 500 µl tube. Add 6 µl of beta mercaptoethanol and mix well. Dispense 15 µl into an appropriate number of sample tubes. Add 15 µl of your sample to each respective tube, and mix.

10. Boil your samples in the thermocycler for 10 minutes.

11. Dispense 25 µl of your samples into the wells of the gel with a P30 micropipette. Avoid using the outermost wells if you don't need them. Be sure to save one lane for your ladder. Fill any unused wells with 1X loading dye.

12. Put the lid into place with concern to the cathode and anode, and run your samples at 165 V for 60 minutes. Be sure to check frequently, as the buffer level between the gels will decrease rapidly while running. To refill it, stop the power, and with a 10 ml pipette draw buffer from the reserve and dispense it back into the center.

13. When the cycle is complete, discard the buffer and remove the clamping frame. Separate the glass plates with the gel releaser. Cut away the stacking gel, and rinse the gels under dH_2O.

14. Rock the gels overnight in a low volume of 1X coomassie solution.

15. Dispose of the used coomassie solution in a hazardous waste container, and rinse the gels with dH_2O. Add destaining solution and rock until the solution needs to be changed. Do this until the gel is fully destained.

16. Observe the bands under bright illumination.

Separating Gel Stock Solutions (ml)	Final Acrylamide Concentration in Separating Gel (%)									
	5	**6**	**7**	**7.5**	**8**	**9**	**10**	**12**	**13**	**15**
30% Acrylamide/ 0.8% Bisacrylamide	2.50	3.00	3.50	3.75	4.00	4.50	5.00	6.00	6.50	7.50
4X Tris-HCl/SDS pH 8.8	3.75	3.75	3.75	3.75	3.75	3.75	3.75	3.75	3.75	3.75
dH$_2$O	8.75	8.25	7.75	7.50	7.25	6.75	6.25	5.25	4.75	3.75
10% APS (Fresh)	0.05	0.05	0.05	0.05	0.05	0.05	0.05	0.05	0.05	0.05
TEMED	0.01	0.01	0.01	0.01	0.01	0.01	0.01	0.01	0.01	0.01

Gel %	**5**	**10**	**15**
Protein Separation Range (kDa)	60-200	16-70	12-45

30% Acrylamide/0.8% Bisacrylamide	
Acrylamide	30 g
N,N'- methylenebisacrylamide	0.8 g
dH$_2$O	q.s. to 100 ml

Keep solution away from light by wrapping the bottle with foil. Heat solution to 37ºC to get chemicals into solution. Filter with 0.45 μm-membrane filter. **Caution!** Acrylamide is a neurotoxin! Take proper precautions!

4X Tris-HCl/SDS Seprating Gel pH 8.8

Tris-HCl	91 g
SDS	2 g
dH$_2$O	q.s. to 500 ml

Stir reagents into solution, pH to 8.8 with HCl, filter through 0.45 µm filter, store at 4ºC

4X Tris-HCl/SDS Stacking Gel pH 6.8

Tris-HCl	6.05 g
SDS	0.4 g
dH2O	q.s. to 100 ml

Stir reagents into solution, pH to 8.8 with HCl, filter through 0.45 µm filter, store at 4ºC

10% Ammonium Persulfate

Ammonium Persulfate	0.1 g
dH$_2$O	0.9 ml

Always prepare this solution fresh before use. Store at -20ºC

2X Sample Buffer

Tris-HCl	1.52 g
Glycerol	20 ml
SDS	2.0 g
Bromphenol Blue	0.001 g
dH$_2$O	q.s. to 100 ml

Stir reagents into solution, pH to 6.8 with HCl, add 20 μl ß-mercaptoethanol per ml sample buffer immediately before use.

10X SDS-PAGE Running Buffer

Tris Base	30.2 g
Glycine	144 g
SDS	10 g
dH$_2$O	q.s. to 1000 ml

Coomassie Blue Solution

Methanol	500 ml
Glacial Acetic Acid	300 ml
Coomassie Blue R	0.5 g
dH$_2$O	q.s. to 1000 ml

Destaining Solution	
Methanol	50 ml
Glacial Acetic Acid	70 ml
dH$_2$O	q.s. to 1000ml

References

T.E. Secott, MnSU-Mankato. Lab Protocol. 2003. <u>Preparation of Reagents for Denaturing Sodium Dodecylsulfate-Polyacrylamide Discontinuous Gel Electrophoresis – Laemmli Method.</u>

Western Blotting

Required: SDS-PAGE Gel, Transfer Buffer, Bio-Ice Cooling Unit with frozen water, Gel-Holder Cassettes, Gel-Transfer Cell, Buffer Tank, Nitrocellulose Paper, Filters, Foam Pads, Power Source, Appropriate Antibody, Diaminobenzidine Solution, Sterile 1X PBST + 1% BSA, 1X PBST, Tube Roller, 50 ml Conical Tubes, Cake Pan, Magnetic Stir Bar, Magnetic Stir Plate,

1. Streamline this protocol from step 15 of SDS-PAGE protocol.

2. Cut a piece of nitrocellulose paper equal in size to the area covered by the migration of your bands in the polyacrylamide gel. Trim 2 Whatman filters (per blot) equal in size to the foam pads.

3. Assemble the gel sandwich as follows: 1) place the gel-holder cassettes in the cake pan, black side down. Pour approximately 400 ml transfer buffer into cake pan. 2) Saturate the foam pads in transfer buffer in cake pan. Place one pad onto each black panel of cassettes. 3) Place one trimmed Whatman filter on top of the saturated foam pad. 4) Place polyacrylamide gel in the center of the wet filter. 5) Carefully lay down the nitrocellulose paper on top of the gel. 6) Place 2nd trimmed Whatman filter on top of the nitrocellulose paper. 7) Saturate 2nd foam pad in running buffer and place overtop wet filter. **Careful!** Be sure to exclude any and all bubbles between any of the layers of your gel sandwich or transfer will be incomplete! Wear nitrile gloves during this procedure. Latex and bare skin will leave residues that can obscure your results!

4. Fold down the clear side of the cassette and clamp shut. Place the cassettes into the gel-transfer cell with the plastic hinges down, and orientated such that the black cassette panels are facing the same direction as the black side of the transfer cell.

5. Pour transfer buffer from the cake pan into the buffer tank, and drop in the stir bar. The stir bar should be able to spin in between the center notches of the cassettes.

6. Place the bio-ice cooling unit (already containing frozen water) into the remaining gap between the buffer tank and the gel-transfer cell. Fill the buffer tank with the remaining transfer buffer until it reaches a few millimeters below the top lip of the buffer tank. Fluid expansion will cause overflow of buffer if filled too high.

7. Set the tank on the magnetic stirrer and turn on to medium speed, being sure it rotates unobstructed. Secure lid to the tank, with concern to the anode and cathode, and run for 1 hour at 100 V.

8. When the cycle completes, pour the buffer back into the original container. It can be reused approximately 5 times, or until distortion of your bands is seen. Deconstruct the sandwich apparatus, and place the nitrocellulose, blot-side up, into a 50 ml conical tube. Pipette 10 ml of filter-sterilized 1X PBST + 1% BSA into conical tube, and slide nitrocellulose paper up and down until bubbles are gone. Put tube into a roller at 4ºC, and rotate for 1 hour.

9. Dump 1X PBST + 1% BSA, and add 5-10 ml 1X PBST + 1% BSA + 1:1000 anti-6XHis antibody and Spin at 4ºC for 1 hour.

10. Save antibody solution for future reuse, and wash nitrocellulose paper for 1 hour by adding 10 ml 1X PBST and spinning at 4ºC for 1 hour. Sequential washes and buffer exchanges may help eliminate background noise.

11. Prepare diaminobenzidine solution by combining the following: 10 ml dH_2O, 60 mg Tris-HCL, 6 mg diaminobenzidine, and pH to 7.2 with HCl.

    Caution! Diaminobenzidine has known health hazards! Take proper safety precautions!

12. Once step 10 wash has completed, dump wash buffer, and add diaminobenzidine solution. Add 6.6 µl 30% H_2O_2 to the solution and mix briefly. Rotate by hand at room temperature. Bands should develop within 15 minutes.

13. Wash nitrocellulose paper with dH_2O to stop the reaction and prevent over development of background. Observe bands.

20X PBST	
Sodium Phosphate (monobasic)	4.4 g
Sodium Phosphate (dibasic)	24 g
Sodium Chloride	170 g
Tween 20	10 ml
dH$_2$O	q.s. to 1000 ml
Dilute 5 ml 20X PBST into 95 ml dH$_2$O to make 1X.	

1X PBST + 1% BSA	
1X PBST	99 ml
BSA	1 g
Mix BSA into solution, sterile filter with 0.22 μm filter. Dispense into two 50 ml conical tubes, store at 4ºC.	

Diaminobenzidine Solution	
Tris-HCl	0.06 g
Diaminobenzidine	0.006 g
dH$_2$O	10 ml
30% Hydrogen Peroxide	6.6 μl
Mix tris into solution and pH to 7.2 with HCl, then add diaminobenzidine. Do not add H$_2$O$_2$ until immediately before use. **Caution!** Diaminobenzidine has known health hazards! Take proper precautions.	

Competent Cell Prep and Electroporation

Required: Competent Cell Line, Shaking Incubator, LB Broth, SOC Broth, 10% Glycerol, Centrifuge Bottles, Centrifuge, Ice, -80ºC Freezer, 2 mm Cuvette, Bio-Rad Gene Pulser Xcell™, LB Agar, Blood Agar, Appropriate Antibiotic, 37ºC Incubator, Sterile Glass Pasteur Pipttes, 6 ml Culture Tubes

1. Dispense 50 ml LB broth (add 0.05% tween 20 if growing *M. smegmatis mc^{2}155*) into a 250 ml Erlenmeyer flask, and inoculate with your cell line. Grow at 37ºC overnight (for *E. coli XL-1*, or 48 hours for *M. smegmatis mc^{2}155*) in a shaking incubator at 2,000 RPM.

2. When the incubation is complete, do a purity check by streaking the culture to blood agar.

3. Put the cultures on ice for 3 hours. Cool the centrifuge and rotor to 4ºC during this time.

4. Centrifuge the cultures at 10,000 x *g* for 10 minutes at 4ºC. Dump supernate, and resuspend the pellet in 50 ml cold-sterile 10% glycerol.

5. Centrifuge as before, and resuspend the pellet in 25 ml cold-sterile 10% glycerol.

6. Centrifuge as before, and resuspend the pellet in 10 ml cold-sterile 10% glycerol.

7. Centrifuge as before, and resuspend the pellet in 2 ml cold-sterile 10% glycerol.

8. Dispense the 2 ml suspension into 50 µl aliquots, keeping all tubes and cultures on ice during the step.

9. Store 50 µl aliquots at -80ºC.

Electroporation

1. Thaw competent cells on ice.

2. Dispense up to 5 µl of your plasmid into the thawed cells, and mix by stirring the pipette. Do not pipette up and down.

3. Pipette the cell/plasmid mix into a cold 2 mm electroporation cuvette. Wipe the metal edges dry with a paper towel.

4. Shock the cells in the Bio-Rad Gene Pulser Xcell™. For *E. coli* strains use the following parameters: 2,500 V, 25 µF, and 200 Ω. For *M. smegmatis* use the following parameters: 1250 V, 25 µF, and 800 Ω. If electrical arcing occurs, lower your DNA concentration or make new competent cells.

5. Immediately following electroporation, use a glass Pasteur pipette to pipette 1 ml pre-warmed SOC broth into the cuvette, pipette up and down to mix, and move to a 6 ml culture tube.

6. Incubate *E. coli* strains for 1 hour, or *M. smegmatis* strains for 2 hours in a shaking incubator at 37ºC.

7. Prepare 2 LB agars supplemented with an appropriate antibiotic.

8. Pipette 100 µl of your culture to the surface of one of the prepared LB-antibiotic agars, and the remaining 900 µl to the other (these volumes may need to be optimized).

9. Spread the volumes evenly across the entire surface of the agar, being sure the liquid is entirely absorbed into the agar before proceeding to the next step (allowing the agars to "dry" in the laminar-flow hood by leaving the lids off for an hour may expedite the process).

10. Incubate *E. coli* cultures overnight, or *M. smegmatis* cultures for 48 hours at 37ºC.

11. Screen colonies by PCR.

12. Subculture multiple colonies that screen positive in LB broth supplemented with the appropriate antibiotic. Store cultures in 10% glycerol at -80ºC and -20ºC in replicate.

10% Glycerol	
Glycerol	10 ml
dH$_2$O	90 ml
Autoclave and store at 4ºC.	

LB Broth	
LB Broth Base	20 g
Tween 20 (if growing *M. smegmatis mc^2 155*)	500 µl
dH$_2$O	1000 ml
Autoclave immediately after prepared, store at 4ºC. Add 10 g/L NaCl for Miller formulation.	

LB Agar	
LB Broth Base	20 g
Agar-Agar	15 g
dH$_2$O	1000 ml
Boil contents into solution. Cool to 50ºC, and dispense into 20 ml aliquots. Autoclave, and store at 4ºC.	

SOC Broth

Sterile Filtered 20% Dextrose	20 ml
1 M $MgCl_2$	10 ml
1 M $MgSO_4$	10 ml
SOB broth	960 ml

1 M $MgCl_2$

$MgCl_2 \cdot 6H_2O$	20.33 g
dH_2O	100 ml

1 M $MgSO_4$

$MgSO_4 \cdot 7H_2O$	24.65 g
dH_2O	100 ml

SOB Broth

Tryptone	20 g
Sodium Chloride	0.5 g
Yeast Extract	5 g
dH_2O	q.s. to 1000 ml

Autoclave SOB broth immediately after preparation. Store SOB, SOC, and 20% dextrose at 4ºC

Recombinant Protein Expression, Cell Lysis, Ni-NTA Chromatography

Expression

Required: 250 ml Erlenmeyer Flasks, LB broth, 50 mg/ml Kanamycin, 500 mM IPTG, 100 mM PMSF in 95% Ethanol, Shaking Incubator, Centrifuge Bottles, Centrifuge, 1 M Tris-HCl pH 8.0, 10% Glycerol, -20ºC Freezer, Spectrophotometer, Spectrophotometer Cuvettes, BugBuster® Reagent

1. Transform *E. coli* BL21 (DE3) with your vector. Once they have been screened for your DNA insert, grow them in a shaking incubator at 37ºC in 50 ml LB broth with 30 µg/ml kanamycin to OD_{590} 0.8. Concentrate into 2 ml 10% sterile glycerol, dispense into 80µl aliquots, and freeze at -80ºC. Note: expression will decrease with extended storage at 80ºC.

2. Dispense 50 ml LB broth into a 250 ml Erlenmeyer flask. Add 30 µl of 50 mg/ml kanamycin for a final concentration of 30 µg/ml.

3. Add 40 µl of concentrated transformed *E. coli* BL21 (DE3) cells from frozen aliquots.

4. Grow cells at 37ºC (shaking) to OD_{590} 0.6-0.8.

5. Induce cells with 1 mM IPTG (100 µl of 500 mM stock IPTG), and continue incubation for 1 hour.

6. Harvest cells by centrifugation at 10,000 x *g* for 10 minutes.

7. Resuspend cells in 10 ml 20 mM Tris-HCl pH 8.0 (200 µl 1 M Tris-HCl pH 8.0 into 9.8 ml dH_2O). Spin as before.

8. Resuspend the cells in 1 ml 1X Ni-NTA binding buffer. Add 1 mM PMSF (10 µl/ml from 100 mM stock) and freeze at -20ºC overnight in a 15 ml conical tube. **Caution!** PMSF is extremely toxic!! Lab coat, respirator, gloves, fume hood! Note: some protocols state that extended storage at -20ºC can cause inclusion bodies to become less soluble.

50 mg/ml Kanamycin

Kanamycin Sulfate	0.05 g
dH$_2$O	1 ml

Store at -20ºC

500 mM IPTG

IPTG	0.119 g
dH$_2$O	1 ml

Store at -20ºC

100 mM PMSF

PMSF	0.087 g
95% Ethanol	5 ml

Store at -20ºC **Caution!** PMSF is extremely toxic! Take proper precautions.

1 M Tris-HCl pH 8.0

Tris-HCl	121.14 g
dH$_2$O	q.s. to 1000 ml

pH to 8.0 with HCl

LB Broth

LB Broth Base	20 g
dH$_2$O	1000 ml

Autoclave immediately after prepared, store at 4ºC. Add 10 g/L NaCl for Miller formulation.

LB Agar

LB Broth Base	20 g
Agar-Agar	15 g
dH$_2$O	1000 ml

Boil contents into solution. Cool to 50ºC, and dispense into 20 ml aliquots. Autoclave, and store at 4ºC.

10% Glycerol

Glycerol	10 ml
dH$_2$O	90 ml

Autoclave and store at 4ºC.

Sonication

Required: Sonifier, 100 mM PMSF, Ice, Lab coat, Respirator, Latex Gloves, Hearing Protection, 1.5 ml Centrifuge Tubes, BugBuster® reagent, 1X Ni-NTA binding buffer, Urea, 15 ml Conical Tubes

1. Thaw cells, immediately add PMSF to final concentration of 1 mM (PMSF has a half-life of ~ 30 min in H_2O).

2. Pulse-sonicate cell suspension inside the fume hood, 6 times for 10 seconds with 30 second breaks on ice. Avoid contact between the probe tip and the tube. If suspension turns to foam while sonicating, allow liquid to settle before continuing.

3. Move the suspension into a 1.5 ml centrifuge tube, and spin at max speed for 10 minutes. Save supernate for analysis by SDS-PAGE.

4. Completely resuspend pellet in 1 ml 1:10 BugBuster® reagent, vortex, and repeat centrifugation.

5. Repeat step 13.

6. Resuspend pellet in 1X Ni-NTA binding buffer. Add an additional 1.25 mg of imidazole for each ml of binding buffer to account for the volume increase from the addition of urea in the following step. Move suspension into a 15 ml conical tube.

7. Add urea to a final concentration of 8 M (48 mg per 1 ml binding buffer). Vortex thoroughly. Note: use of urea can be problematic. Be sure Ni-NTA buffers have a slightly alkaline pH to reduce chances of protein carbamylation, while maintaining an appropriate polyhistidine pKa for the binding of nickel ions.

8. Pulse sonicate the suspension 3 times for 10 seconds between 30 second breaks ON ICE (heating promotes the production of isocyanic acid from urea decomposition).

9. Centrifuge for 30 min at 6000 x *g*. During centrifugation, proceed to following steps

Ni-NTA Chromatography

Required: Novagen® Chromatography Columns, Pierce® Disposable 10 ml Polypropylene Column, Clamp Stand, Tube Clamps, Ni-NTA 50% Resin Slurry, 4X Ni-NTA Bind Buffer, 4X Ni-NTA Wash Buffer, 4X Ni-NTA Elution Buffer, Denaturant (urea), Imidazole, 500 mM NaOH, Ultrapure Water, 15 ml Conical Tubes, 1.5 ml Centrifuge Tubes,

1. Place clamp stand into laminar flow hood, attach clamps, and secure Novagen® chromatography columns.

2. Pipette 1 ml of 50% Ni-NTA slurry into the chromatography column and allow resin to settle by gravity. Once settled, remove end cap and allow fluid to drain. Equate resin by gravity flow with 2 ml 1X Ni-NTA buffer + 8 M urea, using the same calculations for urea and additional imidazole.

3. Send soluble fraction from step 11 through the prepared Ni-NTA resin, collect in a 15 ml conical tube, and send eluate through the resin a second time.

4. Prepare 4 ml 1X Ni-NTA wash buffer and add 1.25 mg imidazole per 1 ml binding buffer, 48 mg urea, and vortex. Note: wait to add urea until you are ready to apply wash buffer to the column.

5. Add 2 ml wash buffer to the column, allow to flow through, and repeat with remaining 2 ml. Note: baseline OD_{280} readings may be necessary to determine when all contaminating proteins have eluted. Imidazole concentration may need to be optimized if contaminating proteins elute downstream.

6. Prepare 2 ml 1X Ni-NTA elution buffer and add an additional 17 mg imidazole. Immediately before use, add 96 mg urea to bring final urea concentration to 8 M, and vortex.

7. Elute into 1.5 ml micro-centrifuge tubes as follows with the following volumes: elution 1) 400 µl; elution 2) 700 µl; elution 3) 500 µl; elution 4) 500 µl.

8. Wash Ni-NTA resin with 5 ml dH$_2$O, cap, add an equal resin volume of 20% EtOH (500 µl assuming 1 ml slurry was added in step 13). Gently pipette up and down and move resin slurry to a capped, Pierce® Disposable 10 ml Polypropylene Column fit with one polyethylene disc placed directly above the reservoir tip. Be sure to assemble column such that there is already fluid in the tip, and no bubbles. Continue collecting used resin from identical-protein extractions in this column for preparation of reuse.

Eluates containing urea can be streamlined directly into SDS-PAGE from step 18. If guanidine-HCl is used as a denaturant in place of urea, eluates from step 18 must be either dialyzed or sent through a buffer exchange system before running through SDS-PAGE. For exchanging buffer, see Desalting Protocol.

Preparation To Reuse Resin:
1. Allow resin to settle in Pierce® column
2. Prepare 15 ml 500 mM NaOH
3. Remove cap and allow fluid to flow through
4. Add 5 ml 500 mM NaOH and allow to flow through
5. Cap column
6. Add 5 ml 500 mM NaOH and let sit for 30 minutes
7. Remove cap and allow to drain
8. Add 5 ml 500 mM NaOH and allow to flow through
9. Wash with 10 ml dH$_2$O
10. Repeat step 9
11. Add 5 ml 20% EtOH and allow to flow through
12. Cap column, add a volume of 20% EtOH equal to that of the resin volume
13. Store at 4ºC

Note 1) Preparing the resin for reuse cannot be done in the Novagen® columns. 500 mM NaOH will degrade the retention disc.

Note 2) This does not recharge the resin; it prepares the resin for reuse with identical proteins. Recharge resin when it losses its color. To do so, see product manual.

4X Ni-NTA Binding Buffer pH 8.0

Sodium Phosphate (monobasic)	0.4 g
Sodium Phosphate (dibasic)	10 g
Sodium Chloride	14 g
Imidazole	0.54 g
dH$_2$O	q.s. to 200 ml
pH to 8.0 with HCl	

4X Ni-NTA Wash Buffer pH 8.0

Sodium Phosphate (monobasic)	0.4 g
Sodium Phosphate (dibasic)	10 g
Sodium Chloride	14 g
Imidazole	1.09 g
dH$_2$O	q.s. to 200 ml
pH to 8.0 with HCl	

4X Ni-NTA Elution Buffer pH 8.0

Sodium Phosphate (monobasic)	0.4 g
Sodium Phosphate (dibasic)	10 g
Sodium Chloride	14 g
Imidazole	13.62 g
dH$_2$O	q.s. to 200 ml
pH to 8.0 with HCl	

500 mM Sodium Hydroxide	
Sodium Hydroxide	0.3 g
dH$_2$O	15 ml

Desalting/Buffer Exchange

Required: D-Salt™ Columns, 1X PBS, 10 mM Tris-HCl pH 6.8, 0.02% Sodium Azide, Spectrophotometer, Clamp Stand, Tube Clamps, 1.5 ml Centrifuge Tubes, Spectrophotometer, Quartz Cuvette,

1. Remove the top column cap and clamp the desalting column into place.

2. Decant the excess buffer from the surface of the top disc. Remove the bottom cap and allow any remaining storage buffer to drip through.

3. Slide the buffer reservoir into place at the top of the column. Add 5 column volumes of 10 mM Tris-HCl pH 6.8 to the top of the column (25 ml for the 5 ml column). Allow to drain completely.

4. Add your sample to the column and proceed to step 5 once it has stopped dripping.

5. In 500 µl increments, add 10 mM Tris HCl pH 6.8 to the top of the column and collect the flow through in 1.5 ml centrifuge tubes. In your initial trials, run a total volume of 5 ml through the column.

6. Take OD_{280} readings from the total volume of each sample to determine which tube(s) contain your sample. Note: Readings will become inaccurate as you approach 3 ml elution volume from the column, as the buffer you are trying to elute from will begin to elute with your exchange buffer.

7. Confirm the presence of your protein by SDS-PAGE.

8. Recharge the column by passing through 10 column volumes of 1X PBS.

9. For storage, send through 5 column volumes of 0.02% sodium azide, and recap the top and bottom when approximately 1 ml remains above the top disc. Store columns upright at 4ºC. **Caution!** Sodium azide is toxic! Take proper precautions.

10 mM Tris-HCl pH 6.8	
Tris-HCl	0.242 g
dH_2O	200 ml
pH to 6.8 with HCl	

20X PBS	
Sodium Phosphate (monobasic)	4.4 g
Sodium Phosphate (dibasic)	24 g
Sodium Chloride	170 g
dH_2O	q.s. to 1000 ml
Dilute 5 ml 20X PBS into 95 ml dH_2O to make 1X.	

0.02% Sodium Azide	
Sodium Azide	0.04 g
dH_2O	200 ml
Caution! Sodium azide is toxic! Take proper precautions.	

Polymerase Chain Reaction

This protocol was developed for amplification from high GC-containing templates.

Required: 200 µl tubes, 1.5 ml Centrifuge tubes, Ultrapure Water, Primers (10 mM working stocks), DNA Template, 10X Buffer with $MgCl_2$, Taq Polymerase, Roche GC-Rich Solution, DMSO, dNTPs, Thermocycler, Ice

1. UV irradiate an appropriate number of 200 µl reaction tubes and 1.5 ml master-mix centrifuge tubes.

2. Combine the following in a 1.5 ml centrifuge tube for a 50 µl master mix:
   a. 32.5 µl ultrapure water
   b. 5 µl 10X buffer with $MgCl_2$
   c. 1 µl 10 mM dNTPs
   d. 5 µl Roche® GC-Rich Solution
   e. 2.5 µl DMSO
   f. 1 µl 10 mM forward primer
   g. 1 µl 10 mM reverse primer
   h. 1 µl DNA template
   i. 1 µl (2 U) DyNAzyme™ II polymerase (increase to 4 U if performing PCR with chaotropes for the purpose of cloning)

3. In a thermocycler, amplify sequence in lanes 7-9 (60.8ºC, 63.5ºC, 66.0ºC) of a thermal gradient ranging from 50ºC to 70.5ºC.

4. Analyze your samples by agarose-gel electrophoresis.

DNA Ligation and Vector Construction

Required: T4 DNA Ligase, 10X Buffer, 200 µl tubes, Restriction-Digested Vector and Insert

1. UV irradiate sterile 200 µl reaction tube.

2. Combine the following:
    a. 120 ng restriction-digested vector
    b. 60 ng restriction-digested insert
    c. 1 µl 10X buffer
    d. 1 µl T4 DNA ligase
    e. Q.s. to 10 µl with nuclease-free H_2O
    f. Incubate overnight at 18ºC

3. Transform electrocompetent or chemically competent cells, select and screen colonies by PCR.

Testing the Effects of RpfB on Dormant Mpt

Required: Dormant *Mycobacterium avium* subsp. *paratuberculosis*, Thermo Scientific®
Evolution 300 UV-Vis™, Quartz Cuvette, Microcentrifuge, 3 cc Syringe, 25 Gauge
Syringe Needles, Middlebrook 7H9C, Sterile 1X PBST, Microcentrifuge Tubes,
Tupperware™ Container, Sterile 96-Well Plate, Mce and RpfB Preps, 37ºC Incubator,
Laminar Flow Hood with UV Light, 70% Ethanol, 95% Ethanol, 15 ml Conical Tube,
Sterile Plastic Reservoirs, Thermo Scientific® Multiskan™ 96-Well Plate Reader.

1. The night before you begin this setup, autoclave the following:
    a. 1X PBST
    b. 200 µl pipette tips (2-3 boxes)
    c. 1000 µl pipette tips (1 box)
    d. 10 ml glass pipettes
    e. Microcentrifuge tubes
    f. Tupperware™ container, with a paper towel in the bottom – damp with roccal,
       and the top cocked off to the side

2. Allow the autoclave to cool to room temperature overnight.

3. The next morning, bleach the inside of the laminar flow hood and wipe down any
   items in the hood with 70% ethanol.

4. Open the autoclave and immediately slide the Tupperware™ lids into place. Move
   all items from the autoclave into the laminar flow hood and irradiate with UV light
   for 15 minutes.

Dormant Cell Prep

1. Gently shake your dormant cells into suspension, breaking up the majority of
   flocculated cells.

2. Place a drop of 95% ethanol on top of the rubber cap of the serum vial containing
   your dormant cells and allow to evaporate in the laminar hood

3. Assemble your syringe in the laminar hood, insert the needle through the rubber cap, and withdraw 2 ml (2 cc) of suspended cells.

4. Dispense the 2 ml into 1 ml aliquots in two 1.5 ml microcentrifuge tubes. Spin at 10,000 x g for 7 minutes in a microcentrifuge.

5. Aseptically dump the supernate, resuspend the cells in 500 µl 1X PBST, and combine the two 500 µl volumes into one tube.

6. Withdraw 500 µl from the 1 ml volume, dispense into the quartz cuvette, and read in the % transmittance (%T) in the Evolution 300 UV-Vis™.

7. Adjust the %T to approximately 30% (between 27% and 33%) by adding 1X PBST in 50 µl increments directly to the cuvette containing the cells. At 30%T your cell density will be approximately 2.0×10^8. Once you have determined the volume necessary to dilute your cells to 30%T, fill the remaining volume of the cuvette with 10% bleach, and wash appropriately.

8. Spin down the remaining 500 µl of cells from step 10 at 10,000 x g for 7 minutes, and resuspend the pellet in an equal volume of M7H9C to that which it took to bring the cell density to 2.0×10^8 (30%T).

9. Using two microcentrifuge tubes filled with 900 µl of M7H9C as your diluent, perform two 1:10 serial dilutions on your cells to bring the concentration to 2.0×10^6. Perform a 3rd dilution (1:100) by dispensing 100 µl of your cells at 2.0×10^6 into 10 ml M7H9C in a 15 ml conical tube. This will bring your cells to a density of 2.0×10^4.

Recombinant Protein Prep

1. Have your protein preps ready and quantitated by BCA standardization.

2. Dilute 10 µl of your protein solution (or appropriate volume depending on the quantitated value) in M7H9C to a final concentration of 1 nM. You will need minimally, a total volume of 100 µl for 5 replicate trials.

Experiment Assembly

Proceed to the following with impeccable and absolute concern to the highest allowable aseptic standards.

1. Dispense 10 ml of M7H9C into a sterile plastic reservoir that conforms to use with a multichannel pipette.

2. Fill the wells of a 96-well plate using the following instructions.

3. Dispense 180 µl M7H9C into row A, columns 1-10.

4. Dispense 100 µl M7H9C into row A, column 11

5. Dispense 100 µl M7H9C into rows B-H, columns 1-11.

6. Dispense 20 µl of Mce and RpfB at 1 nM into their respective wells.
   a. Mce into row A, columns 1-5
   b. RpfB into row A, columns 6-10

7. Serially dilute 100 µl of row A columns 1-10 through rows B-H, columns 2-10. Discard 100 µl from row G.

8. Empty the 10 ml of dormant Mpt at 2.0×10^4 into a sterile plastic reservoir.

9. Add 100 µl of dormant Mpt to rows A-H, columns 1-11.

10. Add 200 µl M7H9C to rows A-H, columns 12.

11. Cover with cap, place into Tupperware™. Incubate cells, tubes containing serial dilutions, dormant cells, and what remains of your protein dilutions to track sources of potential contamination.

Growth Monitoring

1. Scan the optical density of your plates every 2 days.

2. Open the Tupperware™ container in the laminar hood, and irradiate under UV light for 5 minutes.

3. Remove the lid of the 96-well plate and place upside down to allow all condensate to evaporate. Allow the temperature of the media to equilibrate to room temp.

4. Aseptically seal the wells by pressing a transparent Platemax® film over the top, and wipe all surfaces dry. From this point on, this seal will represent "the lid" in step 28.

5. Measure the optical density of the media at 490 nm in the Multiscan™ spectrophotometer.

6. Wipe all surfaces of the plate with 70% ethanol, place back into Tupperware™, and incubate.

20X PBST	
Sodium Phosphate (monobasic)	4.4 g
Sodium Phosphate (dibasic)	24 g
Sodium Chloride	170 g
Tween 20	10 ml
dH$_2$O	q.s. to 1000 ml
Dilute 5 ml 20X PBST into 95 ml dH$_2$O to make 1X.	

Middlebrook 7H9 Broth w/ 2 µg/ml Mycobactin J and 0.05% Tween 80 (M7H9C)	
Middlebrook 7H9 Broth Base	4.7 g
Tween 80	0.5 ml
Mycobactin J	4 ml
dH$_2$O	900 ml
Mix components and autoclave. Cool to 50ºC and aseptically add 100 ml oleic acid-albumin-dextrose-catalase (OADC). Alternatively, filter-sterilize the complete medium. Store at 4ºC.	

A1 Mce 500 pM	A2 Mce 500 pM	A3 Mce 500 pM	A4 Mce 500 pM	A5 Mce 500 pM	A6 RpfB 500 pM	A7 RpfB 500 pM	A8 RpfB 500 pM	A9 RpfB 500 pM	A10 RpfB 500 pM	A11 Dormant Mpt @ 1.0x10^4	A12 M7H9C
B1 Mce 250 pM	B2 Mce 250 pM	B3 Mce 250 pM	B4 Mce 250 pM	B5 Mce 250 pM	B6 RpfB 250 pM	B7 RpfB 250 pM	B8 RpfB 250 pM	B9 RpfB 250 pM	B10 RpfB 250 pM	B11 Dormant Mpt @ 1.0x10^4	B12 M7H9C
C1 Mce 125 pM	C2 Mce 125 pM	C3 Mce 125 pM	C4 Mce 125 pM	C5 Mce 125 pM	C6 RpfB 125 pM	C7 RpfB 125 pM	C8 RpfB 125 pM	C9 RpfB 125 pM	C10 RpfB 125 pM	C11 Dormant Mpt @ 1.0x10^4	C12 M7H9C
D1 Mce 62.5 pM	D2 Mce 62.5 pM	D2 Mce 62.5 pM	D3 Mce 62.5 pM	D4 Mce 62.5 pM	D6 RpfB 62.5 pM	D7 RpfB 62.5 pM	D8 RpfB 62.5 pM	D9 RpfB 62.5 pM	D10 RpfB 62.5 pM	D11 Dormant Mpt @ 1.0x10^4	D12 M7H9C
E1 Mce 31.25 pM	E2 Mce 31.25 pM	E3 Mce 31.25 pM	E4 Mce 31.25 pM	E5 Mce 31.25 pM	E6 RpfB 31.25 pM	E7 RpfB 31.25 pM	E8 RpfB 31.25 pM	E9 RpfB 31.25 pM	E10 RpfB 31.25 pM	E11 Dormant Mpt @ 1.0x10^4	E12 M7H9C
F1 Mce 15.63 pM	F2 Mce 15.63 pM	F3 Mce 15.63 pM	F4 Mce 15.63 pM	F5 Mce 15.63 pM	F6 RpfB 15.63 pM	F7 RpfB 15.63 pM	F8 RpfB 15.63 pM	F9 RpfB 15.63 pM	F10 RpfB 15.63 pM	F11 Dormant Mpt @ 1.0x10^4	F12 M7H9C
G1 Mce 7.81 pM	G2 Mce 7.81 pM	G3 Mce 7.81 pM	G4 Mce 7.81 pM	G5 Mce 7.81 pM	G6 RpfB 7.8 pM	G7 RpfB 7.8 pM	G8 RpfB 7.8 pM	G9 RpfB 7.8 pM	G10 RpfB 7.8 pM	G11 Dormant Mpt @ 1.0x10^4	G12 M7H9C
H1 Mce 3.91 pM	H2 Mce 3.91 pM	H3 Mce 3.91 pM	H4 Mce 3.91 pM	H5 Mce 3.91 pM	H6 RpfB 3.91 pM	H7 RpfB 3.91 pM	H8 RpfB 3.91 pM	H9 RpfB 3.91 pM	H10 RpfB 3.91 pM	H11 Dormant Mpt @ 1.0x10^4	H12 M7H9C

Appendix Figure 1: 96-well plate layout. M7H9C was used as the growth medium in all wells. Columns A1-A10 contain dormant Mpt at 1.0x10^4 CFU/well in addition to the recombinant protein.

A1 Mce 500 pM	A2 Mce 500 pM	A3 Mce 500 pM	A4 Mce 500 pM	A5 Mce 500 pM	A6 RpfB 500 pM	A7 RpfB 500 pM	A8 RpfB 500 pM	A9 RpfB 500 pM	A10 RpfB 500 pM	A11 Dormant Mpt @ 1.0×10^6	A12 M7H9C
B1 Mce 250 pM	B2 Mce 250 pM	B3 Mce 250 pM	B4 Mce 250 pM	B5 Mce 250 pM	B6 RpfB 250 pM	B7 RpfB 250 pM	B8 RpfB 250 pM	B9 RpfB 250 pM	B10 RpfB 250 pM	B11 Dormant Mpt @ 1.0×10^6	B12 M7H9C
C1 Mce 125 pM	C2 Mce 125 pM	C3 Mce 125 pM	C4 Mce 125 pM	C5 Mce 125 pM	C6 RpfB 125 pM	C7 RpfB 125 pM	C8 RpfB 125 pM	C9 RpfB 125 pM	C10 RpfB 125 pM	C11 Dormant Mpt @ 1.0×10^6	C12 M7H9C
D1 Mce 62.5 pM	D2 Mce 62.5 pM	D2 Mce 62.5 pM	D3 Mce 62.5 pM	D4 Mce 62.5 pM	D6 RpfB 62.5 pM	D7 RpfB 62.5 pM	D8 RpfB 62.5 pM	D9 RpfB 62.5 pM	D10 RpfB 62.5 pM	D11 Dormant Mpt @ 1.0×10^6	D12 M7H9C
E1 Mce 31.25 pM	E2 Mce 31.25 pM	E3 Mce 31.25 pM	E4 Mce 31.25 pM	E5 Mce 31.25 pM	E6 RpfB 31.25 pM	E7 RpfB 31.25 pM	E8 RpfB 31.25 pM	E9 RpfB 31.25 pM	E10 RpfB 31.25 pM	E11 Dormant Mpt @ 1.0×10^6	E12 M7H9C
F1 Mce 15.63 pM	F2 Mce 15.63 pM	F3 Mce 15.63 pM	F4 Mce 15.63 pM	F5 Mce 15.63 pM	F6 RpfB 15.63 pM	F7 RpfB 15.63 pM	F8 RpfB 15.63 pM	F9 RpfB 15.63 pM	F10 RpfB 15.63 pM	F11 Dormant Mpt @ 1.0×10^6	F12 M7H9C
G1 Mce 7.81 pM	G2 Mce 7.81 pM	G3 Mce 7.81 pM	G4 Mce 7.81 pM	G5 Mce 7.81 pM	G6 RpfB 7.8 pM	G7 RpfB 7.8 pM	G8 RpfB 7.8 pM	G9 RpfB 7.8 pM	G10 RpfB 7.8 pM	G11 Dormant Mpt @ 1.0×10^6	G12 M7H9C
H1 Mce 3.91 pM	H2 Mce 3.91 pM	H3 Mce 3.91 pM	H4 Mce 3.91 pM	H5 Mce 3.91 pM	H6 RpfB 3.91 pM	H7 RpfB 3.91 pM	H8 RpfB 3.91 pM	H9 RpfB 3.91 pM	H10 RpfB 3.91 pM	H11 Dormant Mpt @ 1.0×10^6	H12 M7H9C

Appendix Figure 2: 96-well plate layout. M7H9C was used as the growth medium in all wells. Columns A1-A10 contain dormant Mpt at 1.0×10^6 CFU/well in addition to the recombinant protein.

A1 Mce 6.4 nM	A2 Mce 6.4 nM	A3 Mce 6.4 nM	A4 Mce 6.4 nM	A5 Mce 6.4 nM	A6 RpfB 6.4 nM	A7 RpfB 6.4 nM	A8 RpfB 6.4 nM	A9 RpfB 6.4 nM	A10 RpfB 6.4 nM	A11 Dormant Mpt @ 1.0×10^4	A12 M7H9C
B1 Mce 3.2 nM	B2 Mce 3.2 nM	B3 Mce 3.2 nM	B4 Mce 3.2 nM	B5 Mce 3.2 nM	B6 RpfB 3.2 nM	B7 RpfB 3.2 nM	B8 RpfB 3.2 nM	B9 RpfB 3.2 nM	B10 RpfB 3.2 nM	B11 Dormant Mpt @ 1.0×10^4	B12 M7H9C
C1 Mce 1.6 nM	C2 Mce 1.6 nM	C3 Mce 1.6 nM	C4 Mce 1.6 nM	C5 Mce 1.6 nM	C6 RpfB 1.6 nM	C7 RpfB 1.6 nM	C8 RpfB 1.6 nM	C9 RpfB 1.6 nM	C10 RpfB 1.6 nM	C11 Dormant Mpt @ 1.0×10^4	C12 M7H9C
D1 Mce 800 pM	D2 Mce 800 pM	D2 Mce 800 pM	D3 Mce 800 pM	D4 Mce 800 pM	D6 RpfB 800 pM	D7 RpfB 800 pM	D8 RpfB 800 pM	D9 RpfB 800 pM	D10 RpfB 800 pM	D11 Dormant Mpt @ 1.0×10^4	D12 M7H9C
E1 Mce 400 pM	E2 Mce 400 pM	E3 Mce 400 pM	E4 Mce 400 pM	E5 Mce 400 pM	E6 RpfB 400 pM	E7 RpfB 400 pM	E8 RpfB 400 pM	E9 RpfB 400 pM	E10 RpfB 400 pM	E11 Dormant Mpt @ 1.0×10^4	E12 M7H9C
F1 Mce 200 pM	F2 Mce 200 pM	F3 Mce 200 pM	F4 Mce 200 pM	F5 Mce 200 pM	F6 RpfB 200 pM	F7 RpfB 200 pM	F8 RpfB 200 pM	F9 RpfB 200 pM	F10 RpfB 200 pM	F11 Dormant Mpt @ 1.0×10^4	F12 M7H9C
G1 Mce 100 pM	G2 Mce 100 pM	G3 Mce 100 pM	G4 Mce 100 pM	G5 Mce 100 pM	G6 RpfB 100 pM	G7 RpfB 100 pM	G8 RpfB 100 pM	G9 RpfB 100 pM	G10 RpfB 100 pM	G11 Dormant Mpt @ 1.0×10^4	G12 M7H9C
H1 Mce 50 pM	H2 Mce 50 pM	H3 Mce 50 pM	H4 Mce 50 pM	H5 Mce 50 pM	H6 RpfB 50 pM	H7 RpfB 50 pM	H8 RpfB 50 pM	H9 RpfB 50 pM	H10 RpfB 50 pM	H11 Dormant Mpt @ 1.0×10^4	H12 M7H9C

Appendix Figure 3: 96-well plate layout. M7H9C was used as the growth medium in all wells. Columns A1-A10 contain dormant Mpt at 1.0×10^4 CFU/well in addition to the recombinant protein.

A1 Mce 6.4 nM	A2 Mce 6.4 nM	A3 Mce 6.4 nM	A4 Mce 6.4 nM	A5 Mce 6.4 nM	A6 RpfB 6.4 nM	A7 RpfB 6.4 nM	A8 RpfB 6.4 nM	A9 RpfB 6.4 nM	A10 RpfB 6.4 nM	A11 Dormant Mpt @ 1.0×10^6	A12 M7H9C
B1 Mce 3.2 nM	B2 Mce 3.2 nM	B3 Mce 3.2 nM	B4 Mce 3.2 nM	B5 Mce 3.2 nM	B6 RpfB 3.2 nM	B7 RpfB 3.2 nM	B8 RpfB 3.2 nM	B9 RpfB 3.2 nM	B10 RpfB 3.2 nM	B11 Dormant Mpt @ 1.0×10^6	B12 M7H9C
C1 Mce 1.6 nM	C2 Mce 1.6 nM	C3 Mce 1.6 nM	C4 Mce 1.6 nM	C5 Mce 1.6 nM	C6 RpfB 1.6 nM	C7 RpfB 1.6 nM	C8 RpfB 1.6 nM	C9 RpfB 1.6 nM	C10 RpfB 1.6 nM	C11 Dormant Mpt @ 1.0×10^6	C12 M7H9C
D1 Mce 800 pM	D2 Mce 800 pM	D2 Mce 800 pM	D3 Mce 800 pM	D4 Mce 800 pM	D6 RpfB 800 pM	D7 RpfB 800 pM	D8 RpfB 800 pM	D9 RpfB 800 pM	D10 RpfB 800 pM	D11 Dormant Mpt @ 1.0×10^6	D12 M7H9C
E1 Mce 400 pM	E2 Mce 400 pM	E3 Mce 400 pM	E4 Mce 400 pM	E5 Mce 400 pM	E6 RpfB 400 pM	E7 RpfB 400 pM	E8 RpfB 400 pM	E9 RpfB 400 pM	E10 RpfB 400 pM	E11 Dormant Mpt @ 1.0×10^6	E12 M7H9C
F1 Mce 200 pM	F2 Mce 200 pM	F3 Mce 200 pM	F4 Mce 200 pM	F5 Mce 200 pM	F6 RpfB 200 pM	F7 RpfB 200 pM	F8 RpfB 200 pM	F9 RpfB 200 pM	F10 RpfB 200 pM	F11 Dormant Mpt @ 1.0×10^6	F12 M7H9C
G1 Mce 100 pM	G2 Mce 100 pM	G3 Mce 100 pM	G4 Mce 100 pM	G5 Mce 100 pM	G6 RpfB 100 pM	G7 RpfB 100 pM	G8 RpfB 100 pM	G9 RpfB 100 pM	G10 RpfB 100 pM	G11 Dormant Mpt @ 1.0×10^6	G12 M7H9C
H1 Mce 50 pM	H2 Mce 50 pM	H3 Mce 50 pM	H4 Mce 50 pM	H5 Mce 50 pM	H6 RpfB 50 pM	H7 RpfB 50 pM	H8 RpfB 50 pM	H9 RpfB 50 pM	H10 RpfB 50 pM	H11 Dormant Mpt @ 1.0×10^6	H12 M7H9C

Appendix Figure 4: 96-well plate layout. M7H9C was used as the growth medium in all wells. Columns A1-A10 contain dormant Mpt at 1.0×10^6 CFU/well in addition to the recombinant protein.

Protein	Mce	Mce	Mce	RpfA	RpfA	RpfB	RpfB	RpfB	RpfC	RpfC	RpfE	RpfE
DNA GC%	66.5	66.3	65.5	75.9	72.9	69.7	68.0	68.8	63.8	62.0	75.0	72.2
Length (a.a.)	435	472	473	250	292	372	416	397	170	206	216	254
Expressed From	Mpt	pMTS079	pMTS088	Mpt	pMTS104	Mpt	pMTS112	pMTS115	Mpt	pMTS113	Mpt	pMTS105
Weight (kDa)	45.78	48.05	50.07	24.82	29.65	39.19	44.09	42.07	18.03	22.60	22.18	26.46
Isoelectric Point	6.26	6.38	6.25	4.84	5.35	5.79	6.08	6.19	8.98	7.16	9.55	8.63
Aliphatic Index	93.031	93.235	93.422	63.120	65.303	87.796	89.468	89.064	78.176	82.371	60.324	65.781
Alanine (A)	11.3	11.5	11.8	20.0	19.2	12.1	12.7	12.3	14.7	15.0	17.1	16.9
Cysteine (C)	0.5	0.4	0.4	0.8	0.7	0.8	0.7	0.8	1.8	1.5	1.4	1.2
Aspartic Acid (A)	5.1	5.1	5.5	6.8	7.2	6.2	6.5	6.0	1.8	3.4	4.6	5.9
Glutamic Acid (E)	3.0	3.3	3.2	3.2	3.8	4.6	4.6	4.8	5.3	5.3	2.3	2.8
Phenylalanine (F)	2.5	2.6	2.5	1.6	1.7	1.3	1.4	1.5	3.5	3.4	1.9	2.0
Glycine (G)	9.9	9.5	9.1	12.0	10.3	9.7	8.7	9.1	11.2	9.2	9.7	8.3
Histidine (H)	1.1	2.4	2.3	2.0	3.8	1.1	2.4	2.5	2.4	4.9	1.9	3.9
Isoleucine (I)	5.5	5.5	5.7	2.0	2.7	4.0	4.3	4.0	5.9	6.3	3.2	3.9
Lysine (K)	3.4	3.5	3.8	0.8	1.7	2.2	2.6	2.3	2.9	3.9	1.9	2.8
Leucine (L)	10.1	10.4	10.1	4.0	4.5	6.2	6.7	6.8	4.7	5.8	3.7	4.7
Methionine (M)	1.6	1.5	1.7	1.2	1.7	2.7	2.9	2.8	2.4	2.4	0.5	0.8
Asparagine (N)	6.4	6.2	5.9	2.0	2.1	3.8	3.4	3.5	5.3	4.9	4.2	3.5
Proline (P)	8.0	7.7	7.6	15.6	13.7	6.5	6.0	6.0	5.9	5.3	19.0	16.9
Glutamine (Q)	3.2	3.3	3.2	4.8	4.5	3.8	3.6	3.8	4.7	4.4	4.2	3.9
Arginine (R)	3.7	3.5	3.4	4.0	4.1	7.3	6.5	6.8	5.3	3.9	6.9	5.9
Serine (S)	5.5	5.3	5.1	4.8	4.5	5.4	5.0	5.3	6.5	5.3	4.2	3.5
Threonine (T)	7.4	7.0	7.4	4.4	4.8	7.5	7.5	7.1	3.5	3.9	4.6	4.7
Valine (V)	7.1	6.8	6.8	6.8	6.2	12.4	11.5	11.8	7.6	6.8	5.6	5.1
Tryptophan (W)	0.7	0.7	0.6	2.0	1.7	1.6	1.4	1.5	2.9	2.4	2.3	2.0
Tyrosine (Y)	3.7	3.5	3.6	1.2	1.0	1.1	1.2	1.0	1.8	1.5	0.9	0.8

Appendix Table 1: Mce and Rpf protein statistics. Statistics were produced using CLC Free Workbench. This figure shows the molecular characteristics of each protein. Numbers to the right of the amino acids represent what percentage of the protein is composed of that amino acid.